A novel framework for real-time adaptive signal control using connected vehicles

POLITECNICO DI BARI

D.R.R.S

07

2018

PhD Program in Environmental and Building Risk and Development

Coordinator: Prof. Michele Mossa

XXX CYCLE
Curriculum: Infrastructures, transport and territory

DICATECh
Department of Civil, Environmental, Building Engineering and Chemistry

Gianvito Palmisano

A novel framework for real-time adaptive signal control using connected vehicles

Prof. Ing. Mauro Dell'Orco
DICATECh
Politecnico di Bari
Dr. Ing. Mario Marinelli
DICATECh
Politecnico di Bari

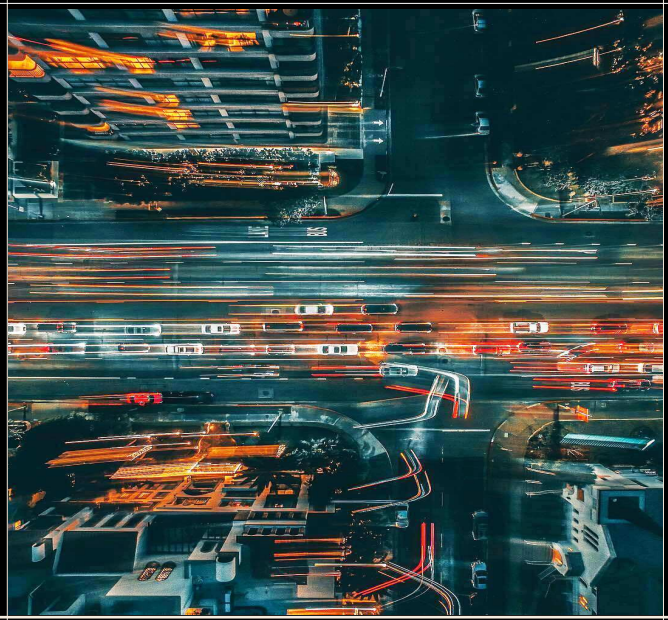

2018 DICATECh
Gianvito Palmisano
A novel framework for real-time adaptive signal control using connected vehicles
07

D.R.R.S

POLITECNICO DI BARI

07

2018

PhD Program in Environmental and Building Risk and Development

Coordinator: Prof. Michele Mossa

XXX CYCLE
Curriculum: Infrastructures, transport and territory

DICATECh
Department of Civil, Environmental, Building Engineering and Chemistry

A novel framework for real-time adaptive signal control using connected vehicles

Prof. Ing. Mauro Dell'Orco
DICATECh
Politecnico di Bari

Dr. Ing. Mario Marinelli
DICATECh
Politecnico di Bari

Gianvito Palmisano

D.R.R.S

POLITECNICO DI BARI

07

2018

Dottorato di Ricerca in Rischio e Sviluppo ambientale, territoriale ed edilizio

Coordinatore: Prof. Michele Mossa

XXX CICLO
Curriculum: Infrastrutture,trasporti e territorio

DICATECh
Dipartimento di Ingegneria Civile, Ambientale, del Territorio, Edile e di Chimica

UN NUOVO MODELLO ADATTIVO IN TEMPO REALE DI CONTROLLO SEMAFORICO MEDIANTE L' UTILIZZO DI VEICOLI CONNESSI

Prof. Ing. Mauro Dell'Orco
DICATECh
Politecnico di Bari

Dott. Ing. Mario Marinelli
DICATECh
Politecnico di Bari

Gianvito Palmisano

Politecnico di Bari

LIBERATORIA PER L'ARCHIVIAZIONE DELLA TESI DI DOTTORATO

Al Magnifico Rettore
del Politecnico di Bari

Il sottoscritto PALMISANO GIANVITO nato a CISTERNINO il 31/12/1987 residente a CRISPIANO in via ARCIPRETE 22 e-mail gianvito.palmisano@poliba.it iscritto al 3° anno di Corso di Dottorato di Ricerca in RISCHIO, SVILUPPO AMBIENTALE, TERRITORIALE ED EDILIZIO ciclo XXX

ed essendo stato ammesso a sostenere l'esame finale con la prevista discussione della tesi dal titolo:

A NOVEL FRAMEWORK FOR REAL-TIME ADAPTIVE SIGNAL CONTROL USING CONNECTED VEHICLES

DICHIARA

1) di essere consapevole che, ai sensi del D.P.R. n. 445 del 28.12.2000, le dichiarazioni mendaci, la falsità negli atti e l'uso di atti falsi sono puniti ai sensi del codice penale e delle Leggi speciali in materia, e che nel caso ricorressero dette ipotesi, decade fin dall'inizio e senza necessità di nessuna formalità dai benefici conseguenti al provvedimento emanato sulla base di tali dichiarazioni;
2) di essere iscritto al Corso di Dottorato di ricerca RISCHIO, SVILUPPO AMBIENTALE, TERRITORIALE ED EDILIZIO ciclo XXX, corso attivato ai sensi del "*Regolamento dei Corsi di Dottorato di ricerca del Politecnico di Bari*", emanato con D.R. n.286 del 01.07.2013;
3) di essere pienamente a conoscenza delle disposizioni contenute nel predetto Regolamento in merito alla procedura di deposito, pubblicazione e autoarchiviazione della tesi di dottorato nell'Archivio Istituzionale ad accesso aperto alla letteratura scientifica;
4) di essere consapevole che attraverso l'autoarchiviazione delle tesi nell'Archivio Istituzionale ad accesso aperto alla letteratura scientifica del Politecnico di Bari (IRIS-POLIBA), l'Ateneo archivierà e renderà consultabile in rete (nel rispetto della Policy di Ateneo di cui al D.R. 642 del 13.11.2015) il testo completo della tesi di dottorato, fatta salva la possibilità di sottoscrizione di apposite licenze per le relative condizioni di utilizzo (di cui al sito http://www.creativecommons.it/Licenze), e fatte salve, altresì, le eventuali esigenze di "embargo", legate a strette considerazioni sulla tutelabilità e sfruttamento industriale/commerciale dei contenuti della tesi, da rappresentarsi mediante compilazione e sottoscrizione del modulo in calce (Richiesta di embargo);
5) che la tesi da depositare in IRIS-POLIBA, in formato digitale (PDF/A) sarà del tutto identica a quelle **consegnate**/inviate/da inviarsi ai componenti della commissione per l'esame finale e a qualsiasi altra copia depositata presso gli Uffici del Politecnico di Bari in forma cartacea o digitale, ovvero a quella da discutere in sede di esame finale, a quella da depositare, a cura dell'Ateneo, presso le Biblioteche Nazionali Centrali di Roma e Firenze e presso tutti gli Uffici competenti per legge al momento del deposito stesso, e che di conseguenza va esclusa qualsiasi responsabilità del Politecnico di Bari per quanto riguarda eventuali errori, imprecisioni o omissioni nei contenuti della tesi;
6) che il contenuto e l'organizzazione della tesi è opera originale realizzata dal sottoscritto e non compromette in alcun modo i diritti di terzi, ivi compresi quelli relativi alla sicurezza dei dati personali; che pertanto il Politecnico di Bari ed i suoi funzionari sono in ogni caso esenti da responsabilità di qualsivoglia natura: civile, amministrativa e penale e saranno dal sottoscritto tenuti indenni da qualsiasi richiesta o rivendicazione da parte di terzi;
7) che il contenuto della tesi non infrange in alcun modo il diritto d'Autore né gli obblighi connessi alla salvaguardia di diritti morali od economici di altri autori o di altri aventi diritto, sia per testi, immagini, foto, tabelle, o altre parti di cui la tesi è composta.

Luogo e data 20/12/2017 Firma

Il/La sottoscritto, con l'autoarchiviazione della propria tesi di dottorato nell'Archivio Istituzionale ad accesso aperto del Politecnico di Bari (POLIBA-IRIS), pur mantenendo su di essa tutti i diritti d'autore, morali ed economici, ai sensi della normativa vigente (Legge 633/1941 e ss.mm.ii.),

CONCEDE

- al Politecnico di Bari il permesso di trasferire l'opera su qualsiasi supporto e di convertirla in qualsiasi formato al fine di una corretta conservazione nel tempo. Il Politecnico di Bari garantisce che non verrà effettuata alcuna modifica al contenuto e alla struttura dell'opera.
- al Politecnico di Bari la possibilità di riprodurre l'opera in più di una copia per fini di sicurezza, back-up e conservazione.

Luogo e data 20/12/2017 Firma

Politecnico di Bari

Department of Civil, Environmental, Building Engineering and Chemistry

RISK AND ENVIRONMENTAL, TERRITORIAL AND BUILDING DEVELOPMENT
Ph.D. Program
SSD: ICAR/05–TRANSPORT

Final Dissertation

A novel framework for real-time adaptive signal control using connected vehicles

by
GIANVITO PALMISANO

_____
Firma leggibile e per esteso

Referee:
Prof. Ing. Borja Alonso
Prof. Ing. Luigi Dell'Olio

Supervisor:
Prof. Ing. Mauro Dell'Orco
Dr. Ing. Mario Marinelli

Coordinator of Ph.D Program:
Prof. Ing Michele Mossa
_____ *firma*

Course n°30, 01/11/2014- 31/10/2017

AD UN GRANDE UOMO, MIO PADRE

AD UNA DONNA SPECIALE, MIA MADRE

AI MIEI FRATELLI

E A MATTEO E SIMONE

"Life is like riding a bicycle. To keep your balance,

you must keep moving"

A. Einstein

EXTENDED ABSTRACT (eng)

Intelligent transportation systems (ITS) work by collections of data in real time. Average speed, travel time and delay at intersections are some of the most important measures, often used for monitoring the performance of transportation systems, and useful for system management and planning. In urban transportation planning, intersections are usually considered critical points, acting as bottlenecks and clog points for urban traffic. Thus, detecting the travel time at intersections in different turning directions is an activity useful to improve the urban transport efficiency. Smartphones represent a low-cost technology, with which is possible to obtain information about traffic state. However, smartphone GPS data suffer for low precision, mainly in urban areas.

In this work, we propose a novel framework for real-time adaptive signal control using connected vehicles (CV). This framework is made of two new methods: the first one is for lane identification and flow estimation, in which we aim to determine the traffic flows on lanes near the intersections controlled by traffic lights, starting from GPS data acquired by smartphones; the second one is for optimal real-time traffic signal settings.

In the first method, we present a fuzzy set-based method for identification of vehicles position within road lanes near intersections using GPS data coming from smartphones. We have introduced the fuzzy sets to consider uncertainty embedded in

GPS data when trying to identify the position of vehicles within the lanes. Moreover, we introduced a Genetic Algorithm to calibrate the fuzzy parameters and to obtain a novel supervised clustering technique.
In more details, for each lane identified by the proposed method, we set up a flow estimation method to optimize signal timings. It is based on the evaluation of the length of the queues and the speed. Finally, the proposed method has been validated through the comparison with the fundamental diagram. Signal timings were optimized using the Webster algorithm.
As for the case study, we have studied a signalized intersection in the city of Bari (Italy), considering three main time periods: 8 a.m. – 9 a.m., 12 a.m. - 1 p.m. and 5 p.m-6 p.m. We acquired data related to location, speed, travel times and trajectories of a vehicle using a smartphone application. Smartphone devices have the advantages of mobile sensors: low investment costs, high penetration, and high accuracy achieved by GPS receivers. In addition, GPS-enabled smartphones can provide accurately not only the position but also speed and travel direction.
First results reveal the effectiveness of the proposed method about the lane identification in comparison with the outcomes of two well-known clustering techniques (Fuzzy C-means, K-means).
The curves calculated by the Greenshields method are comparable with the fundamental diagrams. Results regarding the signal optimization show that the improvements obtained by our method are remarkable: in some cases, we have achieved improvements around 50% for the delay times and in the reduction of average length of queues. Moreover, the computational times are suitable for the use in a real-time traffic control.

key words : connected vehicle, GPS data, real time, ITS

EXTENDED ABSTRACT (ita)

I sistemi di trasporto intelligente raccolgono, elaborano, gestiscono e trasmettono dati relativi ai veicoli, allo stato delle infrastrutture e agli utenti integrandoli tra loro in modo “intelligente”. Gli ITS lavorano per raccolta dati in tempo reale. La velocità media, il tempo di viaggio e il ritardo alle intersezioni sono alcune delle misure più importanti, spesso utilizzate per monitorare le prestazioni dei sistemi di trasporto e utili per la gestione e la pianificazione del sistema. Nella pianificazione dei trasporti urbani, le intersezioni sono generalmente considerate punti critici, che agiscono come strozzature e punti di intasamento per il traffico urbano. Quindi, rilevare il tempo di percorrenza alle intersezioni in diverse direzioni di svolta è un'attività utile per migliorare l'efficienza dei trasporti urbani. Gli smartphone rappresentano una tecnologia a basso costo con cui è possibile ottenere informazioni sullo stato del traffico. Tuttavia, i dati GPS registrati tramite smartphone hanno una bassa precisione, soprattutto nelle aree urbane.

In questo lavoro, proponiamo un nuovo modello capace di gestire e controllare i semafori in tempo reale utilizzando veicoli connessi (CV). Questa metodologia è composta da due nuovi metodi, il primo necessario all’identificazione della corsia e il secondo, invece, permette la stima dei flussi.

In particolare, ci proponiamo di determinare i flussi di traffico su ogni corsia vicino alle intersezioni regolate dal semaforo, partendo dai dati GPS acquisiti dagli smartphone.

Nel primo metodo, presentiamo un metodo basato sulle funzioni di appartenenza Fuzzy per l'identificazione del veicolo in prossimità di intersezioni semaforizzate attraverso l’utilizzo di dati GPS provenienti da smartphone. Abbiamo introdotto i set fuzzy per tener conto dell'incertezza intrinseca nei dati GPS quando si cerca di identificare la posizione

del veicolo all'interno delle corsie stradali. Inoltre, abbiamo introdotto un algoritmo genetico per calibrare i parametri fuzzy per ottenere una nuova tecnica di “clustering supervisionata”.
Successivamente, per ogni corsia individuata dal metodo proposto, abbiamo definito un metodo di stima del flusso per successivamente ottimizzare i tempi di ciclo semaforico. Il metodo di stima si basa sulla valutazione della lunghezza delle code e della velocità. Infine, i risultati di densità, flusso e velocita ottenuti sono stati calibrati attraverso il modello di Greenshield. I tempi del segnale sono stati ottimizzati utilizzando l'algoritmo Webster.
Abbiamo considerato un'intersezione segnalata nella città di Bari (Italia) per valutare i risultati del metodo proposto. Abbiamo preso in considerazione tre fasce orarie principali: dalle 8.00 alle 9.00 dalle 12.00 alle 13.00. e dalle 5.00 alle 6.00. Abbiamo acquisito dati di posizione, velocità, tempi di viaggio e traiettorie del veicolo utilizzando un'applicazione per smartphone. I dispositivi Smartphone combinano i vantaggi dei sensori mobili di cui sopra: bassi costi di investimento, elevata penetrazione e alta precisione ottenuti dai ricevitori GPS. Inoltre, gli smartphone abilitati al GPS sono in grado di fornire in modo preciso non solo la posizione, ma anche la velocità e la direzione di marcia.
I primi risultati rivelano l'efficacia della prima metodologia proposta (identificazione della corsia stradale) quando si confrontano i risultati del metodo proposto con due tecniche di clustering ben noti (Fuzzy C-means, K-means). Dai risultati ottenuti si è riscontrato un errore del 3% sull’intersezione a due corsie e del 6% invece sull’intersezione a tre corsie.
La curva stimata utilizzando il metodo di Greenshield segue l’andamento dei diagrammi fondamentali. Abbiamo osservato che i dati analizzati sono sempre sul ramo stabile del diagramma fondamentale, quindi sempre in condizioni di traffico non congestionato.
I risultati relativi all'ottimizzazione dei segnali stradali mostrano come i miglioramenti ottenuti sono notevoli. Abbiamo ottenuto miglioramenti in alcuni casi nell'ordine del 50% per i tempi di ritardo e la riduzione delle code medi.

Infine, il nuovo modello quindi, può essere utilizzato per il controllo dell'intersezione semaforizzata a livello di corsia stradale. Inoltre, i tempi di calcolo ottenuti sono compatibili per l'utilizzo nel controllo del traffico in tempo reale tramite smartphone.

key words : connected vehicle, GPS data, real time, ITS

INDEX

FIGURE INDEX

TABLE INDEX

INTRODUCTION

The analysis urban movement cars issues has assumed an increasingly important role in recent years. This is due to the fact that the urban traffic conditions greatly slowed down and have become congested, creating not only inconveniences to car drivers for the increase in the average travel time, but also make a less secure circulation on the road increasing air and noise pollution.

In this context the Intelligent Transport Systems and info-mobility development become an opportunities to reduce costs and road congestion, with sustainable timing. Specifically, in the era of multimedia convergence, communication, and sensing platforms, GPS-enabled smartphones are becoming an essential contributor to location-based services. These devices combine the advantages of mobile sensors mentioned earlier: low investment costs, high penetration, and high accuracy achieved by GPS receivers. In addition, GPS-enabled smartphones are able to provide accurately not only position but also speed and travel direction. It is worth noting that phones not only can send but also receive information. Therefore, traffic information can be delivered through this channel. Given the market penetration of mobile phones, this new sensing technology can potentially provide an exhaustive spatial and temporal coverage of the transportation network. In the mobile computing era, due to their numerous sensors (e.g., GPS, accelerometers, gyroscopes) smartphones have become instrumental tools capable to support innovative mobile context-aware systems development.

Real-time traffic reports are usually based on statistical methods. These methods have been also a common practice in studies that use cell phones as traffic sensors,

in which the main goal has been to find the link speed or travel time estimation (Bar-Gera, 2007). Note that the aforementioned study uses cell phone antennas to obtain a cell phone position (i.e. vehicle), which is less accurate than GPS positioning. Krause et al. (2008) have investigated the use of machine learning techniques to reconstruct travel times on a graph based on sparse measurements collected from GPS devices embedded in cell phones and automobiles.

An overview of the GPS techniques is given in Skog (2009). For mapping the vehicle position in the road, sophisticated algorithms have been developed, e.g., Zhao (2015) or Fouque et al. (2012). The usual problem in GPS positioning is that the accuracy is not within a lane-width. Therefore, solutions have to be found to get the accuracy to a lane level. Liu X. et al. (2017) present a recognition system for dangerous vehicle steering based on the low-cost sensors found in a smartphone: i.e., the gyroscope and the accelerometer. To identify vehicle steering maneuvers, we focus on the vehicle's angular velocity, which is characterized by gyroscope data from a smartphone mounted in the vehicle.

Sekimoto et al. (2012) proposed a simple method for using the separation distance (offset) between a smartphone GPS and the center line on a digital road map to determine the lane position of a car.

In this work, we propose a novel framework for real-time adaptive signal control using connected vehicles. This framework is composed by two new methods for lane identification and flow estimation for optimal real-time traffic signal settings. In particular, we aim to determine the traffic flows on each lane near the intersections regulated by the traffic light, starting from GPS data acquired by smartphones. We have considered a signalized intersection in the city of Bari (Italy) to evaluate the outcomes of the proposed method. We have considered three main time slots: 8 a.m. – 9 a.m., 12 a.m. - 1 p.m. and 5 p.m-6 p.m.

The first proposed method (road lane identification) is based on the Fuzzy set theory (Zadeh,1965) as it is useful in dealing with uncertainty embedded in the observed data. We have used fuzzy sets to represent the membership degree of a vehicle position to a lane. Moreover, a road reference system has been defined to process GPS track data

obtained by a smartphone GPS. To find the optimal distributions, we have defined a supervised clustering technique to efficiently evaluate the lane positioning of a vehicle through a Genetic Algorithm.

Going in further details, for each lane identified by proposed method, we proposed a flow estimation method to subsequently optimize signal timings. It is based on the evaluation of the length of the queues and the speed. Finally, the Greenshield's model has been calibrated for the validation of the proposed method through the fundamental diagram. Finally, signal timings were optimized using the Webster algorithm.

This thesis is structured as follows: Chapter 1 presents ITS technologies. In Chapter 2 presents the basic principles of fundamental diagram and traffic lights optimization. In Chapter 3 a summary of works in Macro Fundamental Diagram(MFD) and estimation traffic flow. In Chapter 4 describes a proposed method and in Chapter 5 presents the case of study and shows results.

CHAPTER 1

INTELLIGENT TRANSPORTATION SYSTEMS

1.1 Intelligent Transportation Systems

Information technology (IT) has transformed many fields, including industries, education, health care, government, and is now in the initial stages of transforming transportation systems. While many think that improving a country's transportation system solely means building new roads or repairing aging infrastructures, the future of transportation lies not only in concrete and steel, but also increasingly in using IT.

IT enables elements within the transportation system vehicles, roads, traffic lights, message signs, etc. to become intelligent by embedding them with microchips and sensors and empowering them to communicate with each other through wireless technologies. In the leading nations in the world, IT brings significant improvement in transportation system performance, including reduced congestion and increased safety and traveler convenience.

Unfortunately, the United States lags the global leaders, particularly Japan, Singapore, and South Korea in ITS deployment. This has been the result of two key factors: a continued lack of adequate funding for ITS and the lack of the right organizational system to drive ITS in the United States, particularly the lack of a federally led approach,

as opposed to the “every state on its own approach” that has prevailed to date. Transportation systems are networks, and much of the value of a network is contained in its information. For example, whether a traffic signal “knows” there is traffic waiting to pass through an intersection; whether a vehicle is drifting out of its lane; whether two vehicles are likely to collide at an intersection; whether a roadway is congested with traffic; what the actual cost of operating a roadway is; etc.

Intelligent Transportation Systems (ITS) include a wide and growing suite of technologies and applications.

ITS applications can be grouped within five summary categories:

1) Advanced Traveler Information Systems provide drivers with real-time information, such as transit routes and schedules; navigation directions; information about delays due to congestion, accidents, weather conditions, or road repair work.
2) Advanced Transportation Management Systems include traffic control devices, such as traffic signals, ramp meters, variable message signs, and traffic operations centers.
3) ITS-Enabled Transportation Pricing Systems include systems such as electronic toll collection (ETC), congestion pricing, fee based express (HOT) lanes, and vehicle miles traveled (VMT) usage based fee systems.
4) Advanced Public Transportation Systems allow trains and buses to report their position, so passengers can be informed of their real-time status (arrival and departure information).
5) Fully integrated Intelligent Transportation Systems, such as vehicle-to-infrastructure (VII) and vehicle-to-vehicle (V2V) integration, enable communication among assets in the transportation system, for example, from vehicles to roadside sensors, traffic lights, and other vehicles.

ITS deliver five key classes of benefits by:

- increasing safety;
- improving operational performance, particularly by reducing congestion;
- enhancing mobility and convenience;
- delivering environmental benefits;

- boosting productivity, expanding economic and employment growth.

Given the wide range of intelligent transportation systems, it is useful to organize discussion of ITS applications through a taxonomy that arranges them by their primary functional intent (with the acknowledgment that many ITS applications can serve multiple functions or purposes). While this list is not inclusive of all possible ITS applications, it includes the most prominent ones (see Table 1.1).

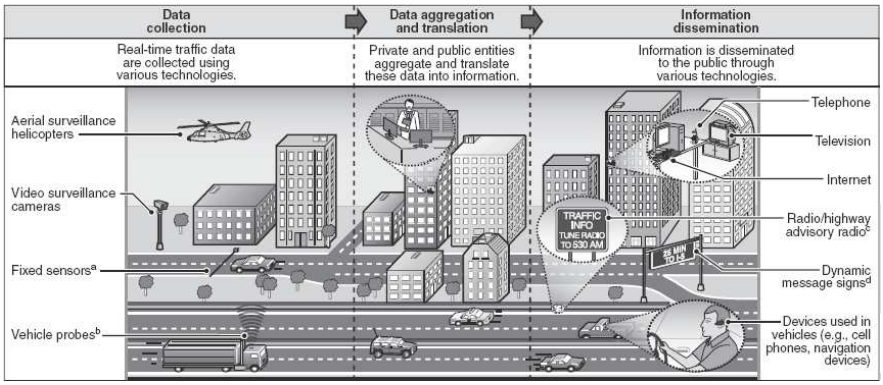

Figure 1.1 *Example of Technologies Associated with Real-Time Traffic Information Systems*

Table 1.1: Classifying Contactless Mobile Payments Applications

ITS Category	**Specific ITS Applications**
Advanced Traveller Information Systems (ATIS)	Real-time Traffic Information Provision
	Route Guidance/Navigation Systems
	Parking Information
	Roadside Weather Information Systems
Advanced Transportation Management Systems (ATMS)	Traffic Operations Centres (TOCs)
	Adaptive Traffic Signal Control
	Dynamic Message Signs (or "Variable" Message Signs)
	Ramp Metering
ITS-Enabled Transportation Pricing Systems	Electronic Toll Collection (ETC)
	Congestion Pricing/Electronic Road Pricing (ERP)
	Fee-Based Express (HOT) Lanes
	Vehicle-Miles Travelled (VMT) Usage Fees
	Variable Parking Fees
Advanced Public Transportation Systems (APTS)	Real-time Status Information for Public Transit System (e.g. Bus, Subway, Rail)
	Automatic Vehicle Location (AVL)
	Electronic Fare Payment (for example, Smart Cards)
Vehicle-to-Infrastructure Integration (VII) and Vehicle-to-Vehicle Integration (V2V)	Cooperative Intersection Collision Avoidance System (CICAS)
	Intelligent Speed Adaptation (ISA)

1.1.1 Advanced Traveller Information Systems

Perhaps the most recognized ITS application, Advanced Traveller Information Systems (ATIS), provides drivers with real-time travel and traffic information, such as transit routes and schedules; navigation directions; and information about delays due to congestion, accidents, weather conditions, or road repair work. The most effective traveler information systems can inform drivers in real-time of their precise location, inform them of current traffic or road conditions on their and surrounding roadways, and empower them with optimal route selection and navigation instructions, ideally making this information available on multiple platforms, both in-vehicle and out.

As Figure 1.1 illustrates, there are three key facets to the provision of real-time traffic information: collection, processing, and dissemination, with each step entailing a distinct set of technology devices, platforms, and actors, both public and private. This report will examine several countries' strategies about the provision of real-time traffic information.

This category also includes in car navigation systems and telematics-based services, such as GM's OnStar, which offers a range of safety, route navigation, crash notification, and concierge services, including location-based services, mobile calling, or in-vehicle entertainment options such as Internet access and music or movie downloads. Vehicles in the United States increasingly have telematics devices, whether a factory-installed GPS system or one purchased after-market, such as those available from Garmin or TomTom

1.1.2 Advanced Transportation Management Systems

Advanced Transportation Management Systems (ATMS) include ITS applications that focus on traffic control devices, such as traffic signals, ramp metering, and the dynamic (or "variable") message signs on highways that give drivers real-time messaging about

traffic or highway status. Traffic Operations Centres (TOCs), centralized traffic management centres run by cities and states worldwide, rely on information technologies to connect sensors and roadside equipment, vehicle probes, cameras, message signs, and other devices together to create an integrated view of traffic flow and to detect accidents, dangerous weather events, or other roadway hazards.

Adaptive traffic signal control refers to dynamically managed, intelligent traffic signal timing. Many countries' traffic lights, including the clear majority of the close to 300,000 signalized intersections in the United States, use static, outdated timing plans based on data collected years or decades before. In fact, an estimated 5 to 10 percent of the congestion on major American roadways amounting to 295 million vehicle hours is attributed to bad signal timing. Giving traffic signals the ability to detect the presence of waiting vehicles, or giving vehicles the ability to communicate that information to a traffic signal, through Dedicated-Short Range Communications(DSRC)-enabled communication (assuming both the vehicle and traffic signal are DSRC-equipped), could enable improved timing of traffic signals, thereby enhancing traffic flow and reducing congestion.

Another advanced transportation management system that can yield significant traffic management benefits is ramp metering. Ramp meters are traffic signals on freeway entrance ramps that break up clusters of vehicles entering the freeway, which reduces the disruptions to freeway flow that vehicle clusters cause and makes merging safer. About 20 U.S. metropolitan areas use ramp metering in some form.

1.1.3 ITS-Enabled Transportation Pricing Systems

ITS have a significant role to play in funding countries' transportation systems. The most common application is electronic toll collection (ETC), also commonly known internationally as "road user charging," through which drivers can pay tolls automatically via a DSRC-enabled onboard device or tag placed on the windshield. The most sophisticated countries, including Australia and Japan, have implemented a single national ETC standard, obviating the need, as in the United States, to carry multiple toll

collection tags on cross-country trips because various highway operators' ETC systems lack interoperability. This particularly has been a problem for the European Union, although the European Committee for Standardization is working to resolve this challenge (and has made considerable progress).

An increasing number of cities throughout the world have implemented congestion pricing schemes, charging for entry into urban centers, usually at certain peak hours, to not only reduce congestion but also to generate needed resources to fund investments in public transportation and to reduce the environmental impact of vehicles. Singapore, Stockholm, London, Oslo, and Jakarta are just some of the cities that have put congestion-pricing systems in place to reduce traffic congestion, smog, and greenhouse gases. By charging more at congested times, traffic flows can be evened out or reduced. As half the world's population now lives in urban areas, some economists believe that urban congestion and emissions will be virtually impossible to reduce without some form of congestion pricing. For example, in Europe, urban areas account for 40 percent of passenger transport but 53 percent of all transport-related emissions. Stockholm's congestion pricing scheme yielded immediate results, reducing traffic by 20 percent in the first month alone as many commuters opted for public transportation. Statistics gathered since the full implementation of Stockholm's congestion pricing scheme in 2007 show that the initiative has reduced both traffic congestion and carbon emissions by 15 percent on a sustained basis. Stockholm's congestion pricing scheme has also generated $120 million in net revenue. If congestion pricing were used in just three to five major American cities, it could save as much fuel as is saved with the fuel economy standards for light vehicles in the United States (Duvall,2008).

High-Occupancy Toll (HOT) lanes reserved for buses and other high occupancy vehicles but that can be made available to single occupant vehicles upon payment of a toll are another ITS-enabled mechanism to combat traffic congestion. The number of vehicles using the reserved lanes can be controlled through variable pricing (via electronic toll collection) to keep free-flowing traffic at all times, even during rush hours, which increases overall traffic flow on a given segment of road. For example, Orange County, California, found that, while HOT lanes represent only one-third of its highway lane

miles, they carry over half of the traffic during rush hours (Ybarra and Staley,2008). By the end of 2009, approximately 25 U.S. cities either had deployed or were beginning to plan or implement HOT lane proposals.

Other ITS-enabled alternative countries are evaluating for financing their transportation systems is vehicle miles travelled (VMT) fee system that charges motorists for each mile driven. VMT fee systems represent an alternative to the current fuel taxes and other fees that many countries and states use to finance their transportation systems. Holland's "Kilometerprijs" (price per kilometer) program is slated to be the world first nationwide VMT system implemented for both passenger vehicles and heavy vehicles. The Kilometerprijs program will replace fixed vehicle (ownership) taxes to charge Dutch citizens by their annual distances driven, differentiated by time, place, and environmental characteristics. The policy, which will begin with distance-based charging for freight transport in 2012, followed by passenger vehicles by 2016, will use advanced satellite technology coupled with an on-board vehicle telematics system to charge travelers based on mileage driven. Germany is already charging for freight transport on this basis. In the United States, the National Surface Transportation Infrastructure Financing Commission recommended in February 2009 moving to a VMT-type "user charge" fee system within a decade, and several states, including Oregon, Washington, and Hawaii, are considering doing so as well.

1.1.4 Advanced Public Transportation Systems

Advanced Public Transportation Systems (APTS) include applications such as automatic vehicle location (AVL), which enable transit vehicles, whether bus or rail, to report their current location, making it possible for traffic operations managers to construct a real-time view of the status of all assets in the public transportation system. APTS help to make public transport a more attractive choice for commuters by giving them enhanced visibility into the arrival and departure status (and overall timeliness) of buses and trains. This category also includes electronic fare payment systems for public transportation systems, such as Suica in Japan or T-Money in South Korea, which

enable transit users to pay fares contactless from their smart cards or mobile phones using near field communications technology (Ezell 2009). Advanced public transportation systems, particularly providing “next bus” or “next train information, are increasingly common worldwide, from Washington, DC, to Paris, Tokyo, Seoul, and elsewhere.

1.1.5 Vehicle-to-infrastructure Integration (VII) and Vehicle-to-vehicle (V2V) Integration

Vehicle-to-infrastructure integration is the archetype for a comprehensively integrated intelligent transportation system. In the United States, the aim of the VII Initiative as of January 2009 rebranded as IntelliDriveSM has been to deploy and enable a communications infrastructure that supports vehicle-to-infrastructure, as well as vehicle-to-vehicle, communications for a variety of vehicle safety applications and transportation operations. IntelliDrive envisions that DSRC-enabled tags or sensors, if widely deployed in vehicles, highways, and in roadside or intersection equipment, would enable the core elements of the transportation system to communicate intelligently with one another, delivering a wide range of benefits. For example, IntelliDrive could enable cooperative intersection collision avoidance systems (CICAS).In these systems, two (or more) DSRC-equipped vehicles at an intersection would be in continuous communication either with each other or with roadside devices. The system could recognize when a collision between the vehicles appeared imminent (based on the vehicles’ speeds and trajectories) and would warn the drivers of an impending collision or even communicate directly with the vehicles to brake them (Atkinson and Castro 2008).

IntelliDrive, by combining both vehicle-to-vehicle and vehicle-to-infrastructure integration into a consolidated platform, would enable a number of additional ITS applications, including adaptive signal timing, dynamic re-routing of traffic through variable message signs, lane departure warnings, curve speed warnings, and automatic detection of roadway hazards, such as potholes, or weather-related conditions, such as icing.

Another application enabled by vehicle-to-infrastructure integration is intelligent speed adaptation (ISA), which aims to assist drivers in keeping within the speed limit by correlating information about the vehicle's position (for example, through GPS) with a digital speed limit map, thus enabling the vehicle to recognize if it is exceeding the posted speed limit. The system could either warn the driver to slow down or be designed to automatically slow the vehicle through automatic intervention. France is now testing deployment of an ISA system that would automatically slow fast-moving vehicles in extreme weather conditions, such as blizzards or icing. The province of Victoria, Australia, is testing a system in which trains could remotely and autonomously brake vehicles to cross their path at railway intersections (Warin 2008).

1.2 Traffic Sensor Types

Many sensors have been developed in the past 50 years designed to collect diverse types of traffic data. In general, traffic data includes flows (number of vehicles per time unit), density (number of vehicles per distance unit), occupancy (percentage of time a vehicle is over of specific location, which is directly related to density), velocity (distance per unit time), and travel time (time to travel between two locations). One more data type possible are vehicle trajectories, which are always represented by a sequence of discrete time/location pairs for each vehicle. From vehicle's trajectory data with a location-reporting frequency of several seconds or less, travel times and short distance velocities can be directly computed. When the location-reporting frequency is more than 10 seconds, directly measuring travel times and velocities become non-trivial.

1.2.1 Loop Detectors

Inductive loop detectors are built into the roadway so that they can detect each vehicle that passes over them. They work by detecting the metal of a vehicle as it passes over the detector. Properly calibrated, a loop detector can provide high-accuracy flow and occupancy data (Chen et al, 2001), the latter of which can be used to infer density (Ji

et al.,2001). When two loop detectors are placed close together, velocity can be measured by looking at consecutive crossing times. While the quality of the measurements from loop detectors is often good, filtering is still needed from producing quality input data to highway estimation models (Claudel et al., 2009). Loop detectors are not capable of directly measuring travel times. Loop detectors are found on most major highways throughout the United States and Europe. Many of these locations have loop detectors connected to an internet connection that can be used to send the data to a central server in real-time (that can subsequently be used in traffic information systems). Many locations throughout the United States and Europe also have loop detectors placed on arterial roads. However, for arterial roads, it is very rare for the loop detector to be connected to the internet for easy transmission of the data to a central server. For this reason, arterial traffic information systems cannot rely on loop detector data as there is not enough of it to estimate conditions overall arterial network.

1.2.2 Radar

Radar detectors can be placed on poles along the side of the road enabling them to collect flow, occupancy, and velocity data. In general, radar detectors give lower accuracy data than loop detectors (Mimbela et al., 2007). As of this writing, dedicated radar detectors that are connected to the internet and giving data in real-time are still rare in the United States and Europe. Where these are available, they are placed exclusively on highways. Radars are not well suited to mass data collection on arterials since accuracy decreases in arterial environments. For this reason and the fact that almost no radar data exists on arterials, they are not considered practical inputs into an arterial traffic information system.

1.2.3 Video

Video recording can be used to collect traffic data in two ways. The first way is to use high-resolution cameras placed high above the roadway to track all vehicles within the

view of the camera. The second way is to use the video cameras to record license plate numbers at specified locations, which is equivalent to using video as a license plate reader. Using high-resolution cameras to track vehicle trajectories does not give data in real-time due to a large amount of post-processing work that needs to be done on the images to turn them into actual vehicle trajectory data. When properly processed, video can provide very high-resolution vehicle trajectories (vehicle positions every tenth of a second). However, this technology is expensive to deploy and can only cover a small portion of the roadway (generally less than a mile). The NGSIM project is an example of the use of this kind of technology, which to date has mostly been used to provide researchers with high-accuracy vehicle trajectories over a small spatiotemporal domain (less than a mile for less than an hour). This kind of data is valuable to arterial traffic estimation research, but given that the data does not come in real-time, it cannot be used in real-time traffic information systems.

1.2.4 Sparsely-sampled GPS

Sparsely-sampled probe GPS data refers to the case where probe vehicles send their current GPS location at a fixed frequency, which is not frequent enough to directly measure velocities or link travel times (i.e. sampling frequency is more than about 10 seconds). There are several challenges associated with this type of data. First, GPS measurements must be mapped to the road network representation used by the traffic information system, which means that the correct position on the road as well as the path in between successive measurements must be decided. This process is known as map matching and path inference. Second, probe vehicles can often travel multiple links between measurements when the sampling frequency is low, which means that one must infer what the travel times on each link of the path here. Sparsely-sampled probe GPS data is now the most ubiquitous data source on the arterial network. An example of this type of data comes from the Cabspotting project, which gives the positions of 500 taxis in the Bay Area approximately once per minute. Figure 1.2 shows one full day of raw data, which proves that even just a single data source such as taxis

can provide broad coverage of a city. This data has some privacy issues as it is possible to track the general path of the vehicle. However, most of this data today comes from fleets of various sorts (such as UPS, FedEx, taxis, etc.). Most of this data is privately held among several companies, but between all sources, there are millions of records per day in many major urban markets. One publicly available source of this kind of data is the Cabspotting project. This project provides one-minute samples of the positions of over 500 taxis in San Francisco, CA. This results in upwards of 500,000 measurements per day. Due to the ubiquity of this data source, it is paramount that it be used in an arterial traffic information system. Indeed, it is the only source that is likely to be available across the arterial network in the next decade.

1.2.5 High-frequency GPS

High-frequency probe GPS data refers to the case where probe vehicles send their current GPS location every few seconds (no more than about every 10 seconds). This kind of data is generally the most accurate kind of vehicle trajectory data possible, especially when sampling every second with a high-quality GPS chip. From this data, one can directly infer velocities and short distance travel times. The issue of map matching is still present as there can be ambiguity around intersections, but the path is usually easy to decide when examining the entire trace. Figure 1.3 depicts a sample of high-frequency data collected as part of the Mobile Millennium project. This figure illustrates the level of detail that can be extracted from high-frequency data but also shows the relatively low percentage of vehicles that were being tracked as there are occasional gaps of five minutes or more between trajectories. Sampling a vehicle's position every few seconds is clearly very privacy invasive and it also comes with large communication costs to send the high volume of data. For these reasons, it is not common to receive this data with any kind of regularity. This data is often collected for specific experimental studies but is not generally available for real-time traffic information systems.

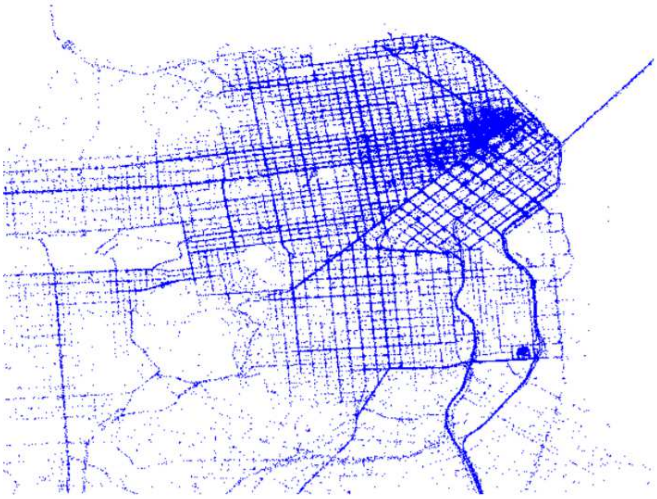

Figure 1.2 One day of sparsely-sampled GPS data from San Francisco taxi drivers as provided by the Cabspotting project

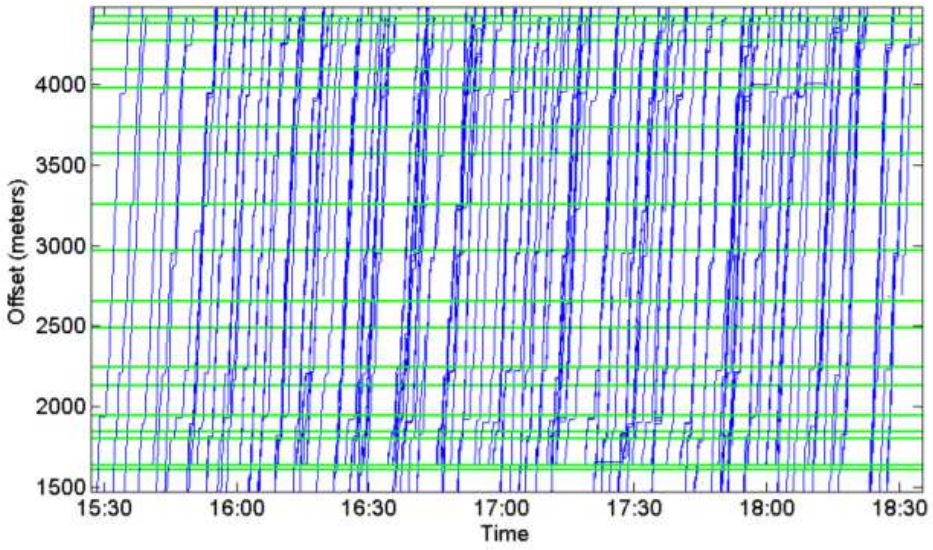

Figure 1 3 Vehicle trajectories from the Mobile Millennium evaluation experiment on San Pablo Avenue in Berkeley, Albany and El Cerrito, California. The high-frequency GPS data in this figure is represented as the distance (meters) from an arbitrary start point upstream of the experiment location. The horizontal lines represent the locations of the traffic signals along the route.

1.2.6 Probe Technology

Probe vehicle technology is a typical application of Intelligent Transportation Systems (ITS), and it provides an innovative way to collect traffic data. It commonly involved a real-time traffic monitoring system including probe vehicles equipped with on-board units such as GPS and wireless communication devices. Some examples of using probe vehicle systems, including Automatic Vehicle Identification (AVI), Automatic Vehicle Location (AVL).

AVI system involves communication between probe vehicle with electronic tags and roadside transceivers. The vehicle is equipped with an electronic transponder and a unique ID, and the antenna transceiver stations are set up in every two to five kilometers. When a vehicle enters the roadside antenna's detection range, the radio signal will contain the information about timestamp and IDs for transponder and antenna, and this information will be sent to the management center by roadside units.

The AVL system has mostly been used by transit agencies for public transit planning. The position and status of the transit fleet vehicles are checked using technologies such as ground-based radio navigation, and signpost-based technologies. For ground-based radio navigation, traffic data is collected by communication between probe vehicles and radio towers. For signpost-based technologies, the communication is between the probes vehicles with transmitters mounted on existing signpost structure.

These probe vehicle systems usually use high-cost, onboard equipment on certain vehicles for traffic data capturing and the penetration rate is usually low. With emerging wireless communication applied with probe system technologies, there is an observing tend to incorporate mobile sensors to obtain real-time traffic information through estimating the device location. Different technologies such as short-range tracking (infrared, radio frequency, Wi-Fi, etc.), GPS, and cell phone network positioning system can be used. The accuracies of detect device locations using these technologies vary, but in general, these new mobile sensors can acquire massive traffic data that covers the wide spatial area and are economically feasible. Short-range traffic

detection involves propagation of a physical wave at fixed time interval. The sensors detect the moving device, pick up the wave emitted from the transmitter, and relay it to the detection software. The device location can be found by inferring antenna coordinates, measuring signal strengths of access points.

1.2.7 Cellular Probe Technology

Cellular networks have become an extensive wireless communication infrastructure with global coverage. Cellular service areas are divided into hexagonally shaped districts/cells, and each of the cells has a cellular tower associated with it. With cell phone signals, a cell phone can be found using triangulation of the cell phone towers near the cell phone location. As a mobile client moves through the network, the mobile device is distributed to the cellular tower with which it is receiving the greatest field strength.

Handoff based location solution is often used in the Global System for Mobiles (GSM) network. The handover data can be regarded as records of mobile probes' trajectories on the road network. When a mobile phone travels from one cell into another, a change of cell-ID indicating handoff is been performed. Theoretically, a handoff is considered to be located on the border of two adjacent cells in the GSM network. When the GSM network is overlapped with the road network, handoff location can be approximated to a point on the matched road link.

Studies have shown that cellular probe technology could be applied to a coordinate-based approach and a handover-based approach to traffic monitoring. The coordinate-based approach requires the coordinates of the cell phone, which is similar to GPS probe technology. Location accuracy is the key issue for this approach. Some researchers tried to exploit network-based solutions using handover approach, and their evaluation results revealed that they could produce promising traffic information (Arulampalam et al.,2002).

The cellular probe technology-based traffic data collection method has several distinct advantages, including large sample size, large spatial coverage, and high penetration rates, over other conventional methods. As of 2007, the global cellular phone penetration rate was over 50%, ranging from 30-40% in developing countries (with an

annual growth rate greater than 30%) to 90-100% in developed countries (Ban et al., 2007). However, the main drawback of cellular probe technology is that its location accuracy is comparatively lower than other technologies, such as GPS. Its location accuracy depends greatly on the density of the cellular towers. A study by Mohr et al. used three different cellular operators in the U.K. and found that the horizontal error varies greatly across urban-rural gradients. The median error was about 246m in a dense urban area, and 626m in a rural area (Ban et al., 2009).

The application of the cellular positioning technique has been investigated in several studies. Lots effort used cell tower signal triangulation to estimate travel time and speed information. Sanwal and Walrand studied the use of probe vehicles to collect traffic data for estimation and prediction of traffic behavior, and key issues involved in the design of such system was discussed (Ban et al., 2009). Bar-Gera examined the performance of a system based on using information from cellular phone service providers to measure traffic speeds and travel times. He compared the cellular measurements with that of dual magnetic loop detectors and found that there is a good match between the two measurement methods and that the cellular phone-based system can be useful for various practical applications (Ban et al., 200). Yim and Cayford conducted an evaluation of the feasibility of using cell phones as traffic probes for the Bay Area Network. The study showed that accurate travel time estimates can be obtained, and assuming a 5% penetration rate, freeway link travel time estimates can achieve 95% accuracy (Bartin et al.,2007).

1.2.8 GPS-Probe Technology

GPS is a satellite-based radio navigation system developed by the United States Department of Defense (Bellman et al., 1962). GPS was initially used as a military system and the operational best accuracies were intentionally degraded by a selective availability (SA) method, which dithered the satellite clocks and caused a range error with a standard deviation of 24 meters (m) (Bickel et al.,2007). Since the SA method was removed in May 2000, the single point accuracy of GPS has dramatically improved

allowing GPS use in more applications. All users with GPS receivers can reach accuracy levels of approximately 18m horizontal, 28 m vertical and 100 nanoseconds (Brand, 1997). GPS consists of three segments: the space segment, the control segment, and the user segment. The Figure 1.4 shows a typical configuration of GPS based probe system.

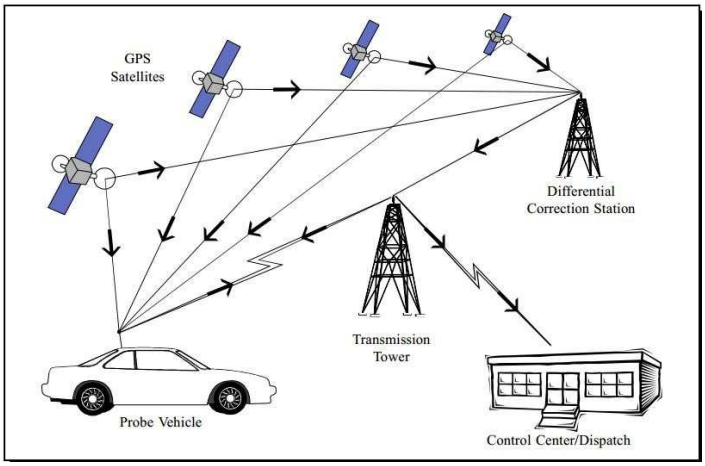

Figure 1.4 Configuration of GPS based probe system

The space segment includes 24 satellites that broadcast navigation signals to receivers through carrier waves. The control segment checks the location and status of the satellites that are in the space segment. The end users of the GPS receivers are the user segment. The receivers calculate the time the radio signals travel from satellites to the receiver and estimate their locations on earth by calculating travel times of signals between the satellites and GPS receivers.

GPS position accuracy varies and changes in different circumstances and is greatly affected by errors, including tropospheric delays, ionospheric delays, satellite clock and ephemeris data, orbital and atmospheric errors, and multipath.

The ionosphere is the layer of the atmosphere ranging in altitude from 50 to 500 km. It consists largely of ionized particles that can exert a perturbing effect on GPS signals. The troposphere is the lower part of the earth's atmosphere that encompasses our

weather. Mathematical models of the atmosphere have been researching to consider the charged particles in the ionosphere and the varying gaseous content of the troposphere.

As GPS became widely used to collect vehicle probe data, the accuracy of the data has been reviewed in different applications. Meaker and Horner proposed an Automatic Position Reporting System (APRS) that uses GPS probe vehicles to collect speed, heading, and position data. The authors compared the speed data retrieved from the probe system and traffic loop sensors and showed that the speeds of the probes and the loop sensors were largely in concordance; however, the detailed statistical analysis was not provided (Charniak,1993). Schussed and Axhausen described a post-processing procedure to process basic raw GPS data. The authors used the proposed procedure for trip and activity detection, and mode detection. The results were compared with the Swiss Micro-census on Travel Behavior 2005, which confirmed that the trip and activity detection works properly, the distance distributions of the individual modes derived from the GPS data were like the census data, and GPS has the advantage with respect to temporal and spatial accuracy.

1.2.9 GPS-Enabled Smartphone Probe

In the era of multimedia convergence, a new data collection approach is based on GPS-enabled smartphones. From 2000, cell phone providers in the United State of America and Canada have started embedding assisted GPS (AGPS) chips in their mobile devices to enhance the location-based services. The AGPS enables the service providers to decide the phone locations within 15 meters (Chen et al.,2003). As there is an increasing number of smartphone users, and more advanced GPS chip feature is deployed, vehicle location estimation based on wirelessly transmitted sparse data via smartphones is a recent area of interest. More correct mobile probe data have been integrated with point detection data to estimate freeway travel times (Chu et al.,2004; Claudel et al., 2010). Aguilar et.al conducted a study on the position accuracy of multimodal data from GPS-enabled cellphones to fill the gap of little quantitative information

about the reliability of GPS data obtained from GPS-enabled cellphones in most real-world application settings. The study result proved the result of location fix attempts over different transportation modes in an urban environment and concluded that location-based transportation applications are feasible using current GPS-enabled cell phone technology. The quantitative data presented in the paper focuses on the percentage of GPS fixes obtained by each mode and the analysis results indicated little significant differences in the number of valid GPS fixes obtained from users (Claudel et al.,2009). A field experiment was conducted by Yim and Cayford in 2001(Coifman et al.,2002) to compare the performance of cellphones and GPS devices for traffic monitoring. The study concluded that the GPS positioning technique is more accurate than cellular tower positioning. If GPS-equipped cellphones are widely used, then they will become an attractive and realistic alternative for traffic monitoring.

1.2.10 Effect of Equipped Vehicle Penetration Rate

As methods for collecting connected vehicle data are defined and implemented, researchers have proposed mobility applications that use wireless communications to improve traffic flow and reduce congestion. Several new algorithms have been developed that, rather than estimate vehicle trajectories from loop detectors or historical data, use the locations and speeds of individual vehicles. A ramp-metering scheme that is based on detecting platoons of vehicles in the mainline rather than aggregated density measurements is an example of an application that requires the locations of individual vehicles. Many of these applications function most effectively when all, or most vehicles are equipped with sensing technology. Simply put, these applications are not designed for the detector or historical data only, but instead need knowledge of individual vehicle locations. Some proposed applications include adaptive traffic signal control, ramp metering, and dynamic gap-out, with others in development. The deployment of mobile sensors among roadway users will not be instantaneous. Band-width shortages and battery life restrict the use of smart phones, and the John A. Volpe National Trans-

portation Systems Center estimated that only 50% of vehicles will have connected vehicle communications capabilities nine years after the program's initiation. In any scenario, there will likely be a transition period where only a portion of vehicles is equipped. The developers of mobile applications have been careful to study the e act of low connected vehicle penetration rates on the application's performance, testing their applications across a wide range of penetration rates. Throughout this dissertation, vehicles that can communicate wirelessly are referred to as equipped vehicles, and those that cannot communicate are referred to as unequipped vehicles.

One can assume that with a reasonable approximation of the locations of unequipped vehicles, the performance of mobility applications that need individual vehicle locations will be signing recently improved. Fortunately, the behavior of equipped vehicles is often in reaction to other nearby unequipped vehicles. With high-resolution data of equipped vehicle positions, speeds, and accelerations, an estimate of unequipped vehicle locations can be made. An attempt to estimate individual unequipped vehicle locations based solely on equipped vehicle behavior has never been tried on freeways, and only on arterials when making several restrictive assumptions.

CHAPTER 2

FUNDAMENTAL PARAMETERS OF TRAFFIC FLOW AND TRAFFIC LIGHT OPTIMIZATION

Traffic engineering pertains to the analysis of the behavior of traffic; its goal is designing the facilities for a smooth, safe, and economical operation of traffic. Traffic flow, like the flow of water, has several parameters associated with it. The traffic stream parameters offer information regarding the nature of traffic flow, which helps the analyst in detecting any variation in flow characteristics. Understanding traffic behavior requires a thorough knowledge of traffic stream parameters and their mutual relationships.

2.1 Traffic stream parameters

The traffic stream includes a combination of driver and vehicle behavior. The driver or human behavior being non-uniform, traffic stream is also non-uniform in nature. It is influenced not only by the individual characteristics of both vehicle and human but also by the way, a group of such units interacts with each other. Thus, a flow of traffic through a street of defined characteristics will vary by both location and time corresponding to the changes in the human behavior.

Thus, the traffic stream itself has some parameters on which the characteristics can be predicted. The parameters can be mainly classified as measurements of quantity, which includes density and flow of traffic, and measurements of quality, which includes speed. The traffic stream parameters can be macroscopic, which characterizes the

traffic as a whole, or microscopic, which studies the behavior of the individual vehicle in the stream with respect to each other.
As far as the macroscopic characteristics are concerned, the parameters can be grouped as a measurement of quantity or quality as described above, i.e. flow, density, and speed. While the microscopic characteristics include the measures of separation, i.e. the headway or separation between vehicles, which can be either time or space headway. Thus, the fundamental stream characteristics are speed, flow, and density.

List of symbols

q *[veh/s]*	flow rate, intensity, volume
k *[veh/m]*	traffic density
u *[m/s]*	instantaneous speed
q_c *[veh/s]*	critical flow / capacity
k_c *[veh/m]*	critical density
k_j *[veh/m]*	jam density
u_c *[m/s]*	speed at critical density

In traffic flow theory, the relations between the macroscopic characteristics of a flow are called 'fundamental diagram(s)'. Three are in use, namely:

- intensity - density $q = q(k)$
- speed - density $u = u(k)$
- speed - intensity $u = u(q)$

It is important to understand that these three relations represent the same information: from one relation one can deduce the other two; See Fig. 2.1.

2.1.1 Special points of the fundamental diagram

Special points of the diagram are:

- *Free speed* u_0: this is the mean speed if $q = 0$ and $k = 0$; it equals the slope of the function *q(k)* in the origin;
- *Capacity qc*: this is the maximal intensity, sometimes called critical intensity;
- *Capacity density or critical density* k_c: i.e. the density if $q = q_c$;
- *Capacity speed* u_c*:* i.e. the mean speed if $q = q_c$;
- *Jam density* k_j*:* i.e. the density if $u = 0$ and $q = 0$.

The part of q(k) with a constant speed is called the 'stable region' of the diagram. As soon as speed decreases with increasing density, one enters the 'unstable region'.
The region in which densities are greater than the capacity density is called 'congestion region' or 'congestion branch'. The entire region with $k < kc$ is sometimes called 'free operation' and the congestion region 'forced operation'.

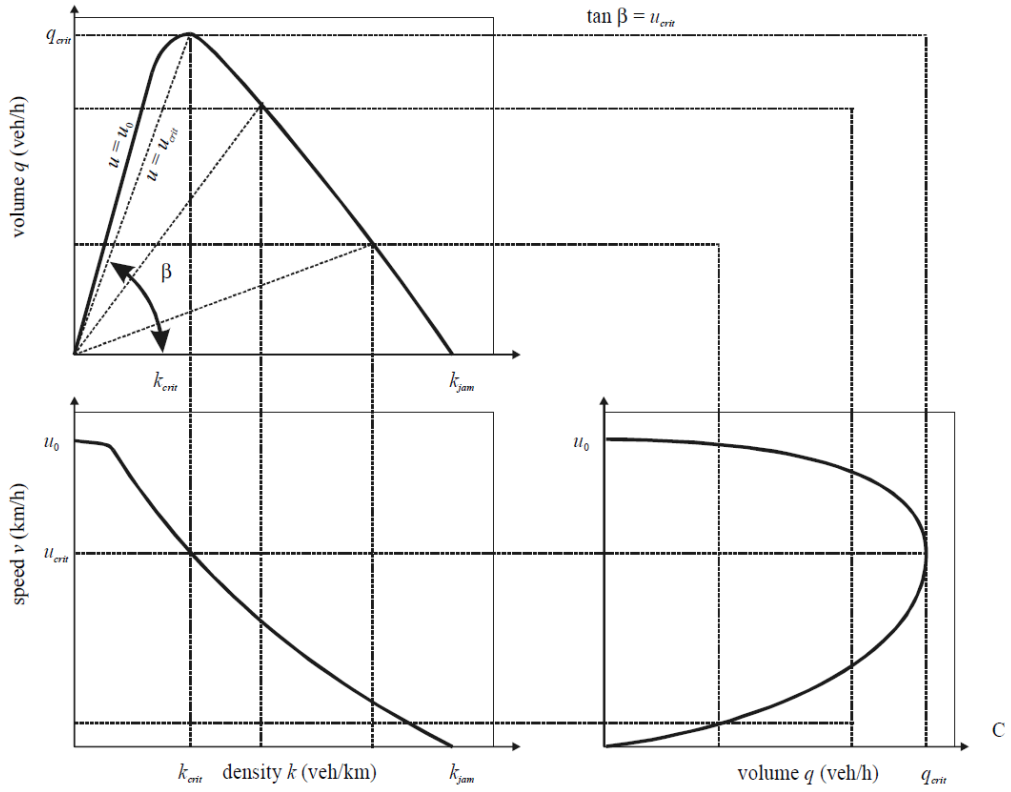

Figure. 2.1 Fundamental diagram

2.2 Greenshield's macroscopic stream models

Macroscopic stream models represent how the behavior of one parameter of traffic flow changes with respect to another. Most important among them is the relation between speed and density. The first and most simple relation between them is proposed by Greenshield. Greenshield assumed a linear speed-density relationship as illustrated in figure 2.2 to derive the model. The equation for this relationship is shown below.

$$v = v_f - \frac{v_f}{k_j} * k \tag{2.5}$$

where v is the mean speed at density k, v_f is the free speed and k_j is the jam density. This equation (2.5) is often referred to as the Greenshields' model. It indicates that when density becomes zero, speed approaches free flow speed illustrated in figure 2.4 (ie. $v \to v_f$ when $k \to 0$).

Figure. 2.2 Relationship between speed-density

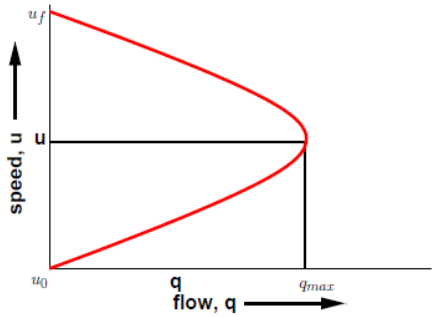

Figure. 2.3 Relationship between speed-flow

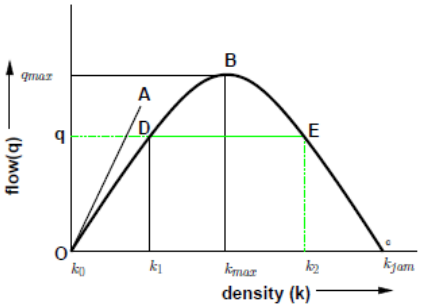

Figure.2.4 Relationship between flow-density

Once the relation between speed and flow is established, the relation with the flow can be derived. This relation between flow and density is parabolic in shape and is shown in figure 2.4. Also, we know that

$$q = k*v \tag{2.6}$$

Now substituting equation 2.4 in equation 2.5, we get

$$q = v_f * k - \left(\frac{v_f}{k_j}\right) * k^2 \tag{2.7}$$

Similarly, we can find the relation between speed and flow. For this, put k = q/v in equation 2.5 and solving, we get

$$q = k_j * v - \left(\frac{k_j}{v_f}\right) * v^2 \tag{2.8}$$

This relationship is again parabolic and is shown in figure 2.3.

2.3 Traffic light Optimization

The problem of traffic optimization involves methods aiming to improve the flow of vehicle traffic within a road network. These methods typically include influencing driver behavior (e.g., traffic lights and signage) and making network modifications (lane additions, turning lanes). Network modifications can result in drastic improvements in traffic flow, but require space that in many cases could be limited or even inexistent. For this reason, more effort has been placed on controlling more efficiently the vehicle flows within the network, using available traffic control devices.

Traffic lights optimization is one of the most effective, and thus most researched, methods of improving vehicles' flow within a traffic network. For obvious safety reasons, conflicting flows present at intersections within a traffic network require regulation and control. The effectiveness of the control method applied to the intersections largely determines the overall performance of the network. The three most important parameters, which determine the behavior of a traffic signal plan, are the phase lengths, signal cycles and offset values. These parameters, as well as the effects of their optimization, are explained below and a graphical representation is included in Figure 2.5.

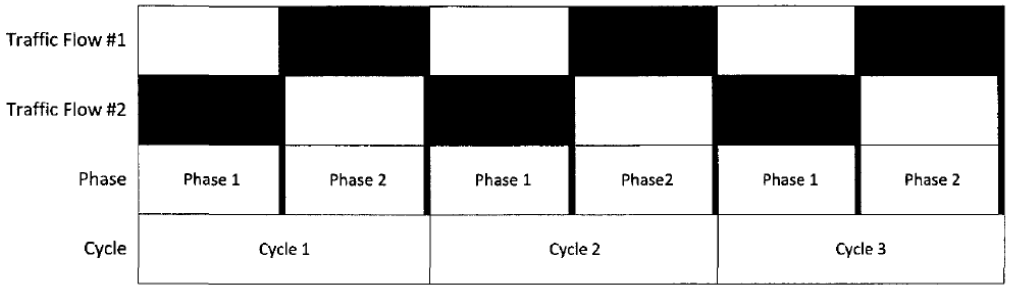

Figure 2.5: Example of cycle and phase relationship with traffic flows, which can (white) and cannot (black) proceed

2.3.1 Phase Lengths

A phase is a time in which certain vehicles may move through the controlled intersection, while others may not. In each phase, a specific set of lights is green and another set of lights is red. These sets, in turn, define which vehicles can go ahead through the intersection and which vehicles must wait. Each phase within a signal plan has a specified length, which decides how long that phase will last during each light cycle. Choosing effective phase lengths allows improving the flow of vehicles through the intersection, since more congested lanes can proceed for a longer time than less congested ones. Optimizing phase lengths for a single intersection, however, can have drastic consequences at other locations within the network, as it can change the vehicle volumes at downstream intersections.

2.3.2 Cycles

A cycle is composed of a number of phases. Generally, a cycle has a fixed time length, which equals the sum of all of its phase lengths. Each traffic light typically implements a single cycle at any given time. This cycle will run through completely, before repeating. There are several different methods of optimizing a signal plan's cycle. First, the length of the cycle can be increased or decreased, allowing phases to repeat more/less often. It is generally thought that shorter cycle lengths can be much more effective with low traffic volumes, as the phases change more quickly to allow sporadically arriving vehicles to proceed (Findler and Stapp, 1992). Higher traffic volumes though can benefit from increased cycle lengths, as more vehicles can proceed through the intersection during a single phase. In addition, a longer cycle length decreases the percentage of time that all traffic flows are stopped, due to safety requirements while switching phases. The order in which phases occur during a cycle can also affect the utility of a signal plan. While the order matters much less at simple intersections, it can become important in more complex control scenarios, where there may be many distinct phases allowing traffic to travel in various directions (e.g., turning lanes with advanced green

lights). Finally, for complex intersections, it may be beneficial to add/remove certain phases depending on the traffic state (observed or predicted) at the current time. As an example, it may be beneficial to have an advanced green light for a turning lane at one point during the day, while it would hinder traffic flow at another point in the day.

2.3.3 Offsets

An offset value specifies at which point in the cycle the first phase will begin, allowing different intersections to begin their cycles at differing times. Improving offset values results in coordination between intersections, which can allow vehicles to proceed through multiple intersections without having to stop. This phenomenon is known in traffic research as a 'green wave' and can be an important factor in improving overall network performance (Robertson and Bretherton, 1991).

2.3.4 Safety Requirements

Since conflicting traffic flows can occur at intersections, a traffic light plan should implement several safety requirements. First, each traffic light plan must ensure that conflicting traffic flows cannot proceed at the same time. In addition, all traffic flows must stop in a specified extent of time before the traffic lights switch from one aspect to another. This extent of time allows vehicles to clear the intersection. As well as safety constraints for vehicles, many local administrations implement procedures to ensure the safety of pedestrians as well. However, in this thesis we will consider only the vehicular traffic.

2.4 Traffic Light Optimization Architecture

Papageorgiou et al. (2003) outlined two different techniques for the traffic light optimization: fixed-time strategies and traffic responsive strategies. Each of these strategies can be further subdivided into strategies for isolated or coordinated intersection. These two approaches will be explained in details in the following two sub-sections.

2.4.1 Fixed-time strategies

Fixed time strategies rely on off-line optimization algorithms, which try to select parameters such that an overall goal is reached (e.g., minimizing travel time, maximizing network capacity). These optimizations are performed using historically observed traffic data, as opposed to real-time observations of traffic state. This, of course, can result in poor overall performance within the traffic network for three reasons. First, there is no guarantee that traffic volumes on a given day will match those that were used to optimize the intersections' signal plans. The larger the difference between current traffic state and historical traffic state, the less effective the signal plans will be. Also, as the historical data ages, it becomes more likely that the underlying traffic volumes will change. This can become especially crucial in an urban environment, where new residential, commercial, or industrial developments can result in an overall traffic volume change for a given area. Once again, these fixed plans do not recognize these changes until new measurements are taken and new plans developed. Finally, traffic volumes can change at any time due to disturbances caused by traffic accidents, work in progress, or other incidents. Fixed controllers do not realize and adapt to these disturbances, resulting in inefficient signal control. The fact that isolated fixed-time strategies do not consider other intersections can result in further problems. For example, one intersection may be optimized in such a way that it allows vehicles to constantly flow in one direction. An intersection downstream from this area, however, will not be expecting the increase in traffic volume because it considers only historical observations when deciding on its own signal plan. The downstream intersection then, will not be prepared for this new situation and will run inefficiently. If the efficiency of the downstream intersection's plan becomes poor enough, major problems can occur as traffic jams form and propagate throughout the network. Coordinated fixed-time strategies address this problem, by analyzing the overall performance of the signal plans at all intersections within the network. While the computational requirements for this analysis

can be extremely high, the off-line optimization allows for the time necessary to find a solution.

2.4.2 Traffic Responsive strategies

Traffic responsive strategies aim to optimize signal plans using real-time traffic state observations. This real-time measurement of traffic is generally achieved through the use of sensors placed within the road network, which is capable of detecting vehicles as they pass. The problem of signal inefficiencies due to measurement aging is eliminated when using real-time observations to decide signal plans. Another issue arises though, as traffic responsive strategies must generate signal plans in real-time and therefore cannot perform as much analysis as the off-line optimization methods used with fixed-time strategies. For this reason, many classic optimization algorithms cannot be used for large traffic networks. Traffic responsive strategies typically implement an architecture such as that shown in Figure 2.6. First, an observation period occurs, in which sensors within the network generate information about the current traffic state. This information is then passed to the optimization algorithm, which performs the steps necessary to generate new signal plans for the network being considered. The traffic lights then implement these new plans until another observation period is completed and the plans change once again. Essentially, traffic responsive signal controllers create a model of traffic flows in real-time and optimize the allocation of resources (green time) based on the predicted traffic volumes. Using this strategy, the signal plans adapt throughout the day to meet the current traffic state, as opposed to a historically observed traffic state. As with isolated fixed-time control strategies, isolated traffic responsive control at an intersection can cause problems at other intersections within the network. This can happen when one intersection implements a plan which results in a traffic volume far from what another intersection has expected. This problem, however, is not costly when using a traffic responsive strategy, because the failing intersection will modify its plan much sooner than a fixed-time control strategy. Still, the level of coordination between intersections, as well as the speed at which intersections can

adapt to unexpected traffic volumes, can greatly affect the overall performance of the network.

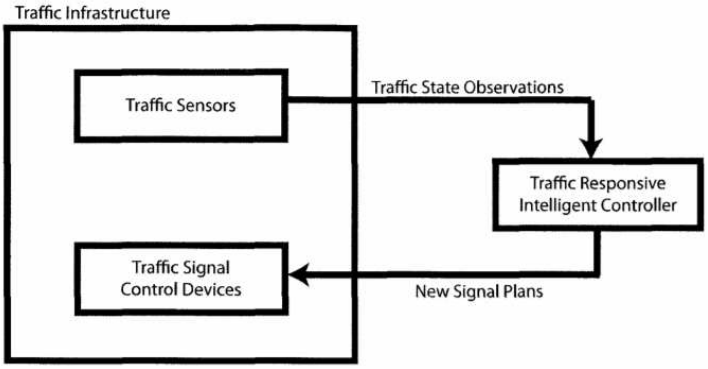

Figure 2.6: A simple responsive traffic system architecture

CHAPTER 3

LITERATURE REVIEW

The analysis of issues related to the urban movement of cars has assumed an increasingly key role in recent years. The urban traffic conditions greatly slowed down and have become congested; in fact, not only create inconveniences to car drivers for the increase in the average travel time but also make a less secure circulation on the road and increase air and noise pollution.

The development of Intelligent Transport Systems and info-mobility represent an opportunity to reduce costs and road congestion, with sustainable timing. In the era of multimedia convergence, communication, and sensing platforms, GPS-enabled smartphones are becoming an essential contributor to location-based services. These devices combine the advantages of mobile sensors mentioned earlier: low investment costs, high penetration, and high accuracy achieved by GPS receivers. In addition, GPS-enabled smartphones can provide accurately not only position but also speed and direction of the travel. Note that phones not only can send but also receive information. Therefore, traffic information can be delivered through this channel. Given the market penetration of mobile phones, this new sensing technology can potentially provide an exhaustive spatial and temporal coverage of the transportation network. In the mobile computing era, smartphones have become instrumental tools to develop innovative mobile context-aware systems because of their numerous sensors such as GPS, accelerometers, gyroscopes. This makes them suitable enablers to capture a wide range of contextual features, like weather and traffic conditions (Miranda-Moreno, 2015).

Real-time traffic reports are usually based on statistical methods. These methods have been also a common practice in studies that use cell phones as traffic sensors,

in which the main goal has been to find the link speed or travel time estimation (Bar-Gera, 2007). Note that the aforementioned study uses cell phone antennas to obtain a cell phone position (i.e. vehicle), which is less accurate than GPS positioning. Krause et al. (2008) have investigated the use of machine learning techniques to reconstruct travel times on a graph based on sparse measurements collected from GPS devices embedded in cell phones and automobiles.

An overview of the GPS techniques is given in Skog (2009). Sophisticated algorithms have been developed to map the vehicle position in the road, see for example Zhao (2015) or Fouque et al. (2012). The usual problem in GPS positioning is that the accuracy is not within a lane-width range. Therefore, solutions have to be found to get the accuracy to a lane level.

Liu et al. (2017) present a recognition system for dangerous vehicle steering based on the low-cost sensors found in a smartphone: i.e., the gyroscope and the accelerometer. To identify vehicle steering manoeuvres, they focus on the vehicle's angular velocity, which is characterized by gyroscope data from a smartphone mounted in the vehicle.

Zheng (2016) develops in his work an innovative approach that uses data from connected vehicles(CVs) to estimate traffic volumes at signalized intersections, particularly under low penetration rate environment. It is well known that traffic volumes are the key inputs to designing and optimizing traffic signal operation. In conventional signal systems, vehicle arrival information can be obtained only by detectors at fixed locations. Different from the detector data, CV data provide detailed trajectories, albeit from a small percentage of vehicles. The challenge here is to estimate overall arrival information using limited CV trajectories. In the proposed algorithm, vehicle arrivals at intersections are modeled as a time-dependent Poisson process with a time-dependent factor characterizing arrival types. For volume estimation, an expectation maximization (EM) procedure is derived that can incorporate different types of CV trajectories. To estimate traffic volume, the basic idea is to take advantage of vehicle arrival information in vehicle trajectories. The arrival information can be reflected from the status whether a vehicle stopped or not. An example is shown in Fig. 3.1. In the figure, CV1 passed

the intersection with a stop and CV2 without a stop. Then, based on CV1's stopping position or departure time, you can calculate a number of vehicles queuing in front of it. Based on the trajectory of CV2 without a stop, it is possible to know that, if a vehicle queue exists, the queue would not be long enough to impact CV2. In other words, the upper bound of possible vehicle arrivals between CV1 and CV2 can be calculated based on the trajectory of CV2 (figure 3.2). By combining this arrival information from vehicle trajectories, the volume of overall vehicle arrivals can be estimated.

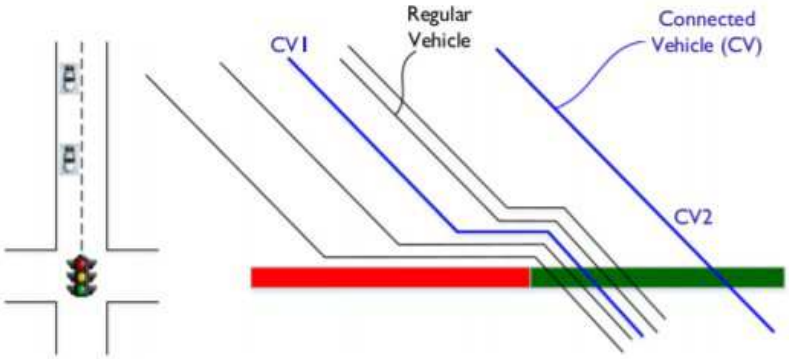

Fig 3.1 Illustration of vehicle arrival information in trajectories

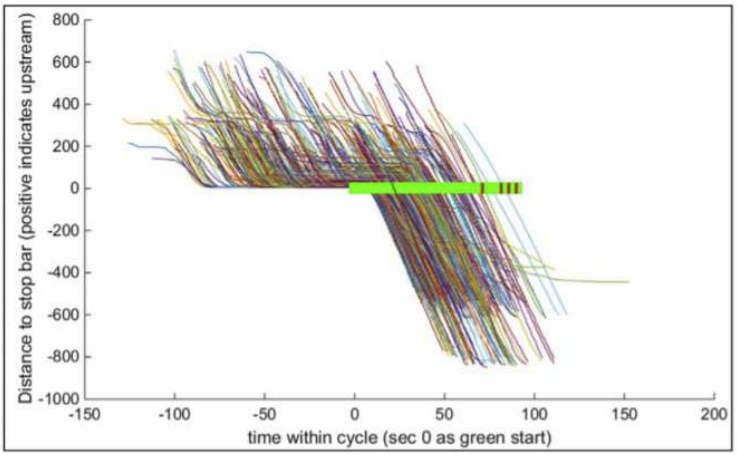

Figure.3.2 Illustration of CV trajectories

Biagioni (2011) reduces the cost and complexity of offering these services by creating EasyTracker, an automatic system for transit tracking, mapping, and arrival time prediction. The system consists of four main components:

a) an off-the-shelf smartphone, installed in each bus or carried by each driver, functioning as an automatic vehicle location system or tracking device;
b) batch processing on a back-end server which turns stored vehicle trajectories into route maps, schedules, and prediction parameters;
c) online processing on a back-end server which uses the real-time location of a vehicle to produce arrival time predictions, and
d) a user interface that allows a user to access current vehicle locations and predicted arrival times.

Using EasyTracker, a transit agency can implement a sophisticated bus-tracking and arrival time prediction system by simply purchasing a number of smartphones and downloading the bus-tracking app to each phone.

Hao et al. (2014) proposed Bayesian Network-based methods to estimate the cycle-by-cycle queue distribution of a signalized intersection. The methods are based on the vehicle index estimation approach, like in Hao et al. (2013). Similar to vehicle index estimation, the proposed methods consider the relationships among the arrival, departure, and vehicle index. They, however, localize the problem around the end of the queue. It first classifies the traffic and sampling conditions to seven cases based on the sample travel times of vehicles from mobile sensors. For the normal case, the method focus on the hidden vehicles between the last queued sample vehicle and the first free-flow sample vehicle. Using Bayes' theorem, they relate the queue length of a cycle to the hidden variables that can be considered as the attributes of the un-sampled vehicles. Then we show the construction and quantification of the BN to infer the hidden variables given sample vehicle travel times and estimated vehicle indices.

Sun and Bun (2013) propose two methods, namely delay-based optimization and estimation models, to estimate the impact of current boundaries, based on which to reconstruct the short trajectory of vehicles. First, they proposed a model based on optimization and demonstrated that this model is difficult to solve because it needs not

only potentially large binary variables, but also a complicated process of evaluation of the objective functions. Then, a simplified optimization model is proposed, which aims to evaluate the combination of boundary points (where the vehicle stops and joins the queue) for several sample vehicles, so that the overall difference between actual and estimated trajectories of the vehicle on the ground was minimized. The simplified method, therefore, explores only a subset of sample vehicle trajectories. To maintain the feasibility, the candidate trajectory points of all sample vehicles can be arranged in a direct and acyclic graph, from which border points can be estimated in a consistent and efficient manner. The delay-based model further simplifies the estimate of the limits. It uses the sample travel times at intersection to deduce the boundary point of a sample vehicle. This model requires less information as it does not require detailed information on the vehicle's trajectory.

Sekimoto et al. (2012) proposed a simple method for using the separation distance (offset) between a smartphone GPS and the centreline on a digital roadmap to determine the lane position of a car.

Victor et al. (2017) present a method to map the lanes on a motorway using data collected. The method exploits the high accuracy and the fact that the most driving is within a lane. It tests a new technique that improves the accuracy of the position based on signals from the Global Positioning System (GPS). The technique does not need expensive equipment and does not rely on vision or radar, hence works in all weather and light conditions. Since most digital maps do not show separate lanes yet, the main contribution is a technique to find automatically the lanes, based on trajectories collected using the GPS technique. In this way, measurement points obtained by the GPS Precise Point Positioning (PPP) can lead to a map where other trajectories can be mapped upon.

Figure 3.3 shows the steps needed to obtain the digital map with identified lanes.

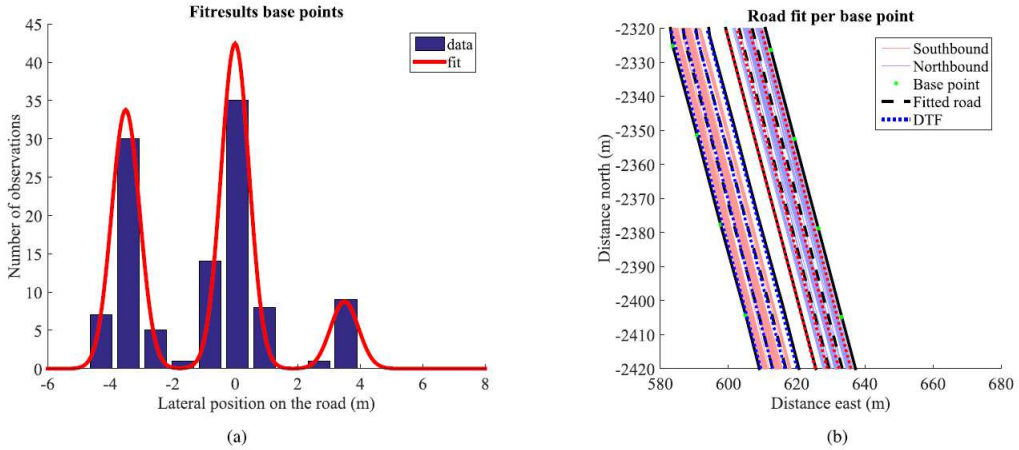

Figure 3.3 Results of the lane finding methodology. (a) Fitting for one base point. (b) Lanes on the map with base point fitting. The red and blue lines are all trajectories measured.

$$p(y) = \sum_{l=1}^{L} \phi_l N(z - l\omega, \sigma) \tag{3.1}$$

In equation 3.1, y is the lateral position, l the lane number, L the number of lanes, ϕ_l the fraction of the flow in lane l, N(X,μ) the normal probability fuction with mean X and standard deviation μ; z is the offset of the first lane compared to the base path, ω is the width of a lane and σ the width of the distribution of vehicles within a path.

This function calculates the probability that a vehicle is in a certain lateral position as a probability that the vehicle is in a lane multiplied by the normal distribution hypothesized for the distribution of vehicles within the lane, summed up on all lanes. The distance of mid points of distributions per lane is equal to the lane width

3.1 Macroscopic Fundamental Diagram (MFD)

The main idea of the Macroscopic Fundamental Diagram (MFD) is that it can describe the traffic at an aggregated level. In a similar way that the Fundamental Diagram (FD) relates the flow and the density in a link or a road section, the MFD extends this relationship to an urban area or a network.

In this section, we tried to answer to the question set in the technical literature about the range of the possible applications of the MFD. Actually, the MFD has various applications, aiming to improve mobility in urban networks: it can help traffic managers in monitoring their systems and assessing whether operations are at the desired level, or can provide information for an efficient traffic control. Keyvan-Ekbatani et al. (2012) stated that, although the MFD is still under research, we can use it as a very good and reliable tool for control strategies.

Geroliminis and Daganzo (2008), proposed to use the outflow rate provided by the MFD as an evaluation of the accessibility of a city and a suggestion on how improve it. If a new control strategy is implemented or an infrastructure change occurs, the MFD should change, showing whether the measure was successful or not. Of course, the effect of the measure could be overestimated if the evaluation of MFD is carried out in a narrow area. For example, the implementation of a new traffic control at an intersection could improve the flow at that intersection, but possibly because drivers choose a different path. Examining the results in the complete network should avoid these questionable assessments.

Daganzo (2007) proposed a solution to decrease congestion by developing an adaptive perimeter control mechanism that uses the MFD to monitor and control the total vehicles amount that enters a neighborhood. The idea was tested by Geroliminis and Daganzo (2007) at two simulated sites in Lincoln Avenue in Los Angeles and in Downtown San Fransisco. They tried to maximize the outflow by maintaining at the optimal level the total number of vehicles in the network and limiting the entry of more vehicles.

Also Keyvan-Ekbatani et al. (2012) analyzed the application of a perimeter control strategy. More specifically, they proposed the use of the MFD to apply a "feedback-based gating". A test application of the gating strategy with simulation offered encouraging results with fewer delays and higher speeds in the simulated network. Geroliminis et al. (2013) proposed a perimeter control as well, but by applying a model predictive control solution. To test their method, they used various examples of two-region urban networks with different levels of congestion and different amounts of noise and errors in the data. The results are very interesting, showing that the model predictive algorithm

performs much better than the "greedy" feedback control. These encouraging results of the perimeter control can be further used for the development of efficient traffic control strategies in any urban network.
Another example of the application of the MFD is a congestion pricing strategy that was proposed by Geroliminis and Levinson (2009). Their research uses the MFD to sketch a network-based congestion-pricing scheme.
Simoni et al. (2015) proposed a methodology to derive time-dependent toll prices using the Network Fundamental Diagram. They tested their methodology in a simulated case study of the city of Zurich. They suggested that this approach is more realistic than the analytic methods that are usually applied to decide tolling schemes.
Furthermore, the proposed approach needs only a few information and offers a very good representation of the traffic dynamics. Thus, it could be implemented effectively in real cases.
As well as applications proposed by the gating and pricing strategies, the MFD could also be used to implement a routing strategy to spread the vehicles over the network, as proposed by Knoop et al. (2012). Yildirimoglu et al. (2015) proposed a "route guidance advisory control system" showing that their method can produce a system optimum for the network.
Overall, various studies have already investigated the advantages of applying the MFD to support new traffic control strategies or to assess existing strategies. These findings strengthen the affirmation that, although the MFD is simple and parsimonious, it can be very useful and powerful. We could actually say that its simplicity is one of its strongest points and this motivates us to research more about it.

3.1.2. Using real traffic data

Geroliminis and Daganzo (2008) first derived a smooth network fundamental diagram from real data. For the purposes of their study, they used loop detector data from downtown Yokohama in Japan. They realized that the flow-occupancy relationship produced by the data from individual detectors contained a lot of scattering, as seen in Figure

3.4. However, when aggregating the detector data, a smooth relationship resulted as it can be seen in Figure 3.5.

Since the detectors did not cover the entire network, they tried to produce the same relationship using GPS taxi-data that had a full network coverage. From these data, they created the relationship between space-average speed and density. Indeed, a smooth graph was again produced, indicating that an MFD can exist for the entire urban network and that it is a characteristic of the network. The formulas that they used for traffic flow q, occupancy o and density k derived from the generalized definitions of Edie (1963).

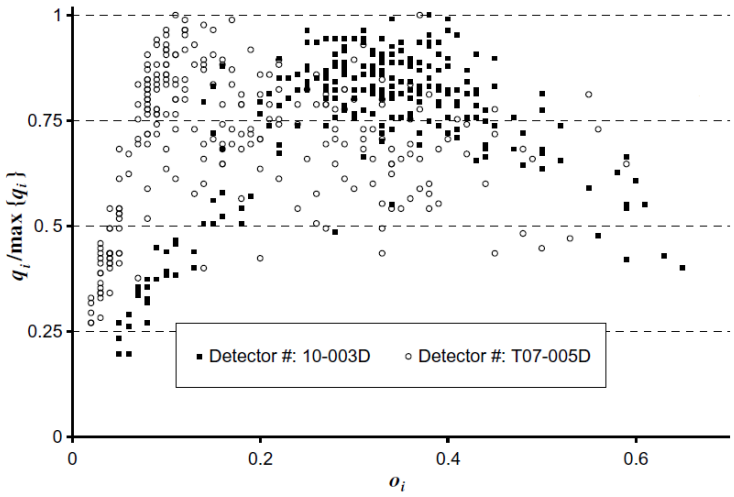

Figure 3.4: Graph of flow vs. occupancy for two individual detectors of Yokohama

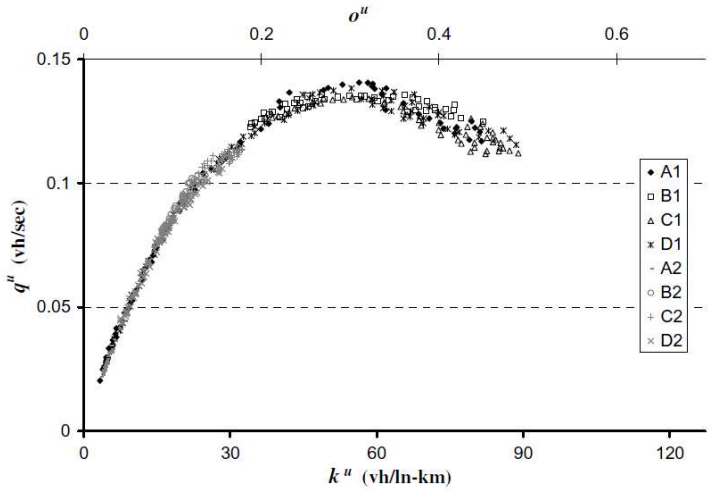

Figure 3.5: The Macroscopic Fundamental Diagram after aggregating the detector data of Yokohama

Buisson and Ladier (2009) used the unweighted mean formulas with loop detector data from both the highway and the surface road network in order to create an MFD in Toulouse, France (Figure 3.6). They observed the evolution of flow and occupancy throughout the chosen days of the analysis with the goal to see what happens if heterogeneity applies in the network. More specifically, they examined the homogeneity issue for different road types, distances of the loop detectors from the stop line, and congestion levels throughout the network and investigated how each one of these parameters influences the scatter on the MFD.

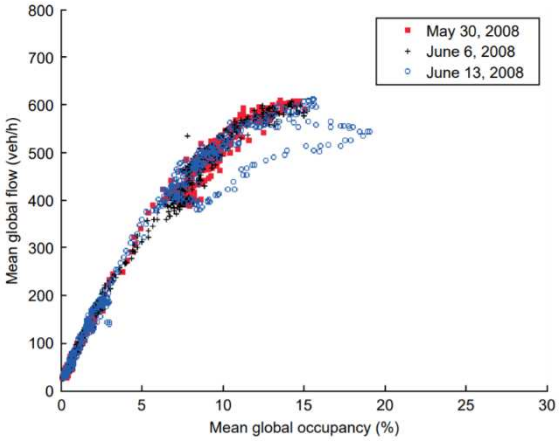

Figure 3.6: The Macroscopic Fundamental Diagram from Buisson and Ladier (2009)

Also Cassidy et al. (2011) used real data to estimate the MFD. They used detailed vehicle trajectories data from freeway stretches. Their results showed that the MFD could be produced only if the network is either in congested or in uncongested state, not in a mixed state. They also discovered that the MFDs for the freeways could be produced also by loop detector data as long as there is at least one detector per link and the data are filtered to meet a single regime condition.

3.1.2 Using simulation traffic data

Geroliminis and Daganzo (2007) performed various microsimulations in downtown San Francisco and first produced a diagram relating the production to the accumulation of vehicles, with the aim of applying macroscopic feedback control strategies. They used Edie's definitions (Edie, 1963) to estimate mean flow and mean density.

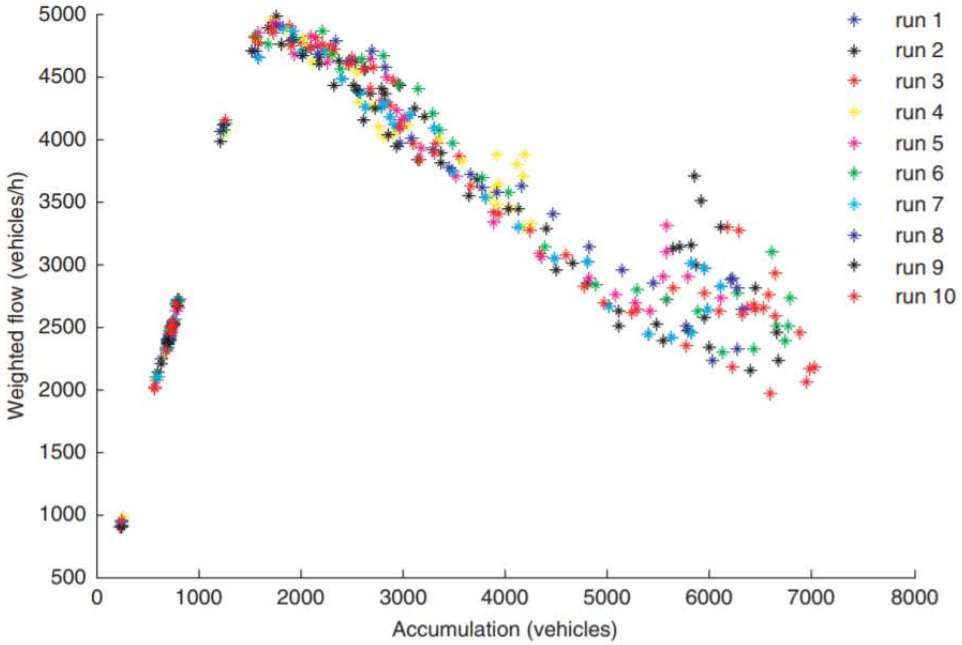

Figure 3.7: The Macroscopic Fundamental Diagram with simulation data of Amsterdam from Ji et al. (2010)

Ji et al. (2010) also used microsimulation data for the city of Amsterdam because the collected traffic data were not adequate to describe the traffic flow. Figure 3.7 shows their resulting MFD .

The goal of their research was to examine the factors influencing the shape of the MFD. To calculate the flow, they used the formula of the weighted average flow q_w as in Geroliminis and Daganzo (2008), while for accumulation n_i they used the following formula:

$$n_i = \sum_i k_i l_i$$

The goal of the research carried out by Courbon and Leclercq (2011) was comparing the results of three different ways to produce the MFD, using a microsimulation model.

For this reason, they tried to avoid the bias resulting from empirical data, having a complete control over both the urban environment and the traffic phenomena occurring in it. They followed three different approaches:

1. Using loop detector data and weighted averages as in Geroliminis and Daganzo (2008).
2. The analytical method with cuts proposed by Daganzo and Geroliminis (2008).
3. Using data from vehicle trajectories.

The network they considered was very simple, with road sections of similar length and same traffic light cycle.

Since their results showed that the trajectory method can produce very accurate values of MFD in any network shape, they propose this method as a benchmark.

Keyvan-Ekbatani et al. (2012) used simulation data of the city of Chania, Greece to produce the MFD and test their proposed gating measures to improve mobility. They state that an MFD can be either "ideal" or "operational". In the first case, it includes precise traffic data of all network links, so it can be derived only from simulation environments; in the second case, it includes the available traffic data from a subset of the network links. An "operational" MFD is "complete" if the available traffic data cover the entire set of network links. For their test, they produced a "complete operational" MFD, which describes the traffic situation in combination with a moderate amount of real-time measurements, and determine the appropriate gating strategy. For their case, they used all measurements of the links to detect the point on the MFD that their network was operating. However, they suggest that this information, required for gating, can be obtained using less real-time measurements.

Ortigosa et al. (2014) used a microsimulation model of the inner city of Zurich. They used only loop detector data, since they supposed that floating car data were not broadly available yet; vice versa, their method could be implemented in any urban areas. The purpose of their study was to find the minimum number of links necessary to obtain the MFD. Thus, they created the complete MFD from all the links and incomplete MFDs with only some links. Then, they compared the incomplete to the complete MFDs on the basis of density ratios and accuracy. To estimate the average flow and density,

the weighted averages proposed by Geroliminis and Daganzo (2008) were used again in this study. Their results showed that a network coverage of minimum 25% provides sufficient accuracy with a small error at the density ratios.

CHAPTER 4

THE PROPOSED METHOD

4.1 A new Intelligent Transportation System for Traffic Light Regulation

This section presents a new intelligent transportation system for traffic light regulation. The proposed system is made of the following modules (Fig. 4.1):

(1) Connected vehicles equipped with GPS smartphone and/or satellite receiver position system (GPS), used together or as an alternative for vehicles location;
(2) Internet
(3) Central server for data collecting and processing;
(4) Traffic lights.

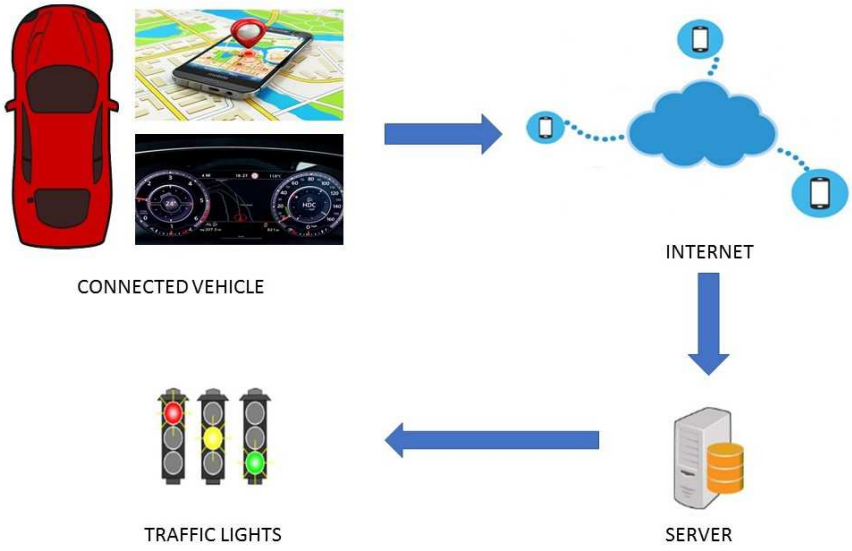

Figure 4.1: General system

The data recorded by the device (smartphone or GPS), when connected to the vehicle, are sent to the main server. On its turn, the server calculates by these data vehicle position, speed, and travel time, and establishes the signal phases, which are communicated to the control unit that activates the phases.

Figure 4.2 shows the server structure: a first part containing the data collection and another part devoted to the data processing. This part is the heart of the model, made of two additional models. The first model, explained in detail in the section 4.1.1, allows identifying the running lane of the connected vehicle. A second model, explained in detail in the section 4.1.2, estimates traffic flows for each lane.

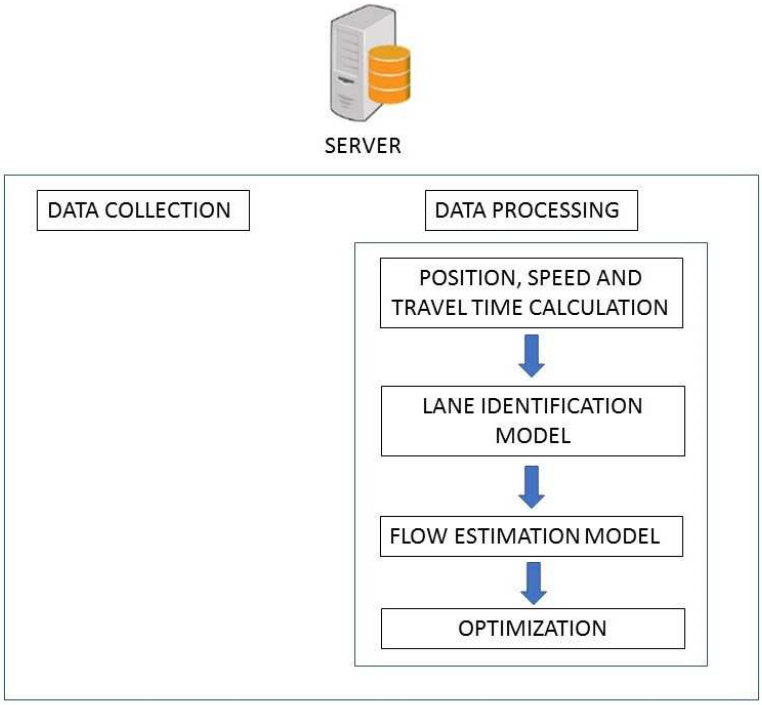

Figure 4.2: The server structure

After having estimated flows, through any optimization method, we can determine the new traffic light cycle time. To simulate and verify the improvements obtained from the system, we used the Webster method described in Section 4.1.3
The system can combine information about vehicular traffic obtained both from FCD and from traditional traffic count systems (magnetic loop detector, microwave radar sensors, etc.). Moreover, it would allow priority vehicles to move faster on the network.

4.2 The lane identification model

In this section, we explain the method used to find the position of a vehicle on a lane in the proximity of any signalized road intersection. We use the GPS data recorded by smartphone devices. First, we need to define the observation area, where the main road references and the definition of the virtual sections take place. A set of base points at the roadside identify the virtual sections. To determine the roadside starting from two sampling points A and B we used the following relation:

$$y = \frac{(y_B - y_A)(x - x_A)}{x_B - x_A} + y_A \tag{4.1}$$

while the equations of the relative virtual sections are:

$$y_{VS_j} = -\frac{(x - x_j)}{m} + y_j \tag{4.2}$$

where $m = \frac{y_B - y_A}{x_B - x_A}$, VS_j is the virtual section j, and x_j, y_j are the coordinates of the j-th base point. Figure 4.3 shows the steps to obtain the input data from the acquired GPS track data.

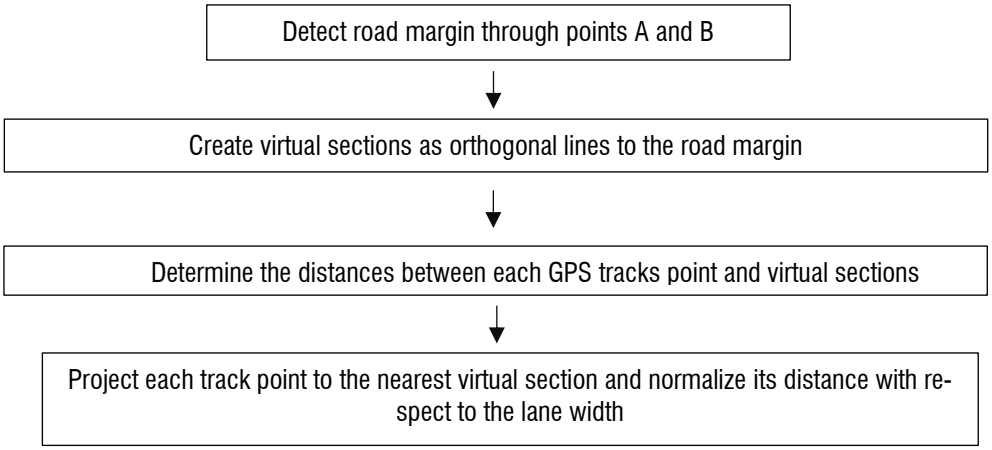

Fig. 4.3. Steps to obtain the input data

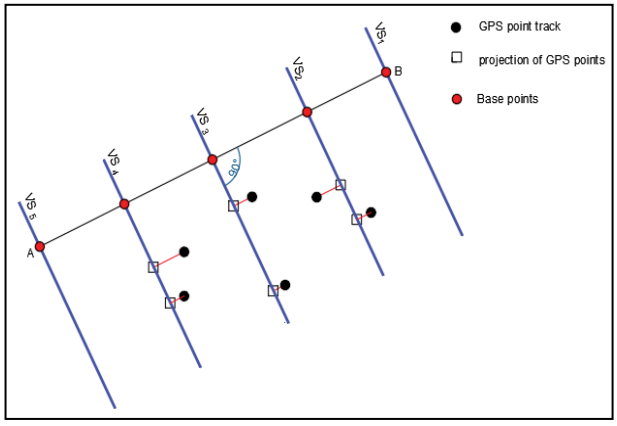

(a)

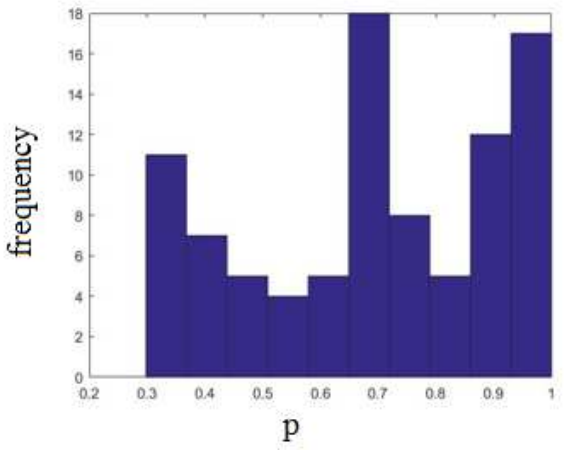

(b)

Fig. 4.4. (a) Creation of virtual sections, and (b) statistical trend of the recorded GPS data.

Figure 4.4a shows the roadside and five sections. The base points A and B have coordinates (x_A, y_A) and (x_B, y_B), used in Eq. 4.1 to find the roadside. Starting from these base points, we created five virtual sections, VS_1 to VS_5; the GPS data projections on these virtual sections (square dots in Fig. 4.4a) have been obtained considering for each GPS point *i* (black dots in Fig. 4.4a) the minimum distance $d_{i,j}$ from every virtual section VS_j, as follows:

$$i \in VS_j \mid j \ni ' \quad d_{i,j} = min(d_{i,k}), \quad j,k = 1,\dots,n_s; \tag{4.3}$$

where n_s is number of virtual section.

The distances from the roadside of the GPS data projections, i.e. the lateral positions of the GPS points, have been normalized with respect to the lane width.

The values of the normalized lateral positions $p_{i,j}$ of points i on a virtual section j have been calculated using the following expression:

$$p_{i,j} = \frac{\sqrt{(x_j - x_i)^2 + (y_j - y_i)^2}}{D_j} \tag{4.4}$$

where D_j is the lane width of the virtual section j.

To test our method, we considered a set of measurements carried out by a smartphone device, in a three-lanes road. In Fig. 4.4b there is the histogram of the normalized lateral positions of surveyed points. A three normal probability distribution fits the histogram, where three high-frequency points can be observed. Each one of these points can be associated with the midpoint of a lane in the considered road.
Thus, in general, we can define the probability distribution for each virtual section j through the following expression:

$$\Phi_j(p_i) = \frac{1}{\sigma\sqrt{2\pi}} e^{-\frac{(p_i-\mu)^2}{2\sigma^2}} \tag{4.5}$$

where the characteristic parameters are the mean μ and the standard deviation σ; p_i is the lateral position of the point i on the section j, as defined by Eq. 4.4.
Due to the uncertainty embedded in the GPS data, we considered fuzzy distributions to represent a point into a road lane. We used Gaussian-shaped Fuzzy Sets to represent a membership function Π_l of a lane *l* and defined as follows:

$$\Pi_{l,j}(p_i) = e^{-\frac{(p_i-\mu_{l,j})^2}{2\sigma_{l,j}^2}} \tag{4.6}$$

where the parameter μ_l for a lane l is the central value of the distribution, defined as:

$$\mu_{l,j} = \frac{1}{N_l}\sum_{i=1}^{N_l} p_{i,j} \tag{4.7}$$

in which N_l is the number of normalized projections belonging to a lane *l*. The standard deviation $\sigma_{l,j}$ for each virtual section j is defined as follows:

$$\sigma_{l,j} = \sqrt{\frac{1}{N_l-1}\sum_{i=1}^{N_l} |p_{i,j} - \mu_{l,j}|^2} \tag{4.8}$$

The correct parametrization of the membership functions for each lane a key problem, to maximize the accuracy of the position identification.
The membership degree of a projection p_i (lateral position) to a Π_l function is evaluated and the associated lane C is determined as follows:

$$C(p_i) = l \ \ if \ \Pi_l(p_i) = \ max\{\Pi_j(p_i)\} \ \ , 1 \leq j \leq n_l \tag{4.9}$$

where n_l is the number of lanes.
The set W of correctly identified lane positions is such that:

$$\hat{C}_i \in W \ \Leftrightarrow \hat{C}_i = C_i \tag{4.10}$$

where C_i is the lane associated with GPS data and $\hat{C}_i$ the value estimated by the method. In this way, the identification error ε is defined as:

$$\varepsilon = 1 - \frac{N_c}{N_t} \tag{4.11}$$

in which N_c is the number of correct estimations and N_t is the total number of the GPS points considered.
The objective is to determine the optimal parameters, the mean μ and the standard deviation σ, of the membership functions. We can consider the proposed method as a supervised clustering technique for uncertain GPS data. In the following, we propose a genetic algorithm for an optimal parametrization.

4.2.1 Calibration with Genetic Algorithms

In this section, we present an approach based on genetic algorithms (GA) to calibrate the parameters (σ_l, μ_l) as described above. We chose GA due to their high flexibility, robustness and global search capabilities. For each virtual section, the aim is to find the optimal parameters of the Gaussian membership function Π_l as defined in eq. 4.6. The objective function associated to the optimization problem is defined through the following expression:

$$max \ Z_j = \frac{n_c}{N} * 100 + \frac{1}{N} \sum_{\substack{i=1 \\ i \in N_c}}^{N} \sum_{l=1}^{n_l} |\Pi_{max}(p_i) - \Pi_l(p_i)| \tag{4.12}$$

where is n_c is the number of correct identifications, $\frac{n_c}{N}$ is the accurancy rate, i.e. the percentage of correct identifications globally made N, N_c is the set of corrected estimated points, $p_{i,j}$ is the normalized projection value on a given virtual section, $\Pi\max(p_i) = \max\{\Pi_C(p_i)\}$, $c=1,\ldots,n_l$.

In the proposed genetic algorithm, a chromosome has been encoded considering the parameters μ and σ. Each pair of genes represents a couple of parameters (μ, σ) related to the membership function of a lane l in a given section. The resulting encoding is reported in Figure 4.5.

μ_1	σ_1	…	…	μ_{n_l}	σ_{n_l}	

Fig. 4.5 Chromosome structure of the genetic algorithm.

The optimization problem is subject to lower and upper bounds of decision variables μ and σ, respectively $0 \leq \mu \leq 1$ and $0.01 \leq \sigma \leq 0.5$.

4.3 Traffic Flow Estimation model

Our method can estimate traffic flow in proximity of any signalized road intersection with the use of GPS data recorded by smartphone devices.

First, we need to define the observation area and identify coordinates of the stop lines.

Figure 4.6 shows the steps we followed to estimate the traffic flow.

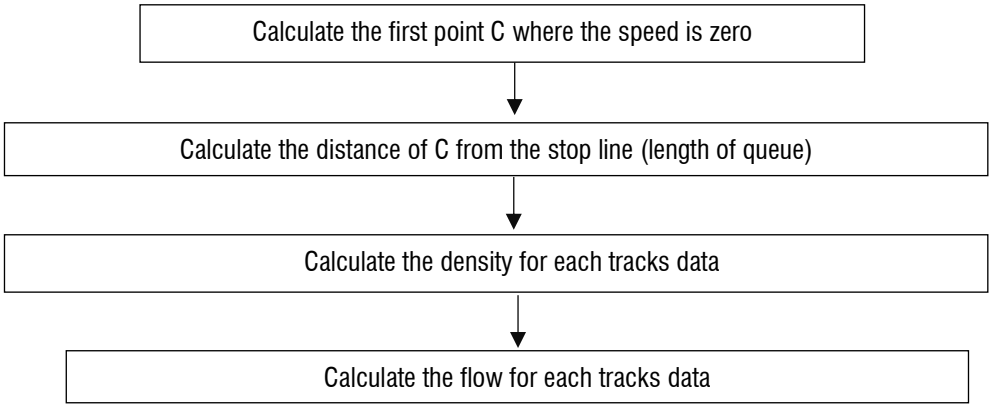

Fig. 4.6. Steps to obtain the input data for our method

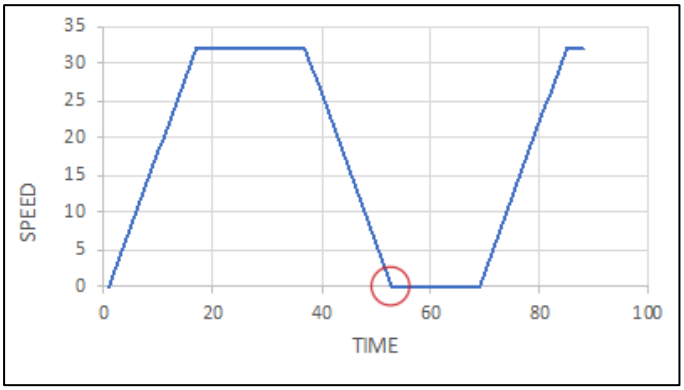

Fig. 4.7 An illustrative example of a speed-time diagram

Figure 4.7 shows an example of a speed-time diagram. To estimate the length of queue, we analyzed all the speed-time diagrams of each run and filtered the data according to the speed value. It is possible to determine the length of queue, taking into account the first speed value equal to zero(red circle in figure 4.7),
We can determine the distance of this point related to stop line virtual section, according to the eq. 4.1.

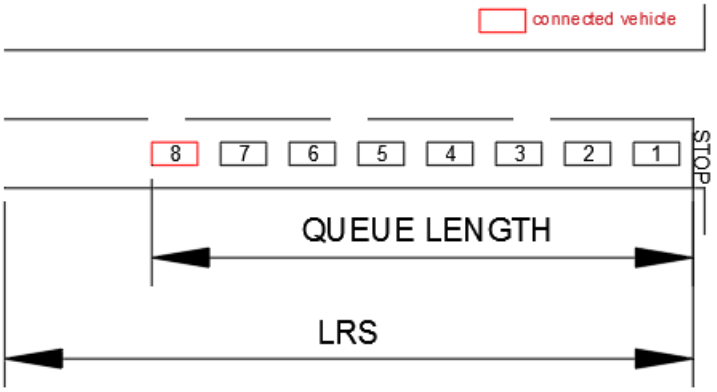

Fig. 4.8. Queue length evaluation according to connected vehicle position

The density k (or concentration) is defined by the 'number of vehicles per distance unit'.

$$k = \frac{number\ of\ vehicles}{LRS} \tag{4.13}$$

where LRS is the length of reference section, equal to 500 m, as shown in figure 4.8.

The number m of vehicles that occupy the road at a time instant is given by.

$$m = \frac{queue\ length}{Average\ vehicle\ length} \tag{4.14}$$

where the average vehicle length is 5.5 m.

In this way, we can calculate the flow through the fundamental relationship

$$q = \ k * v \tag{4.15}$$

where v is the speed the vehicles have when crossing the reference section.

4.3.1 The Greenshields' Model

Macroscopic models represent how the behavior of one parameter of traffic flow changes with respect to another. Most important among them is the relation between speed and density. The first and most simple relation between them is proposed by Greenshield. Greenshield assumed a linear speed-density relationship as illustrated in figure 4.9, 4.10 and 4.11 to derive the model. The equation for this relationship is shown below.

$$v = v_f - \frac{v_f}{k_j} * k \tag{4.16}$$

where v is the mean speed at density k, $v_f$is the free speed and k_j is the jam density. In equation 4.17 is often referred to as the Greenshields' model. It indicates that when density becomes zero, speed approaches free flow speed (ie. $v \to v_f$ when $k \to 0$).

$$q = v_m * k - \frac{v_m}{k_{max}} * k^2 \tag{4.17}$$

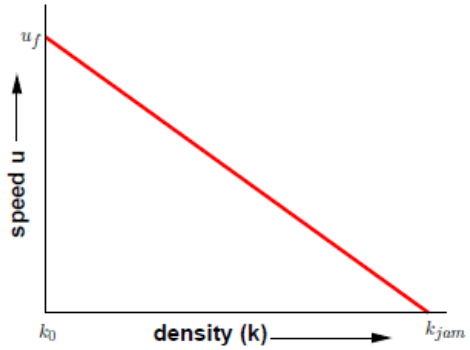

Fig. 4.9. Relation between speed and density

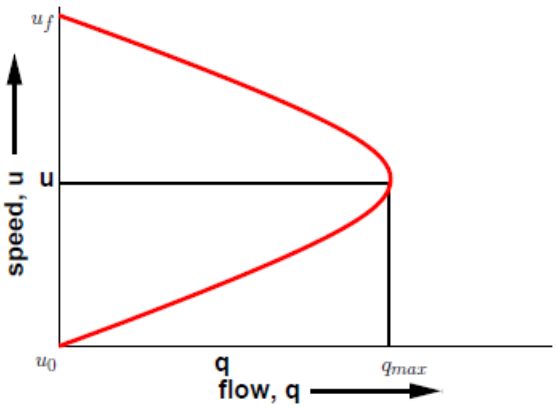

Fig. 4.10. Relation between speed and flow

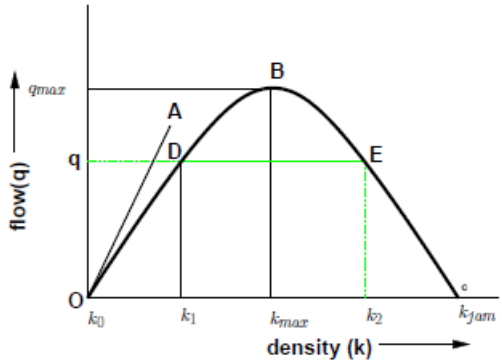

Fig. 4.11. Relation between flow and density

4.4 Optimization of traffic lights with Webster method

In the Webster delay model, the average delay time consists of three components: the delay time due to the uniform traffic flow (d_1), the delay time due to the random traffic flow (d_2), and compensation term due to the different traffic environment (d_3). Three parameters, α, and were introduced. α is the correction coefficient of the first component of delay time; β is the correction coefficient of the second component of delay time; γ is the correction coefficient of the third component of delay time. The corrected Webster delay model is given as

$$d = \alpha d_1 + \beta d_2 + \gamma d_3 \tag{4.19}$$

$$d_1 = \frac{C(1-\lambda)^2}{2(1-\lambda x)}$$

$$d_2 = \frac{x^2}{2q(1-x)}$$

$$d_3 = -0.65\left(\frac{C}{q^2}\right)^{\frac{1}{3}} x^{2+5\lambda}$$

Where d represents the average vehicle delay time; c represents the uniform delay time; d2 represents the random delay time; d3 represents the delay compensation value, C represents the cycle length, q represents the maximum traffic volume of the intersection in 15 minutes, pcu/15 min,where PCU is Passenger Car Unit.

The traffic data of the selected signalized intersection, including the traffic volume, delay time, cycle length, green split, and saturation, were investigated, among which the direct traffic data were traffic volume and cycle length and the indirect traffic data delayed time, green split, and saturation. The calculation methods of the indirect traffic data were shown as follows.

Delay Time. The individual sample survey method was used to determine the delay time, which is given as

$$D = N * t$$

$$\bar{d} = \frac{D}{V} \tag{4.20}$$

Where *D* represents the total delay time and *N* represents the total number of suspended vehicles; *t* represents the interval time; $\bar{d}$ the average delay time of each vehicle at the approach; and *V* represents the total volume at the approach.

Green Split: The green split is given as

$$\lambda = \frac{g}{C'} \tag{4.21}$$

Where λ represents the green split; g represents the effective green time; and C represents the cycle length.

Saturation: The saturation is given as

$$x_i = \frac{q_i}{\lambda_i s_i} \tag{4.22}$$

$$X = max\{x_i\}, \;\; i = 1,2,3, \ldots., n \tag{4.23}$$

Where x_i represents the saturation for phase i; q_i represents the traffic volume; $\lambda_i$represents the green split; $s_i$represents the saturation traffic volume and X represents the saturation degree of the intersection.

As can be seen, the model is a multivariate linear regression equation. Thus, the unknown coefficients can be calibrated using the least square method. The result is as follows:

$$d_i = 1.16\frac{C(1-\lambda_i)^2}{2(1-\lambda_i x_i)} + 0.66\frac{x_i^2}{2q_i(1-x_i)} - 0.79\left(\frac{C}{q_i^2}\right)^{\frac{1}{3}} x_i^{2+5\lambda_i} \tag{4.24}$$

The green time split λ_i is given as:

$$\lambda_i = \frac{g_i}{C} = \frac{C-L}{C}\frac{y_i}{Y} = \left(1-\frac{L}{C}\right)\frac{y_i}{Y} \tag{4.25}$$

Where L represents the total lost time; g_i represents the green time for phase *i*; $y_i$represents the maximum traffic volume ratio for phase *i*, which can be calculated by $y_i = q_i/s_i$ and Y represents the sum of traffic volume ratio of all phases.

Thus, the saturation in (eq. 4.22) can be calculated as

$$x_i = \frac{q_i}{\lambda_i s_i} = \frac{q_i}{s_i\left(1-\frac{L}{C}\right)\left(\frac{y_i}{Y}\right)} = \frac{y_i}{\left(1-\frac{L}{C}\right)\left(\frac{y_i}{Y}\right)} = \frac{Y}{\left(1-\frac{L}{C}\right)} \tag{4.26}$$

Therefore, (eq.4.24) can be rewritten as

$$d_i = 1.16\frac{C(1-\lambda_i)^2}{2(1-y_i)} + 0.66\frac{(Y/(1-L/C))^2}{2q_i\left(1-Y/(1-L/C)\right)} - 0.79\left(\frac{C}{q_i^2}\right)^{\frac{1}{3}}\left(\frac{Y}{1-\frac{L}{C}}\right)^{2+5\lambda} \quad (4.27)$$

The assumption for the optimization cycle length model is that the total delay of all the phases should be minimized, which is given as

$$Min\ d_{total} = Min\sum_i q_i d_i \quad (4.28)$$

Where d_{total} represents the total delay time of all phases, q_i represents the traffic volume, and d_i represents the delay time of phase *i*.

As can be seen from (eq. 4.27), the total delay time d_{total} is a function of only one parameter C. Therefore, the optimum of (eq 4.28) can be found at $\partial d_{total}/\partial C = 0$

Thus, the parameter C is a gives as

$$c = \frac{1{,}45L + 3}{1 - Y} \quad (4.29)$$

where L represents the total lost time and Y represents the sum of traffic volume ratio of all phases.

According to (eq.4.24), when the saturation x_i is close to 1, the delay will tend to be infinity. It is implausible and not realistic. Thence, (eq. 4.29) does not apply to all the traffic conditions. The cycle length model should be rewritten as follows:

$$c = \frac{1{,}45L + 3}{1 - Y} \quad Subject\ to\ \ C_{min} \le C \le C_{max} \quad (4.30)$$

The C_{min} and C_{max} are discussed as follows.

When the traffic volume is low, the important consideration is the pedestrian rather than the vehicle. Therefore, the crossing time for the pedestrian should be focussed on. The minimum green time for the pedestrian crossing on the street is given as

$$g_{min} = 7 + \frac{L_P}{v_P} \tag{4.31}$$

where L_P represents the length of the crossing street for the pedestrians; v_p represents the average speed of the pedestrian. Therefore, the cycle length can be calculated as

$$C_{min} = \sum_i \left(7 + \frac{L_P}{v_p}\right) + L \tag{4.32}$$

L represents the total lost time.

When the traffic flow is crowded, saturation is large and it is no longer able to solve the problem of traffic congestion by an optimal cycle length. Thus, the main factor for determining the cycle length should focus on avoiding the anxiety of drivers for waiting a long time. Therefore, the suggested optimization cycle length is 180 seconds, that is C_{max}=180.

In summary, the optimization traffic signal cycle length model is given as

$$c = \frac{1{,}45L + 3}{1 - Y} \quad Subject\ to \quad C_{min} \leq C \leq C_{max} \tag{4.33}$$

With

$$C_{min} = \sum_i \left(7 + \frac{L_P}{v_p}\right) + L \tag{4.34}$$

$$C_{max} = 180$$

Note that the development process of optimization traffic single cycle length model is not dependent on any particular phase-control scheme. Therefore, it is for 2-phase, 3-phase and 4-phase-control signalized intersection.

The green time for the above three case is determined as follows

The total green time is g_{totat}= C- L; thus the green time for phase I is given as:

$$g_i = g_{min,i} = 7 + \frac{L_{p,i}}{v_{p,i}} \ for\ c = C_{min} \tag{4.35}$$

$$g_i = (C - L)\frac{y_i}{Y} \ for\ c = C, c = C_{min}, subject\ to\ g_i \geq g_{min,i}$$

CHAPTER 5

CASE OF STUDY: CITY OF BARI

The application environment for the traffic estimation needs to be as realistic as possible since the same process applied to theoretical data could be applied also to real data. Thus, the main requirements that the simulation model needs to fulfill are: assigning trips based on an accurate demand model; being dynamic, so that the impact of spillback is taken into consideration; finally, including characteristics of real driver's behavior, such as gap acceptance, preferred speed, lane-changing and car-following choices. Furthermore, traffic lights should be included, in order to have both controlled and priority intersections, such as in real networks.

We have considered a five-way signalized intersection in the city of Bari (Italy). The first way consists of three lanes eastbound and two lanes westbound (via Omedeo); both the second and third way are made of two lanes northbound and two lanes southbound (via Amendola), fourth way consists of two lanes eastbound and two lanes westbound (Ponte Padre Pio), while the fifth one is made of one lane eastbound and one lane westbound (Str. Privata Stoppelli) as shown in Figure 5.1 and Figure 5.2. Note that the fourth way is the ramp of a bridge, and the fifth passes under that bridge for a U-turn.

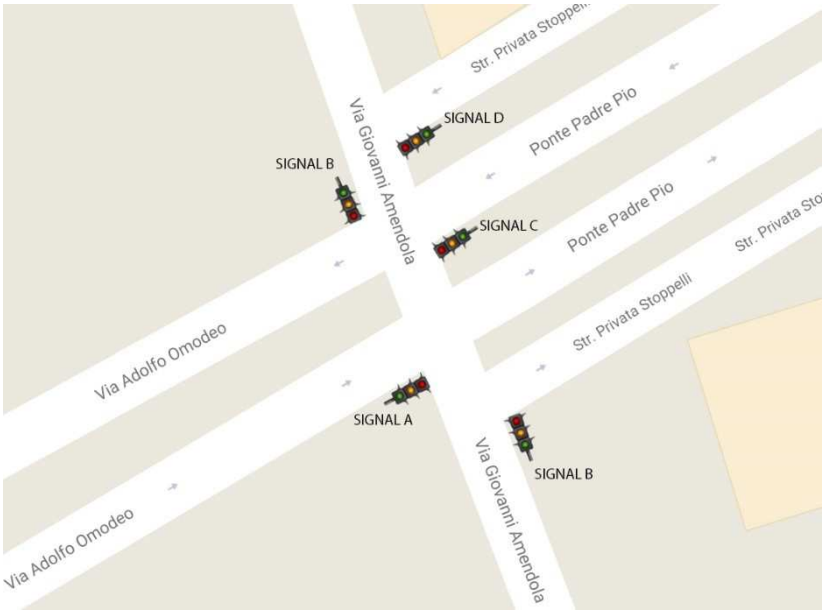

Fig. 5.1 Signalized intersection in the city of Bari (Italy).

Fig. 5.2 Signalized intersection in the city of Bari (Italy).

The intersection is controlled by a traffic light with a total cycle time of 102 seconds. Figure 5.3 shows the green times of the respective traffic lights and Figure 5.4 shows the respective phases

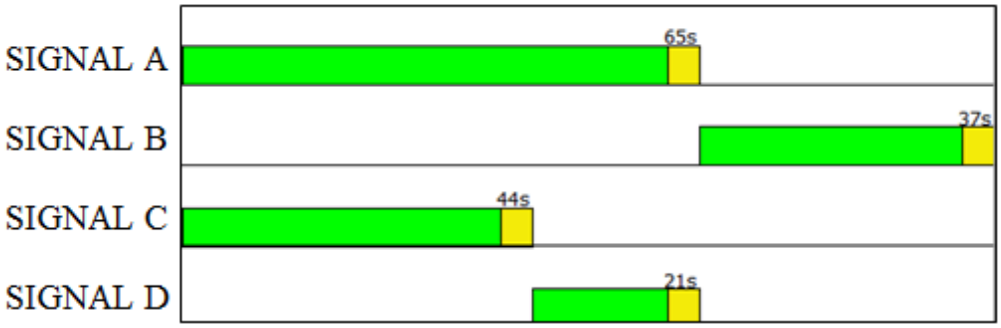

Fig. 5.3 Cycle length

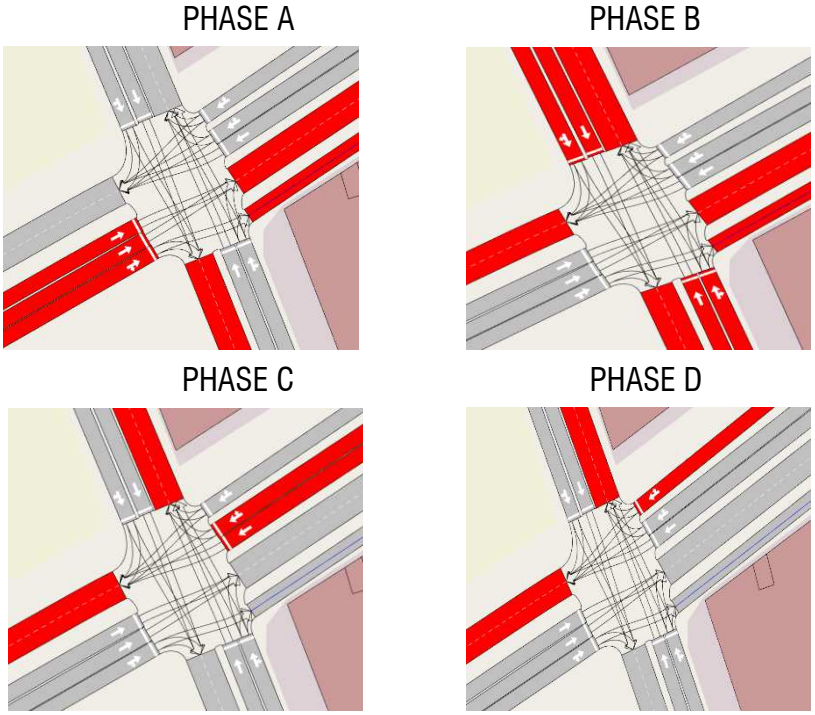

Fig. 5.4 Phases of traffic lights

5.1 Lane Identification Through a Gps Smartphone

For this model, we have considered the GPS track data relative to two main roads converging to a signalized intersection in the city of Bari (Italy). The first road consists of three lanes eastbound, while the second one consists of two lanes in the westbound. GPS track data have been acquired using a *connected vehicle* equipped with an Android smartphone. The acquired database consists of 86 runs (54 on the two-lane road, 32 on the three-lane road) with 1 Hz of data acquisition frequency.

Fig. 5.5 Construction of virtual sections for the two-lane road.

Figure 5.5 shows the five virtual sections (VSs) considered for each road, where the first section is the farthest one from the intersection stop line. Figure 5.6 and 5.7 report the acquired GPS tracks relative to each run for each considered road. Blue points refer to the GPS points projected on each associated virtual section according to Eq. 3.

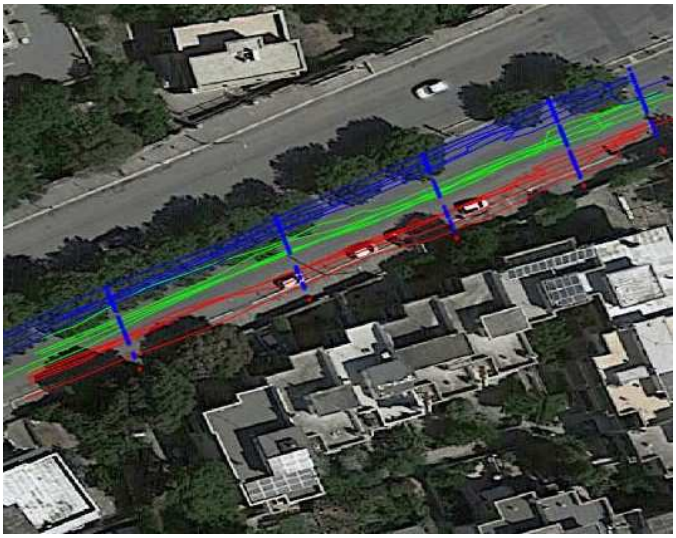

Fig. 5.6. The considered roads with three lanes and recorded GPS tracks.

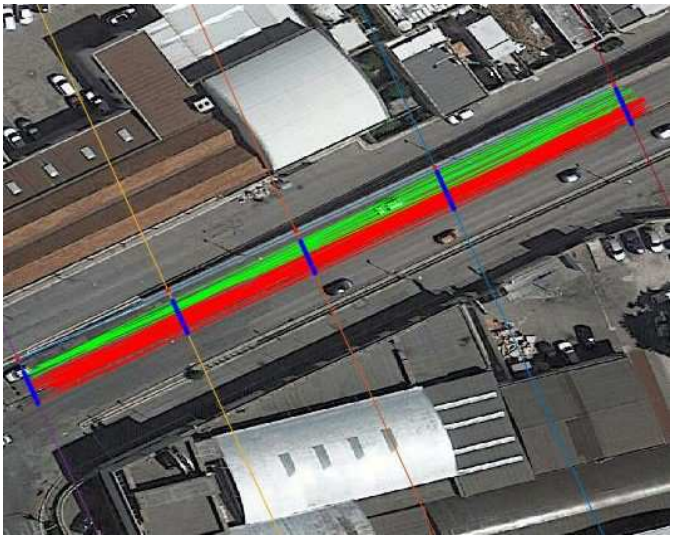

Fig. 5.7. The considered roads with two lanes and recorded GPS tracks.

To calibrate the fuzzy parameters related to lanes' membership functions, we have used a dataset made of 50% of the overall acquired data (calibration set). The remaining 50%

(validation set) has been used to validate the identification performances of the proposed method.

In Table 5.1 and 5.2, the results of the calibrated parameters μ and σ of the membership function are reported for each lane in correspondence of each considered virtual section.

Table 5.1. Resulting calibrated parameters μ and σ of the membership function for the road with 2 lanes

	Lane 1		**Lane 2**	
	σ	**μ**	**σ**	**μ**
VS_1	0.19	0.69	0.13	0.27
VS_2	0.18	0.68	0.12	0.27
VS_3	0.19	0.72	0.08	0.34
VS_4	0.25	0.75	0.08	0.34
VS_5	0.27	0.79	0.08	0.34

Table 5.2. Resulting calibrated parameters μ and σ of the membership function for the road with 3 lanes

	Lane 1		**Lane 2**		**Lane 3**	
	σ	**μ**	**σ**	**μ**	**σ**	**μ**
VS_1	0.18	0.25	0.14	0.61	0.08	0.85
VS_2	0.17	0.24	0.13	0.61	0.08	0.87
VS_3	0.16	0.25	0.11	0.58	0.11	0.89
VS_4	0.11	0.22	0.13	0.55	0.16	0.91
VS_5	0.11	0.28	0.08	0.55	0.16	0.77

In Figures 5.8 and 5.9, the two-lane and three-lane routes are reported, the membership functions obtained by the calibration process described above.

We compared the proposed method with two well-known clustering methods: Fuzzy C-means (FCM) and K-means. Table 5.3 shows the lane identification error ε obtained by the proposed method and by the FCM and K-means methods. We can observe that the proposed method outperforms the other clustering techniques for both calibration and validation set.

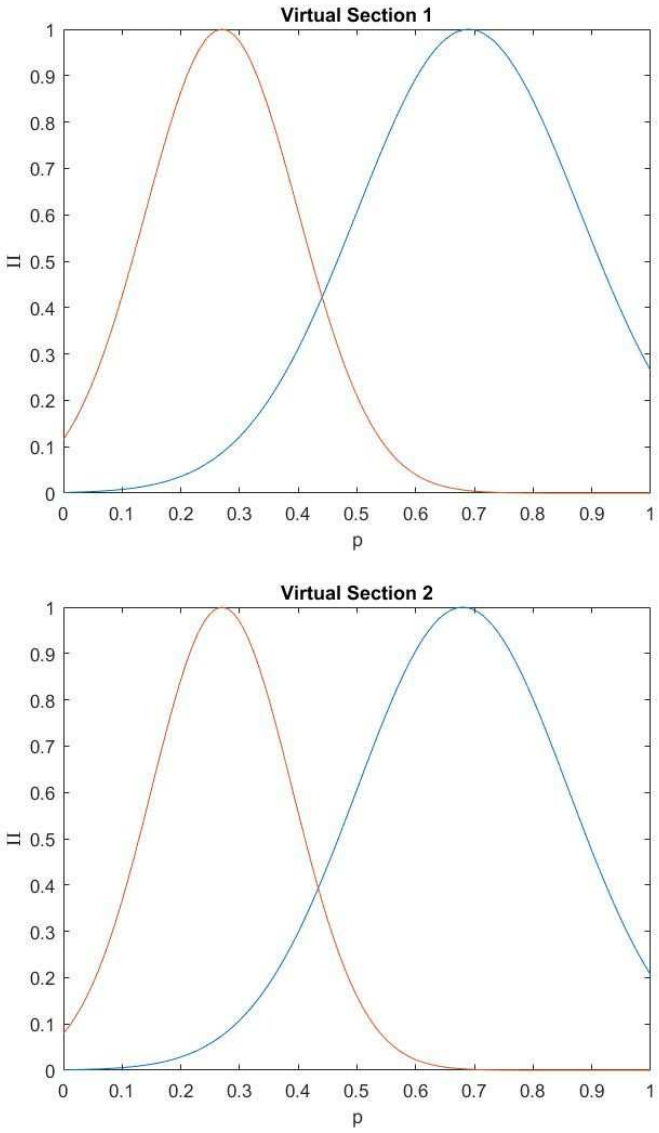

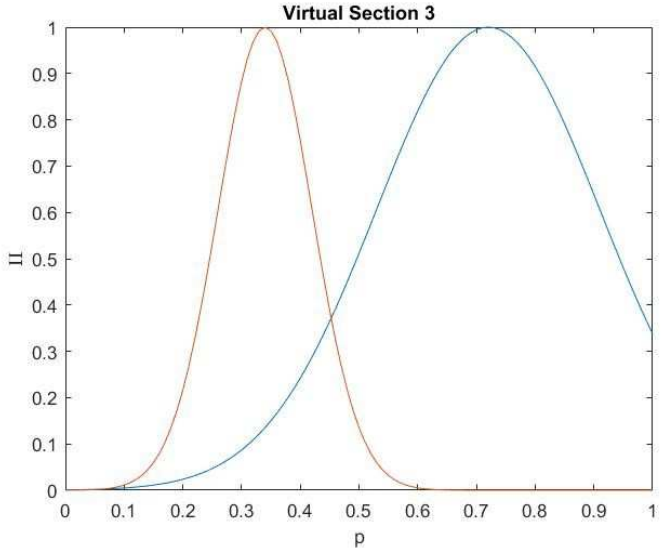
Virtual Section 3
Π
p
0
0.1
0.2
0.3
0.4
0.5
0.6
0.7
0.8
0.9
1

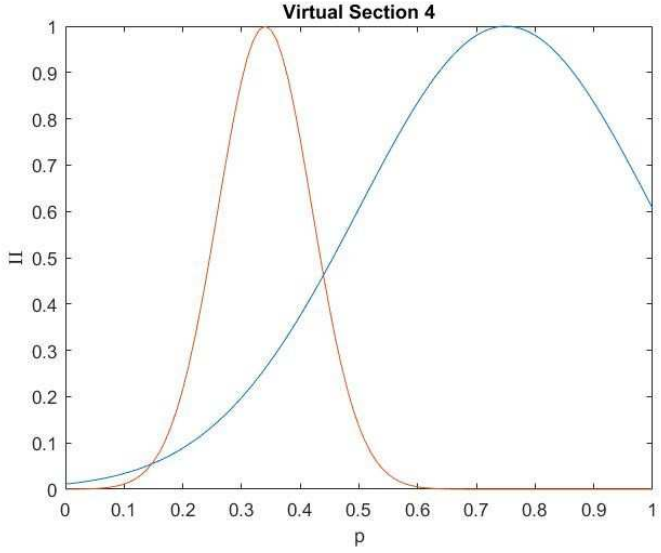
Virtual Section 4
Π
p
0
0.1
0.2
0.3
0.4
0.5
0.6
0.7
0.8
0.9
1

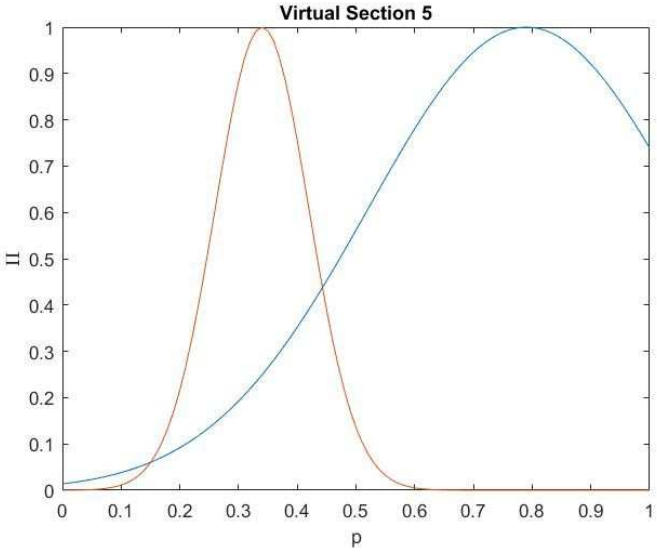

Fig. 5.8. Membership functions related to a virtual section for the two-lane road

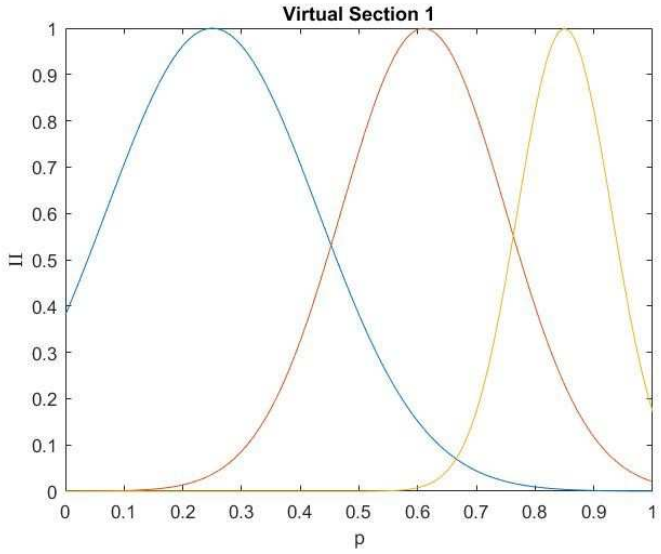
Virtual Section 1
Π
p
0
0.1
0.2
0.3
0.4
0.5
0.6
0.7
0.8
0.9
1

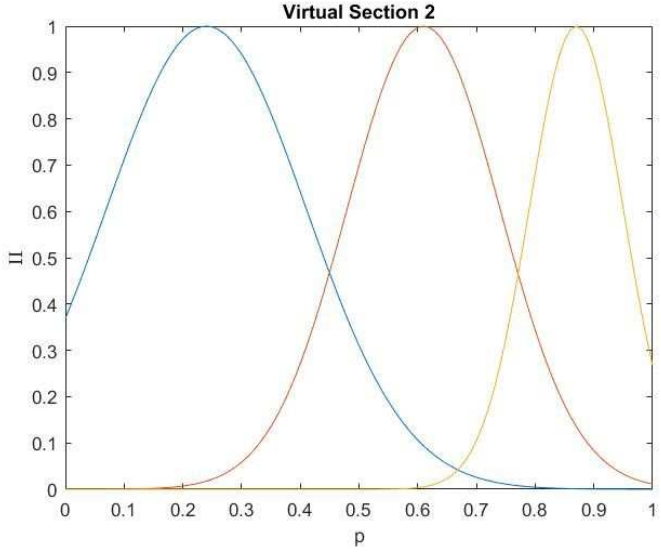
Virtual Section 2
Π
p
0
0.1
0.2
0.3
0.4
0.5
0.6
0.7
0.8
0.9
1

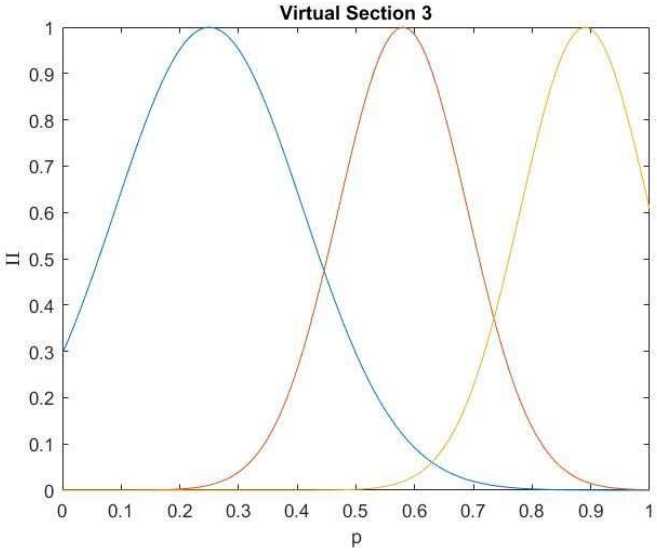
Virtual Section 3
Π
p
0
0.1
0.2
0.3
0.4
0.5
0.6
0.7
0.8
0.9
1

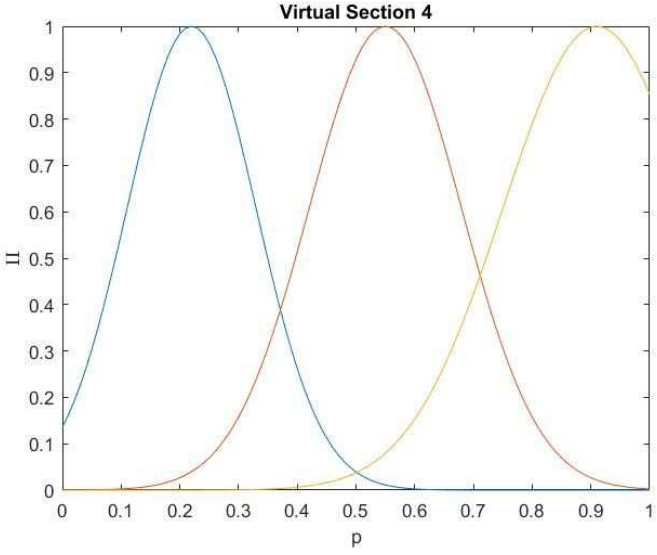
Virtual Section 4
Π
p
0
0.1
0.2
0.3
0.4
0.5
0.6
0.7
0.8
0.9
1

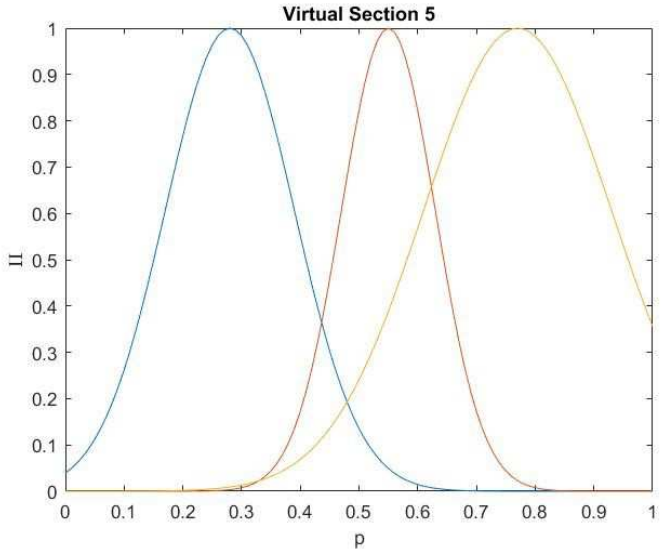

Fig. 5.9. Membership functions related to a virtual section for the three-lane road

Table 5.3. Comparison of the proposed method with C-means and K-means clustering methods

ROAD	VS	Calibration set			Validation set		
		Proposed method	FCM	K-means	Proposed method	FCM	K-means
3 LANES	1	9.10%	18.20%	19.30%	8.82%	75.90%	72.99%
	2	2.30%	27.60%	28.70%	1.08%	66.25%	60.63%
	3	0.00%	29.80%	30.60%	0.00%	70.25%	62.13%
	4	0.00%	43.10%	44.00%	3.05%	56.66%	60,48%
	5	0.00%	13.30%	14.50%	9.49%	89.11%	90.57%
2 LANES	1	2.22%	12.80%	13.33%	10.07%	23.17%	26.63%
	2	4.82%	5.97%	6.02%	7.77%	12.86%	14.06%
	3	0.00%	0.00%	0.00%	3.38%	11.85%	11.12%
	4	0.00%	0.00%	0.00%	1.08%	10.68%	10.66%
	5	0.00%	5.18%	5.26%	1.97%	9.37%	10.05%

5.2 Macroscopic Model for Traffic Flow Estimation

We have considered the same four-way signalized intersection in the city of Bari (Italy) in Figure 5.10.

GPS track data have been acquired using a vehicle equipped with an Android smartphone. The acquired database consists of 250 runs with 1 Hz of data acquisition frequency and has a 2,5% of penetration rate. The penetration rate is defined as the number of equipped vehicles divided by the total number of equipped and unequipped vehicles.

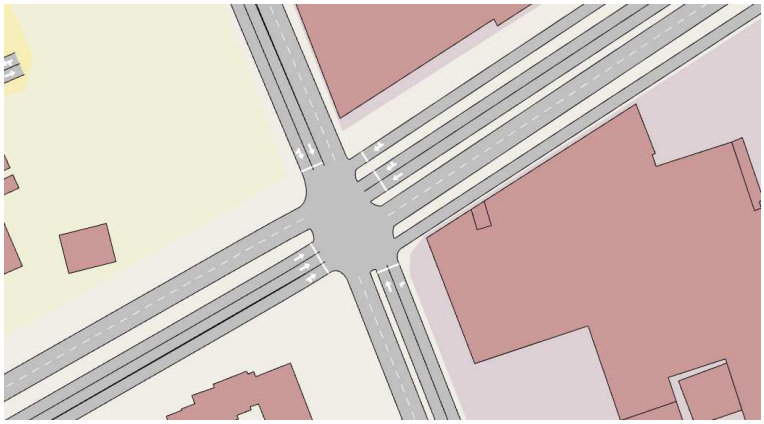

Fig. 5.10. Resulting membership functions related to a virtual section for (a) two-lane and (b) three-lane road.

5.2.1 Data processing

The Gps information was processed as follows. First, we selected for the survey a direction in the considered intersection, its associated signal phase, and a specific time interval, for example, 8-9, 12-13, and 17-18. Then, based on the CV trajectories, we selected the GPS data associated with those direction and time period and prepared the

corresponding data about the signal statuses. On the other hand, based on road geometry, we calculated from GPS positions the CVs' longitudinal position along the road, and generate time-space trajectories as shown in table 5.4. To calculate the waiting time and the length of the queue, we need to locate the first point at zero speed and the last point provided by GPS. The difference provides the value of the waiting time and the value of the queue length as shown in Figure 5.11.

Table 5.4. Gps data tracks.

Latitude	Longitude	Altitude	Speed (Km/h)	Timestamp	Date & Time
41.105.232	16.886.427	212.9	10.33	9	2017-07-14 08:11:07:532
41.105.255	16.886.412	209.68	10.33	1009	2017-07-14 08:11:08:532
411.053	16.886.404	206.45	13.28	2009	2017-07-14 08:11:09:532
4.110.535	1.688.638	209.68	19.08	3009	2017-07-14 08:11:10:532
41.105.404	16.886.356	209.68	23.29	4009	2017-07-14 08:11:11:532
4.110.547	16.886.324	206.45	28.26	5009	2017-07-14 08:11:12:532
41.105.553	16.886.284	206.45	30.6	6009	2017-07-14 08:11:13:532
4.110.563	16.886.248	206.45	30.6	7009	2017-07-14 08:11:14:532
41.105.698	16.886.204	203.23	31.36	8009	2017-07-14 08:11:15:532
41.105.793	16.886.164	200.0	36.0	9009	2017-07-14 08:11:16:532

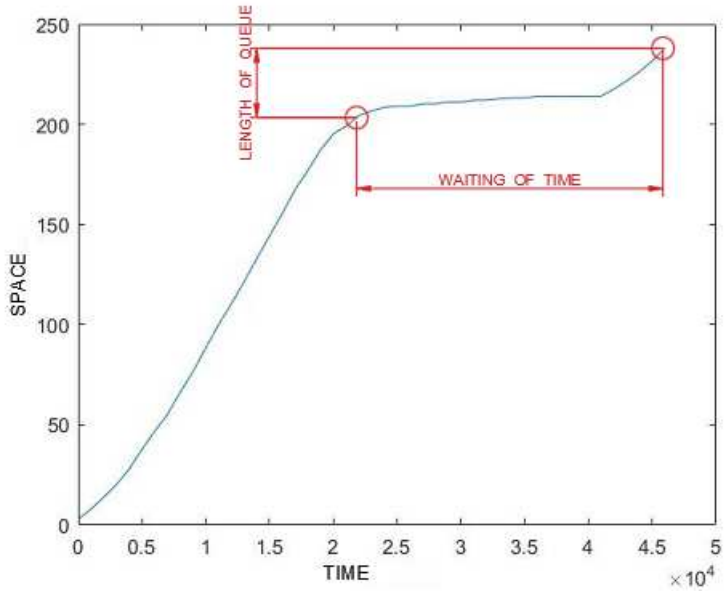

Fig. 5.11. Time space trajectories diagram

5.2.2 Traffic flow estimation model

As described in the previous chapter, once known the length of the queue for each run, we determined the vehicular density for a stretch of 500 m (Fig 5.12)

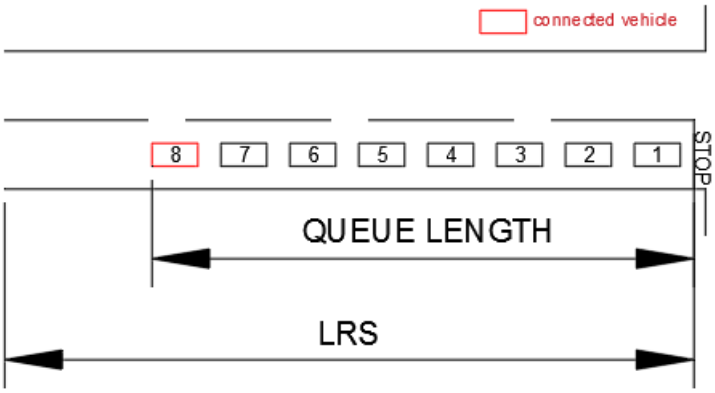

Fig. 5.12. Queue length evaluation according to connected vehicle position

Figures 5.12 and 5.13 show the traffic flow pattern according to the tracks recorded in the time interval 8-9 AM in the lane 1(Fig. 5.13) and lane 2(Fig 5.14) of via Amendola.

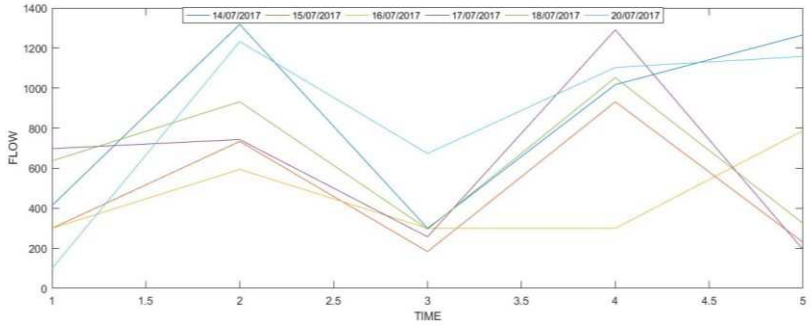

Fig. 5.13. Diagrams of Traffic flow estimation with connected vehicle in the time interval 8-9 AM in via Amendola, lane 1

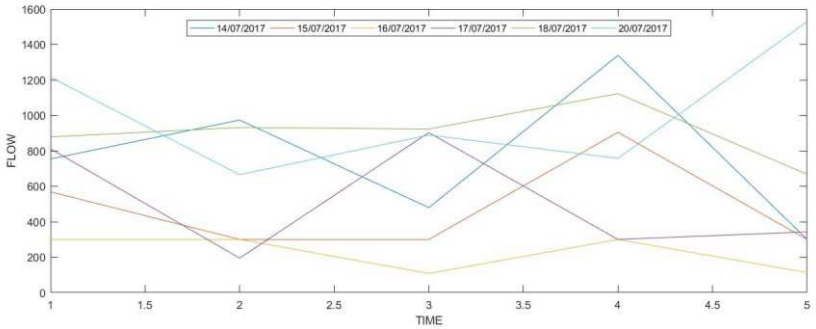

Fig. 5.14. Diagrams of Traffic flow estimation with connected vehicle in the time interval 8-9 AM in via Amendola, lane 2

5.2.3 Calibration With Greenshields Model

In section 4.2.1, the eqs. 4.17 and 4.18 correlate density, flow, and speed according to the Greenshields model. The relations are recalled below:

$$v = v_f - \frac{v_f}{k_j} * k$$

where v is the average speed at density k, v_f is the free-flow speed and k_j is the jam density.

$$q = v_m * k - \frac{v_m}{k_{max}} * k^2$$

$$q = k_j * v - \left(\frac{k_j}{v_f}\right) * v^2$$

where k_{max} is the maximum density, calculated as the maximum number of vehicles of 5.5 meters long in the 500 meters, equal to 90.
The free flow speed of 50 km/h, the average speed is equal to the average of the observed speeds.
Figures 5.15, 5.16, 5.17 show how the estimated data fit the Greenshields model.
Another results are shows In the Annex 1

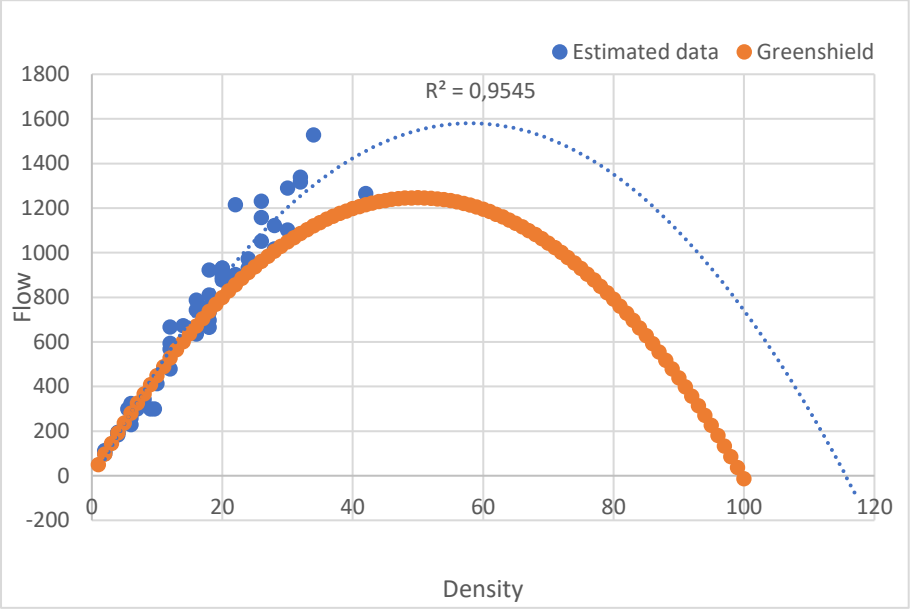

Fig. 5.15. MFD Density- flow at 8-9 AM in Via Amendola northbound

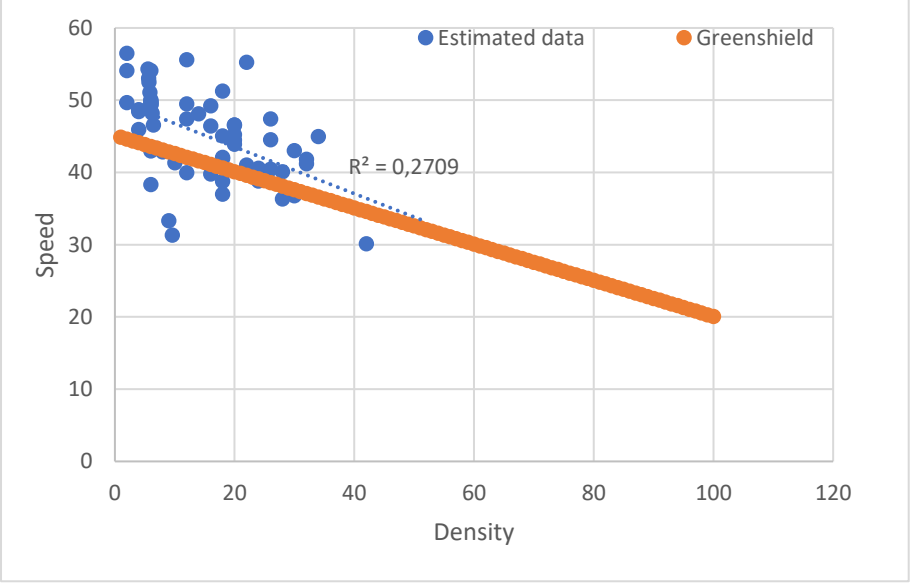

Fig. 5.16. MFD Density- Speed at 8-9 AM in Via Amendola northbound

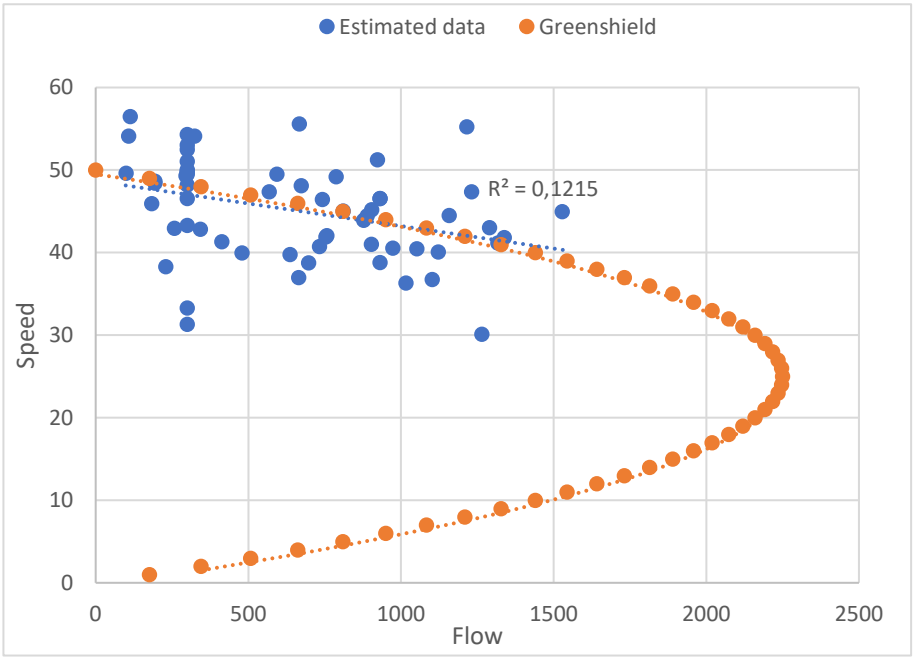

Fig. 5.17. MFD Flow - Speed at 8-9AM in Via Amendola northbound

The relationship between flow and density is the best fitted (Fig. 5.15). For the other ones (Fig. 5.16 and Fig. 5.17), it should be noted that there is a remarkable split of data, but their trends follow the Greenshields curves. Graphs for other lanes and other time intervals (12-13 and 17-18) are given in Annex 1.

5.3 Optimization with Webster method and simulation with Aimsun software

In this section, first, we have built the Origin-Destination (O-D) matrix, whose table 5.5 shows an example, where the flows used to build the matrix correspond to the estimated flows, obtained from the traffic estimation model previously described.
From the results obtained, we have highlighted the different traffic flows for different times of passing of the connected vehicle.
We carried out a day-by-day estimation of flows at each passing of a connected vehicle and determined the respective O-D matrix. Due to the big amount of data, we chose to

analyze in this work only one day, namely July 14th, 2017. All matrices obtained are shown in Annex 2.

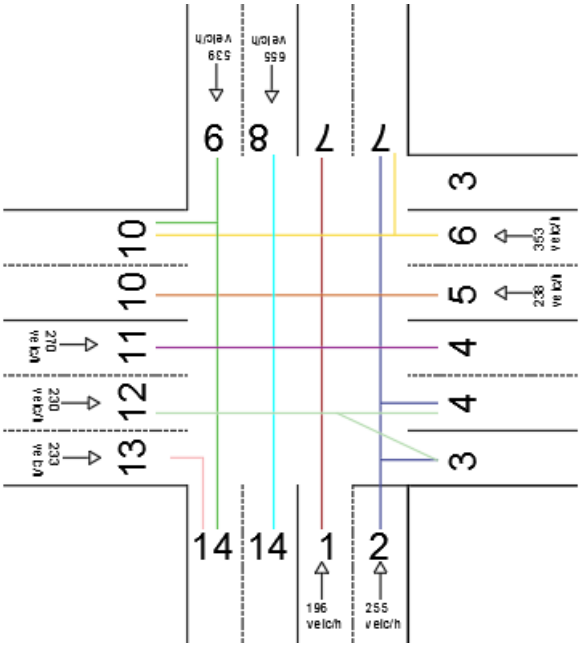

Fig. 5.18. Intersection analyzed and possible turning maneuvers

The figure 5.18 shows the intersection analyzed, the lanes numbered as traffic centroids and the possible turning maneuvers for each lane. Therefore, after estimating the flows of each lane, we calculated the percentages of turns through the available video data. Considering lane 2, we determined that 10% of the total flow turned toward lane 3, 30% turning toward lane 4 and the remaining 60% moved straight ahead towards lane 7. Similarly, for lane 6, 30% turned toward lane 7, while the remaining 70% moved straight ahead towards lane 10. For lane 12, we determined 30% turning toward lane 3 and the remaining 70% moving straight ahead towards lane 7. The incoming flow in lane 3 is redistributed by 30% to lane 7 and the remaining 70% to lane 10.

Table 5.5. O/D matrix

	1	2	3	4	5	6	7	8	9	10	11	12	13	14
1	0	0	0	0	0	0	777	0	0	0	0	0	0	0
2	0	0	62	185	0	0	370	0	0	0	0	0	0	0
3	0	0	0	0	0	0	18	0	0	74	0	0	0	0
4	0	0	0	0	0	0	0	0	0	0	0	0	0	0
5	0	0	0	0	0	0	0	0	0	238	0	0	0	0
6	0	0	0	0	0	0	35	0	0	318	0	0	0	0
7	0	0	0	0	0	0	0	0	0	0	0	0	0	0
8	0	0	0	0	0	0	0	0	0	0	0	0	0	589
9	0	0	0	0	0	0	0	0	0	166	0	0	0	388
10	0	0	0	0	0	0	0	0	0	0	0	0	0	0
11	0	0	0	270	0	0	0	0	0	0	0	0	0	0
12	0	0	30	200	0	0	0	0	0	0	0	0	0	0
13	0	0	0	0	0	0	0	0	0	0	0	0	0	333
14	0	0	0	0	0	0	0	0	0	0	0	0	0	0

The figure 5.18 shows the centroids considered for the construction of the O/D matrix and figure 5.19 reports a snapshot of the simulation carried out with the software Aimsun

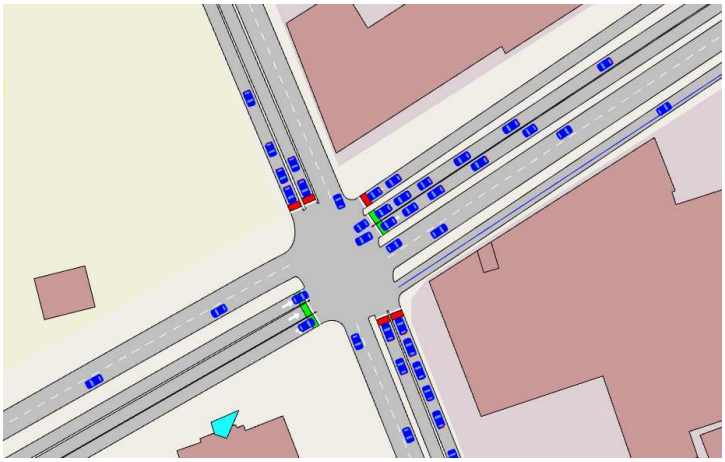

Fig. 5.19. Snapshot of the simulation carried out with the software Aimsun

We have optimized the traffic lights cycle length through Webster's method. The method imposes that the total delay of all phases is minimized, as given by eq. 4.28:

$$Min\ d_{total} = Min \sum_i q_i d_i$$

We recall that d_{total} is the total delay time of all phases; q_i is the traffic volume, and d_i is the delay time of phase *i*.

The parameter C is given by eq 4.29 :

$$c = \frac{1{,}45L + 3}{1 - Y}$$

where L is the total lost time and Y is the sum of traffic volume ratio of all phases.

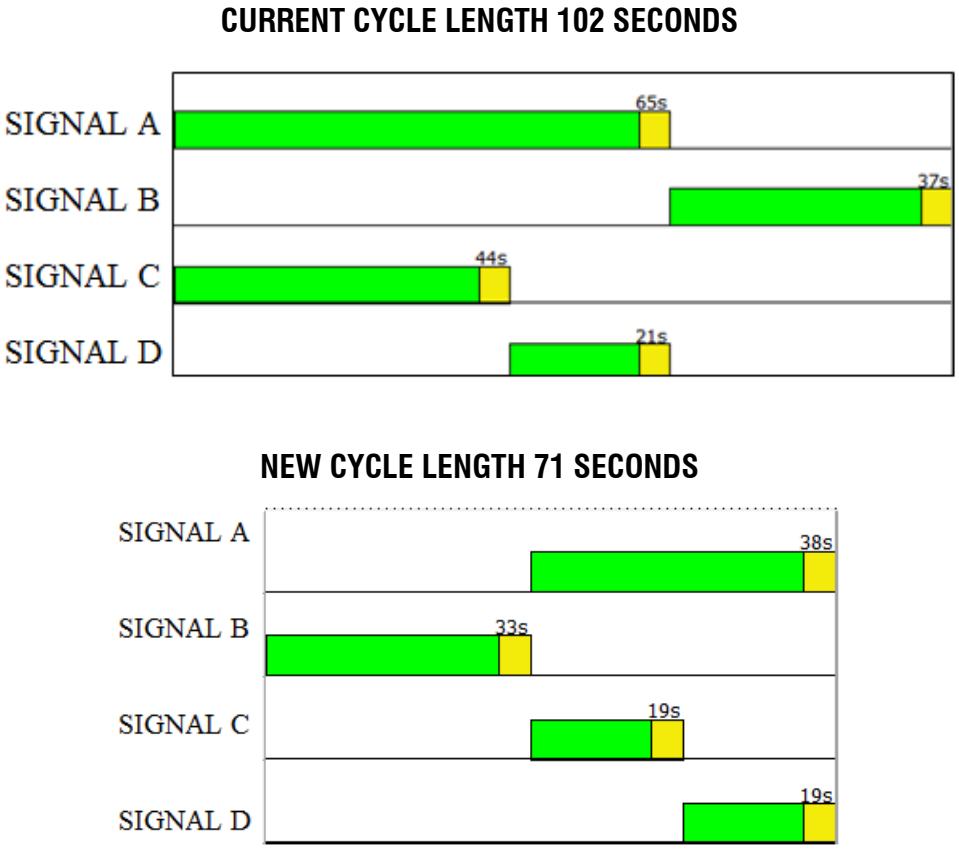

Fig. 5.20. Cycle and phases of traffic lights

The total time of new cycle we obtained through Webster's optimization model is 71 s while the time of the current cycle is 102 s. The Figure 5.20 shows the new traffic lights cycle and the new phases. It can be noticed that the after-optimization time for light B is 33 s compared to 37 s of the current situation. The time for light A, after optimization is equal to 38 s; instead, in the current situation is 65 s.

Finally, we run again the simulation, to evaluate the improvements obtained.

We have analyzed the following indicators:

- *Delay time:* average delay time per vehicle per kilometer. This is the difference between the expected travel time (the time it would take to traverse the system under ideal conditions) and the travel time. It is calculated as the average of all vehicles and then converted into time per kilometer. It does not include the time spent in virtual queue;
- *Density:* average number of vehicles per kilometer for the whole network;
- *average queue:* average queue in the network during the simulation period. It is measured in number of vehicles;
- *Speed:* average speed for all vehicles that have left the system. This is calculated using the mean journey speed for each vehicle;
- *Stop time:* average time at standstill per vehicle per kilometer;
- *Total number of Stops:* total number of stops in the network during the simulation period;
- *Total travel time:* total travel time experienced by all the vehicles that have crossed the network. It does not include the time spent in virtual queue;
- *Travel Time:* average time a vehicle needs to travel one kilometer inside the network. This is the mean of all the single travel times (exit time - entrance time) for every vehicle that has crossed the network, converted into time per kilometer.

Table 5.6. Results of 1st connected vehicle

Time Series	Current cycle length	New cycle length	Improvement
Delay Time – Car [sec/km]	147.95	65.97	55%
Density – Car [veh/km]	8.67	6.17	29%
Mean Queue – Car [veh]	43.26	21.21	51%
Speed – Car [km/h]	27.69	32.31	17%
Stop Time – Car [sec/km]	124.19	49.33	60%
Total Number of Stops - Car	11292.28	9110.95	19%
Total Travel Time – Car [h]	83.36	59.45	29%
Travel Time – Car [sec/km]	214.22	132.02	38%

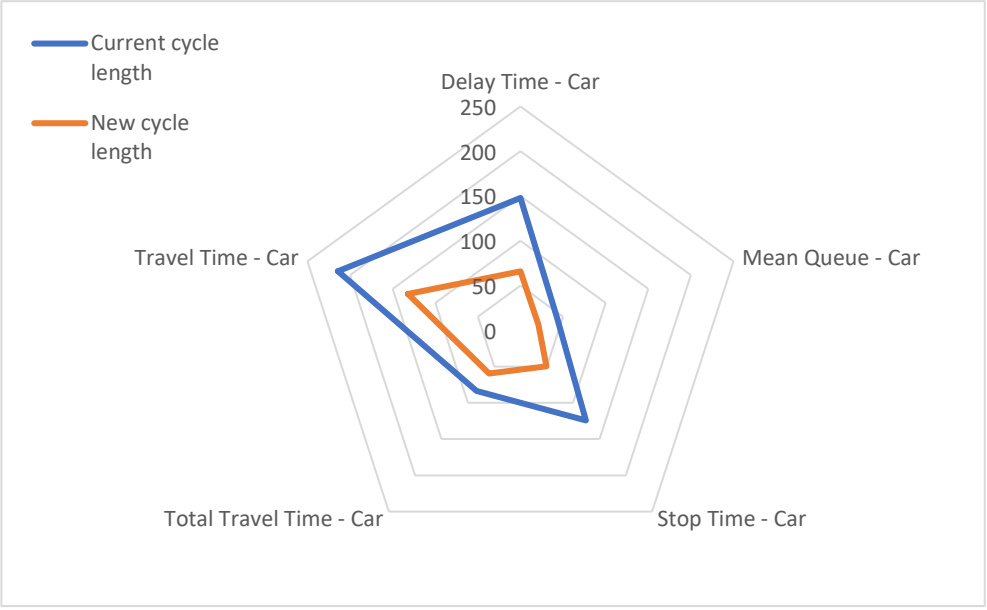

Fig. 5.21. Improvement

Table 5.6 and figure 5.21 shows the improvements for each indicator, related to the passage of the first vehicle connected, between the current scenario and the new scenario. It shows how with the new cycle we get improvements of 55% for delay time and 51% for the mean queue.

Table 5.7. Results of 2nd connected vehicle

Time Series	Current cycle length	New cycle length	Improvement
Delay Time – Car [sec/km]	121.87	56.95	53%
Density – Car [veh /km]	8.05	5.65	30%
Mean Queue – Car [veh]	38.13	18.2	52%
Speed – Car [km/h]	27.24	33.61	23%
Stop Time – Car [sec/km]	100.93	42.71	58%
Total Number of Stops - Car	10297.82	7879.08	23%
Total Travel Time – Car [h]	77.59	54.63	30%
Travel Time – Car [sec/km]	187.99	123.05	35%

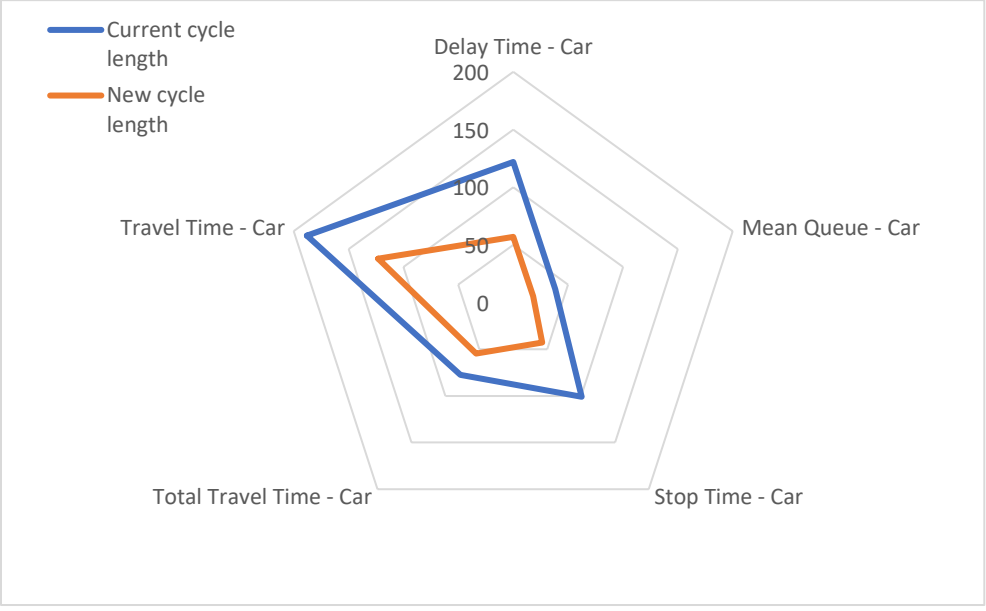

Fig. 5.22. Improvement

Table 5.7 and figure 5.22 show the improvements for each indicator, related to the passage of the second vehicle connected, between the current scenario and the new scenario. It shows how with the new cycle we get improvements of 53% for delay time and 52% for the mean queue.

Table 5.8. Results of 3rd connected vehicle

Time Series	Current cycle length	New cycle length	Improvement
Delay Time – Car [sec/km]	88.17	56.75	36%
Density – Car [veh/km]	6.56	5.7	13%
Mean Queue – Car [veh]	26.72	18.7	30%
Speed – Car [km/h]	30.36	33.71	11%
Stop Time – Car [sec/km]	71.4	43.25	39%
Total Number of Stops - Car	7923.67	7451.23	6%
Total Travel Time – Car [h]	63.33	55.09	13%
Travel Time – Car [sec/km]	154.32	122.86	20%

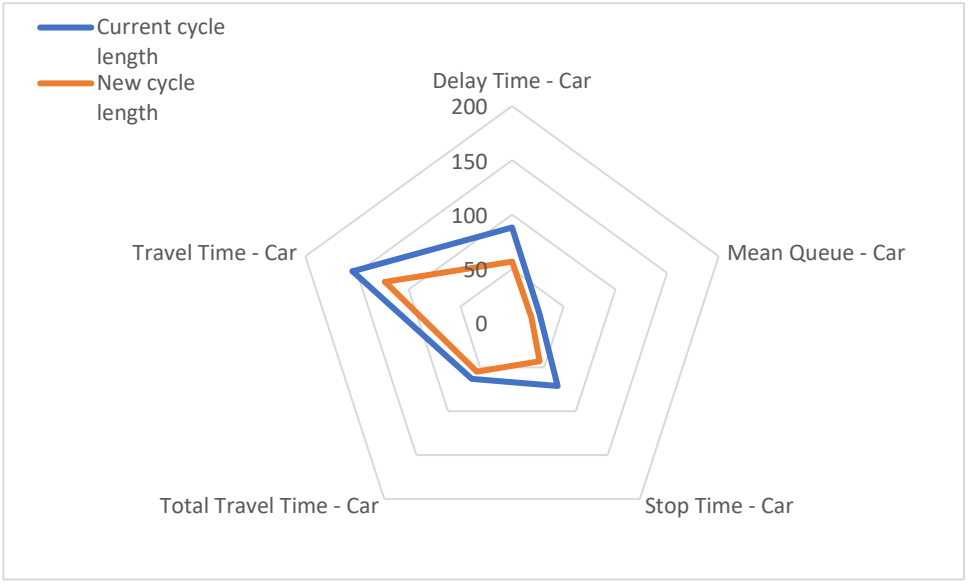

Fig. 5.23. Improvement

Table 5.8 and figure 5.23 shows the improvements for each indicator, related to the passage of the third vehicle connected, between the current scenario and the new scenario. It shows how with the new cycle we get improvements of 36% for delay time and 30% for the mean queue.

Table 5.9. Results of 4th connected vehicle

Time Series	Current cycle length	New cycle length	Improvement
Delay Time – Car [sec/km]	205.06	89.57	56%
Density – Car [veh/km]	11.3	7.25	36%
Mean Queue – Car [veh]	64.24	28.03	56%
Speed – Car [km/h]	23.56	29.64	26%
Stop Time – Car [sec/km]	172.5	67.71	61%
Total Number of Stops - Car	14387.08	11916.19	17%
Total Travel Time – Car [h]	108.22	69.42	36%
Travel Time – Car [sec/km]	271.05	155.66	43%

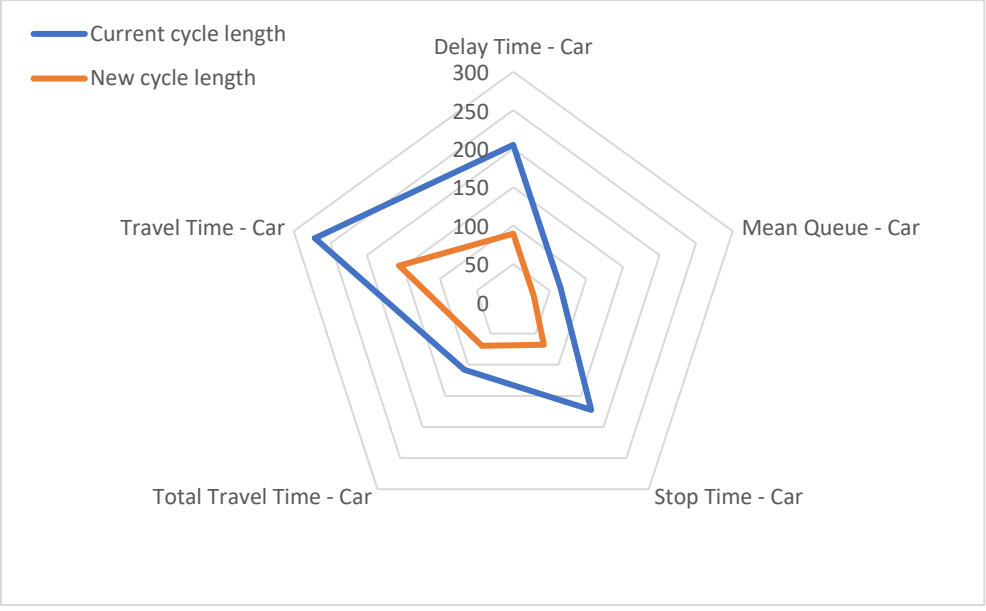

Fig. 5.24. Improvement

Table 5.9 and figure 5.24 shows the improvements for each indicator, related to the passage of the fourth vehicle connected, between the current scenario and the new scenario. It shows how with the new cycle we get improvements of 56% for delay time and 56% for the mean queue.

Table 5.10. Results of 5th connected vehicle

Time Series	Current cycle length	New cycle length	Improvement
Delay Time – Car [sec/km]	165.07	77.58	53%
Density – Car [veh/km]	9.6	7.06	26%
Mean Queue – Car [veh]	50.52	26.97	47%
Speed – Car [km/h]	25.03	30.52	22%
Stop Time – Car [sec/km]	138.53	58.84	58%
Total Number of Stops - Car	12913.24	10476	19%
Total Travel Time – Car [h]	92.11	68.07	26%
Travel Time – Car [sec/km]	231.16	143.67	38%

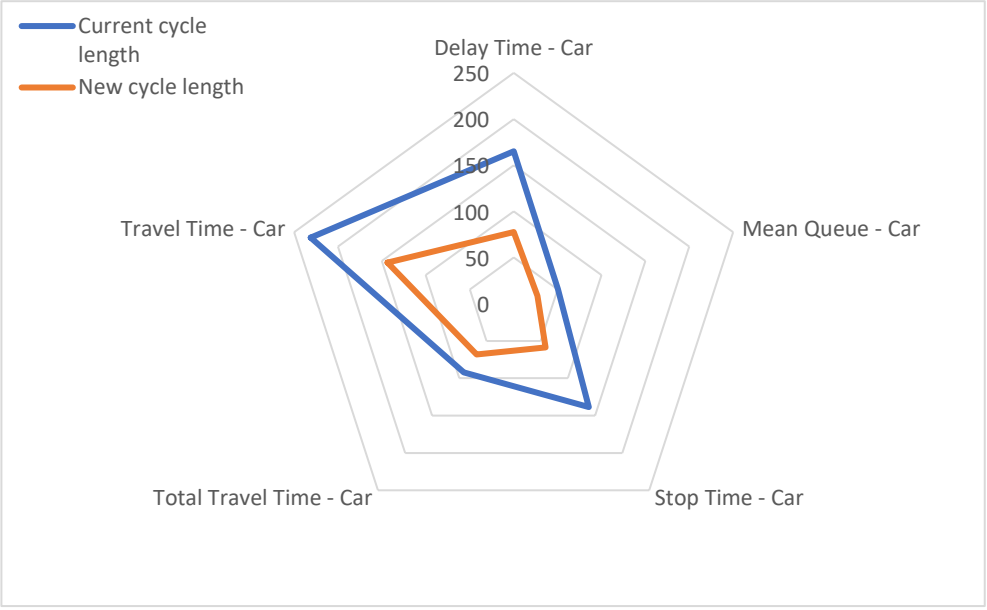

Fig. 5.25. Improvement

The results obtained show that, with the new cycle, results in substantial improvement. For example, Table 5.10 and Figure 5.25, shows the improvements for each indicator, related to the passage of the fifth vehicle connected, between the current scenario and

the new scenario. It shows how with the new cycle we get improvements of 53% for delay time and 47% for the mean queue.

The results for other time periods analyzed (12-13 and 17-18) are shown in Annex 3. Significant improvements are in all time periods. With the new 71-second cycle time, increasing the frequency, we have experienced an average improvement of 50% for delay times and 27% reduction in total travel time. We found also 47% reduction in the average length of queues and 55% reduction in stop time, as well as an average speed improvement of 18%

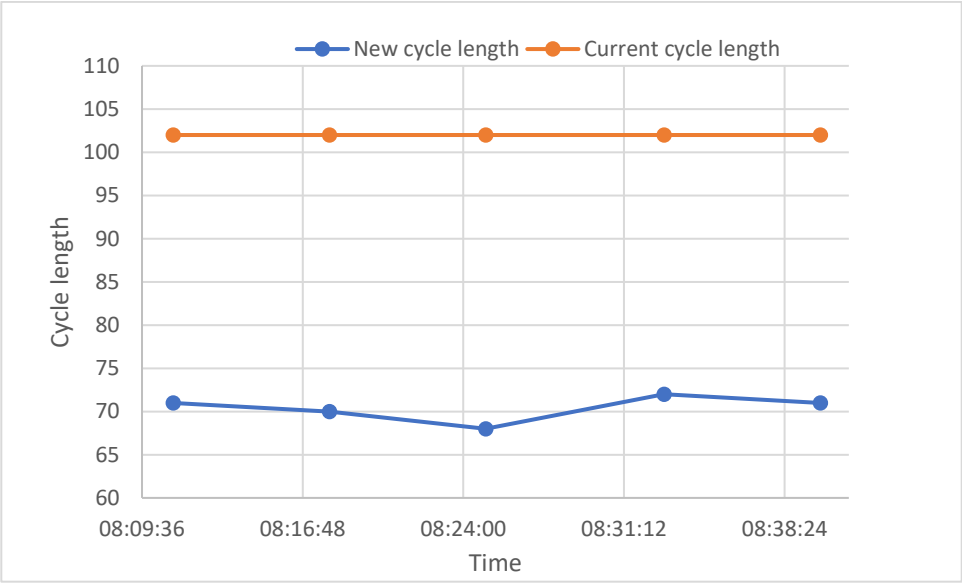

Fig. 5.26. Cycle length

Figure 5.26 shows the values of the traffic light cycles obtained from the optimization. The cycle length is around 70 s; there is a small difference between the length of 68 s, related to the passage of the third connected vehicle, and the length of 72 s, related to the fourth vehicle. As mentioned above, a significant reduction in the cycle time is achieved after optimization, from 102 s to 68 s.

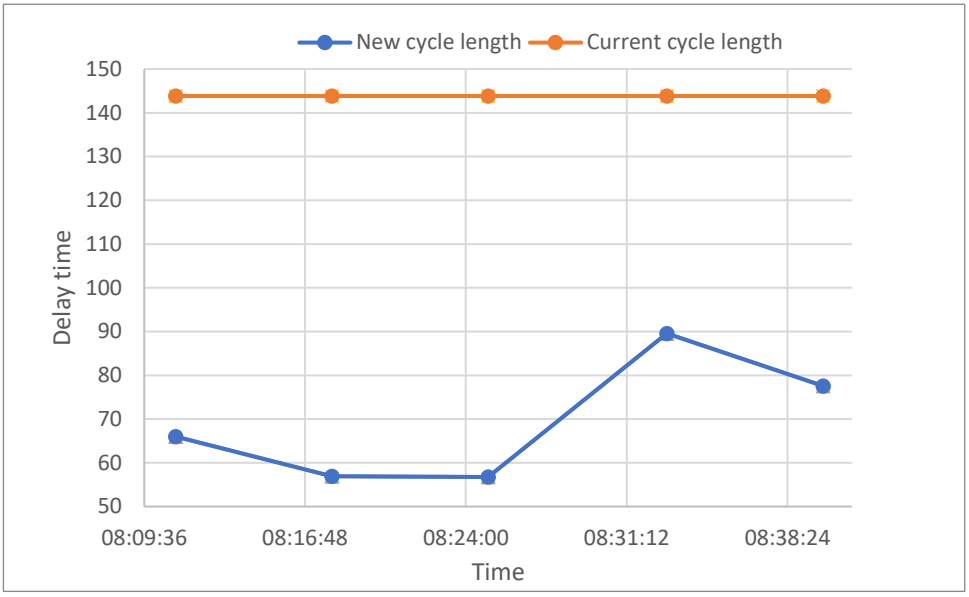

Fig. 5.27. Delay time

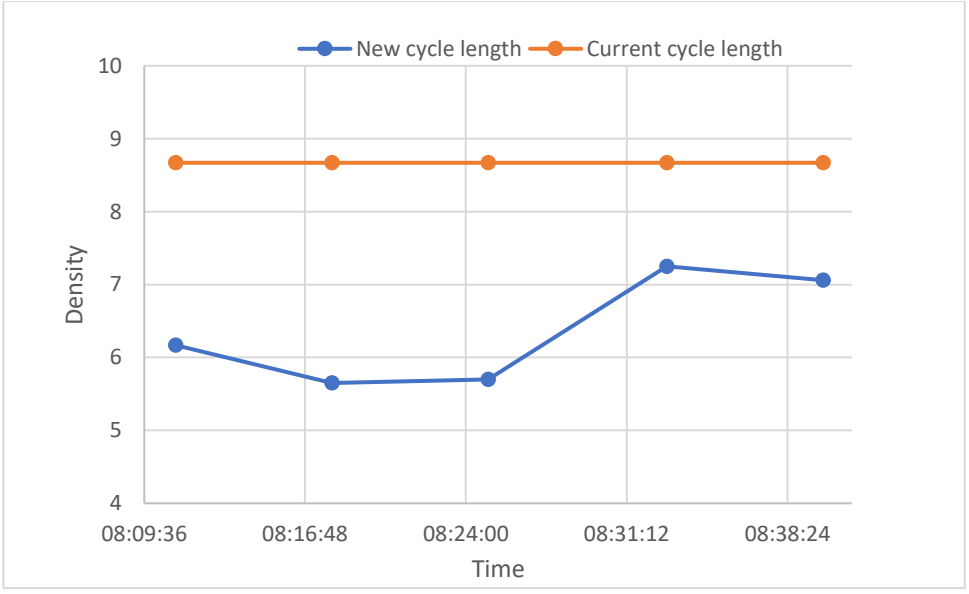

Fig. 5.28. Density

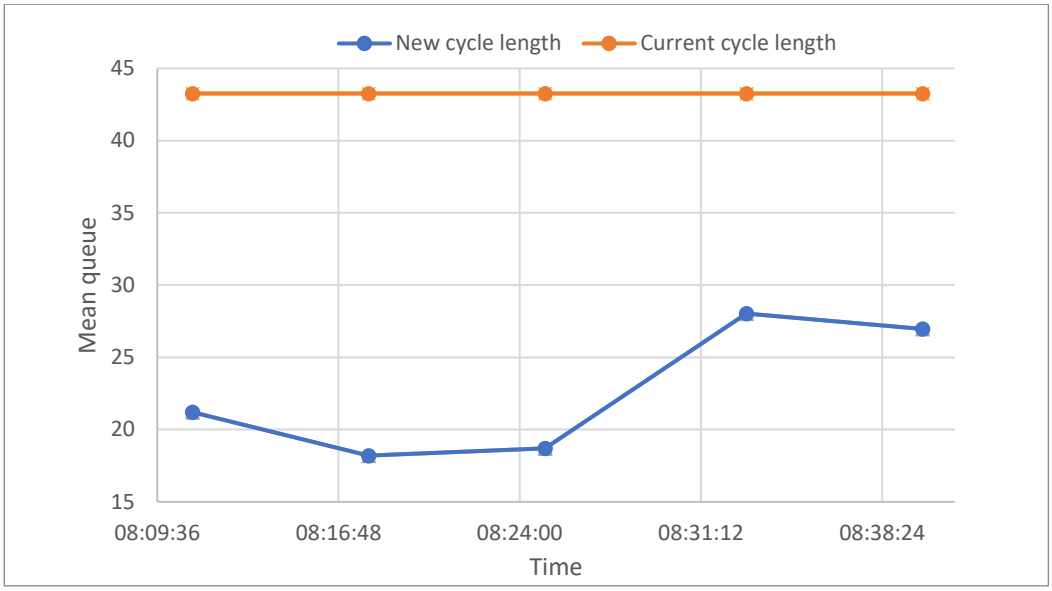

Fig. 5.29. Mean queue

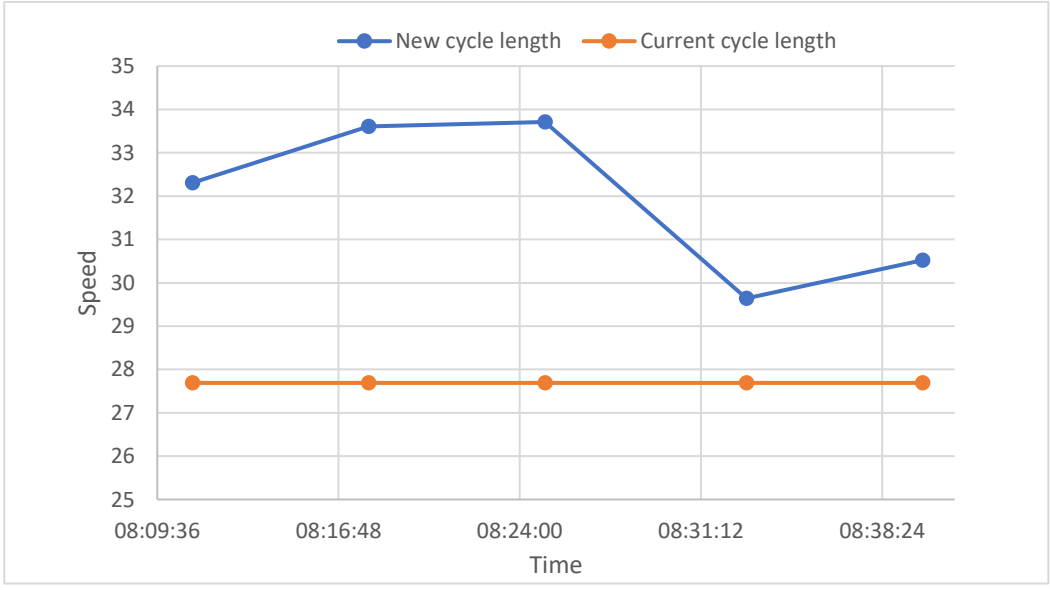

Fig. 5.30. Speed

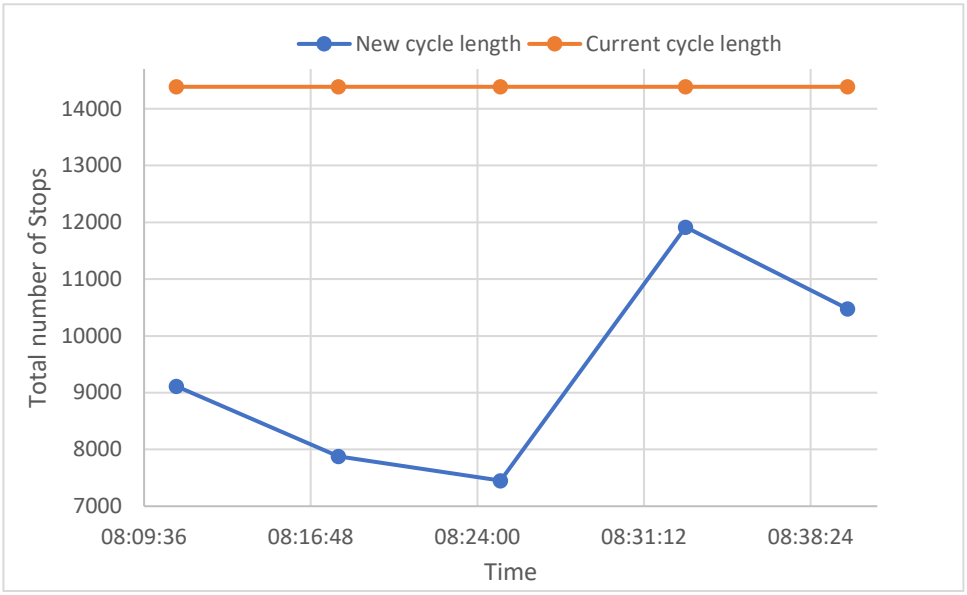

Fig. 5.31. Total number of Stops

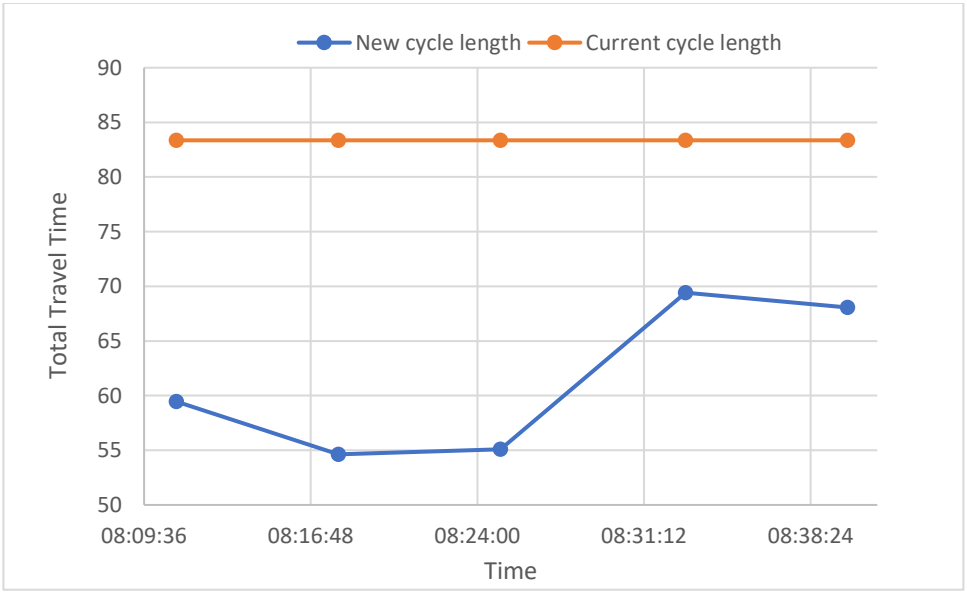

Fig. 5.32. Total travel time

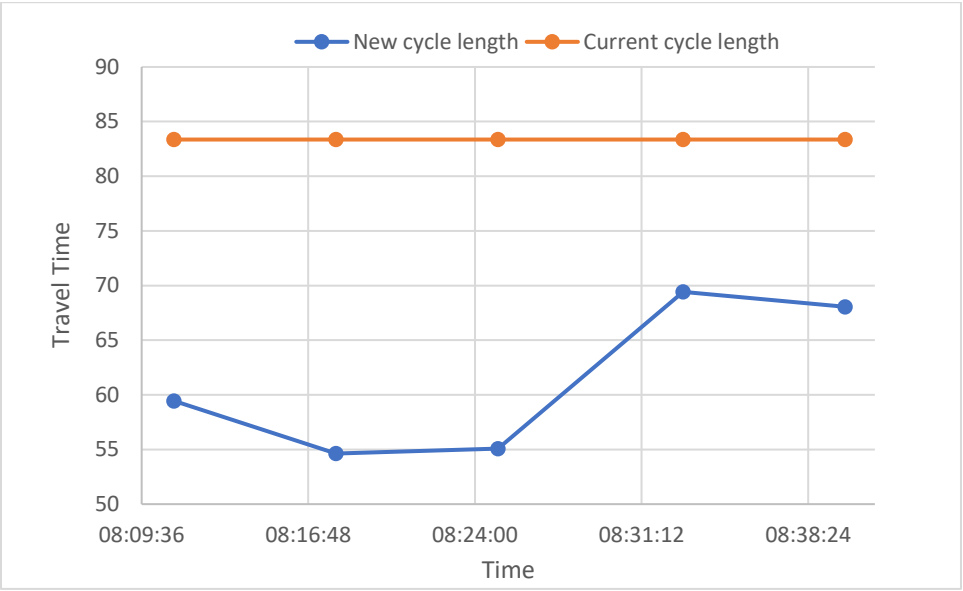

Fig. 5.33. Travel time

The values of indicators related to the new cycle are always better than those of the current state, as one can see in the above figures. In fact, almost in all figures, the values of optimized cycles are lower than the current state, except in the Fig. 5.30, in which the current speed results lower than the optimized speed.

All results obtained in time 12 a.m – 1 p.m and 5 p.m -6 pm are shows in Annex 3.

CONCLUSION

In this work, we propose a novel framework for real-time adaptive signal control using connected vehicles. This framework is composed of two new methods for lane identification and flow estimation for optimal real-time traffic signal settings. To evaluate the outcomes of the proposed method, we have studied a signalized intersection in the city of Bari (Italy), considering three main time periods: 8 a.m. – 9 a.m., 12 a.m. - 1 p.m. and 5 p.m-6 p.m. We acquired data related to location, speed, travel times and trajectories of the vehicle using a smartphone application. Smartphone devices combine the advantages of mobile sensors: low investment costs, high penetration, and high accuracy achieved by GPS receivers. In addition, GPS-enabled smartphones can provide accurately not only position but also speed and travel direction.

The first method represents a supervised clustering technique based on fuzzy sets and Genetic Algorithms. Results reveal a good accuracy in identification of the vehicle position within a lane. Thus, the proposed method allows overcoming the problems related to the "noise" that affects the measurements, and the errors related to obstruction or reflection of GPS data.

The second method estimates the traffic flow based on the queue length and has shown good results. Finally, the optimization performed applying the Webster algorithm to the estimated data obtained remarkable improvements, in some cases about 50%, in terms of delay times and reduction of average length of queues. Future developments aim at the synchronization of traffic lights and integration that model, in real ITS.

REFERENCES

Arulampalam, M., Maskell, S., Gordon, N., and Clapp, T.. "*A tutorial on particle filters for online nonlinear/non-Gaussian Bayesian tracking*". IEEE Transactions on signal processing, 50(2), 2002.

Atkinson and Castro, "*Digital Quality of Life*" 107, 2008

Ban, X., Chu, L., and Benouar, H.. "*Bottleneck identification and calibration for corridor management planning*". Transportation Research Record, 1999:40, 53, 2007.

Ban, X., Herring, R., Hao, P., and Bayen, A.. "*Delay pattern estimation for signalized intersections using sampled travel times".* In Proceedings of the 88th Annual Meeting of the Transportation Research Board, Washington, D.C., January 2009.

Ban, X., Herring, R., Margulici, J., and Bayen, A.. "*Optimal sensor placement for freeway travel time estimation*". Proceedings of the 18th International Symposium on Transportation and Traffic Theory, July 2009.

Ban, X., Li, Y., Skabardonis, A., and Margulici, J.. "*Performance evaluation of travel time methods for real time traffic applications*". In Proceedings of the 11th World Congress on Transport Research (CD-ROM), 2007.

Bar-Gera, Hillel., 2007. "*Evaluation of a cellular phone-based system for measurements of traffic speeds and travel times: a case study from Israel*". Transp. Res. Part C 15 (6), 380–391.

Bartin, B., Ozbay, K., and Iyigun, C.. "*A clustering based methodology for determining the optimal roadway configuration of detectors for travel time estimation*". Transportation Research Record, 2000:98{105, 2007.

Bellman, R. and Dreyfus, S.. Applied Dynamic Programming. Princeton University Press, 1962.

Biagioni, J., Gerlich, T., Merrifield, T., and Eriksson, J. "*Easytracker: Automatic transit tracking, mapping, and arrival time prediction using smartphones*" in Proc. ACM SenSys, 2011, pp. 1–14.

Bickel, P., Chen, C., Kwon, J., Rice, J., Van Zwet, E., and Varaiya, P.. "*Measuring traffic*". Statistical Science, 22(4):581{597, 2007.

Buisson, C. and Ladier, C. "*Exploring the impact of homogeneity of traffic measurements on the existence of macroscopic fundamental diagrams*". Transportation Research Record: Journal of the Transportation Research Board, (2124):127–136, 2009

C. Claudel and A. Bayen. Lax-Hopf based incorporation of internal boundary conditions into Hamilton-Jacobi equation. Part II: Computational methods. IEEE Transactions on Automatic Control, 55(5):1158{1174, 2010. doi:10.1109/TAC.2010.2045439.

C. Claudel and A. Bayen. Lax-Hopf based incorporation of internal boundary conditions into Hamilton-Jacobi equation. Part I: theory. IEEE Transactions on Automatic Control, 55(5):1142{1157, 2010. doi:10.1109/TAC.2010.2041976.

C. Claudel, M. Nahoum, and A. Bayen. "*Minimal error certificates for detection of faulty sensors using convex optimization*". In Proceedings of the 47th Annual Allerton Conference on Communication, Control, and Computing, Allerton, IL, Sep. 2009.

Cassidy, M., Jang, K., and Daganzo, C. "*Macroscopic fundamental diagrams for freeway networks: theory and observation*". Transportation Research Record: Journal of the Transportation Research Board, (2260):8–15, 2011

Charniak, E.. "*Statistical Language Learning*". MIT Press, Cambridge, Massachusetts, 1993.

Chen, C., Kwon, J., Rice, J., Skabardonis, A., and Varaiya, P.. Detecting errors and imputing missing data for single-loop surveillance systems. Journal of Transportation Research Board, 1981:160{167, 2003.

Chen, C., Petty, K., Skabardonis, A., and Varaiya, P., Freeway performance measurement system: mining loop detector data. In 80th Annual Meeting of the Transportation Research Board, Washington, D.C., January 2001.

Chen, C., Petty, K., Skabardonis, A., and Varaiya, P.. Freeway performance measurement system: mining loop detector data. In 80th Annual Meeting of the Transportation Research Board, Washington, D.C., January 2001.

Chu, L., Liu, X., and Recker, W.. Using microscopic simulation to evaluate potential intelligent transportation system strategies under nonrecurrent congestion. Transportation Research Record, 1886:76{84, 2004.

Claudel, C., Nahoum, M., and Bayen, A., Minimal error certificates for detection of faulty sensors using convex optimization. In Proceedings of the 47th Annual Allerton Conference on Communication, Control, and Computing, Allerton, IL, Sep. 2009.

Coifman, B.. Estimating travel times and vehicles trajectories on freeways using dual loop detectors. Transportation Research A, 36(4):351{364, 2002.

Courbon, T. and Leclercq, L. Cross-comparison of macroscopic fundamental diagram estimation methods. Procedia-Social and Behavioral Sciences, 20:417–426, 2011

Daganzo, C. F. Urban gridlock: Macroscopic modeling and mitigation approaches. Transportation Research Part B: Methodological, 41(1):49–62, 2007

Duvall, T., Acting Undersecretary of Policy at U.S. Department of Transportation under George W. Bush, presentation at 15th ITS World Congress, November 17, 2008.

Edie, L. C. Discussion of traffic stream measurements and definitions. Port of New York Authority, 1963.

Ezell, S., "Explaining International Leadership in Contactless Mobile Payments," Information Technology and Innovation Foundation, November 17, 2009, 25, http://www.itif.org/files/2009-mobile-payments.pdf

Findler, N.V. and Stapp, J.. A Distributed Approach to Optimized Control of Street Traffic Signals. *Journal of Transportation Engineering,* 118:99-110, 1992.

Fouque, C., Bonnifait, P. Matching Raw GPS Measurements on a Navigable Map Without Computing a Global Position. IEEE Transactions on Intelligent Transportation Systems, IEEE, 2012, 13 (2), pp.887-898.

Geroliminis, N. and Daganzo, C. F. Macroscopic modeling of traffic in cities. In TRB 86th annual meeting, number 07-0413, 2007.

Geroliminis, N., Haddad, J., and Ramezani, M. Optimal perimeter control for two urban regions with macroscopic fundamental diagrams: A model predictive approach. Intelligent Transportation Systems, IEEE Transactions on, 14(1):348–359, 2013

Hao, P., Sun, Z., Ban, X., Guo, D., Ji, Q., 2013. Vehicle index estimation for signalized intersections using sample travel times. Transportation Research, Part C 36 (1), 513–529.

Ji, Y., Daamen, W., Hoogendoorn, S. P., Hoogendoorn-Lanser, S., and Qian, X. Investigating the shape of the macroscopic fundamental diagram using simulation data.

Transportation Research Record: Journal of the Transportation Research Board, (2161):40–48, 2010.

Jia, Z., Chen, C., Coifman, B., and Varaiya, P., The PeMS algorithms for accurate, real-time estimates of g-factors and speeds from single-loop detectors. In 4th IEEE Conference on Intelligent Transportation Systems, Oakland, CA, August 2001.

Keyvan-Ekbatani, M., Kouvelas, A., Papamichail, I., and Papageorgiou, M. Exploiting the fundamental diagram of urban networks for feedback-based gating. Transportation Research Part B: Methodological, 46(10):1393–1403, 2012.

Krause, E., Horvitz, A., Kansal, and F. Zhao. Toward community sensing. In ACM/IEEE International Conference on Information Processing in Sensor Networks (IPSN), St.Louis, MO, April 2008.

Liu, X., Mei, H., Lu, H., Kuang, H., Ma X. A Vehicle Steering Recognition System Based on Low-Cost Smartphone Sensors. Sensors, 2017. 17(3): p. 633.

M. Brand. Coupled hidden Markov models for modeling interacting processes. Technical report, The Media Lab, Massachusetts Institute of Technology, Boston, MA, 1997.

Mimbela, L., Klein, L., Kent, P., Hamrick, Luces, J. K., and Herrera, S.. Summary of Vehicle Detection and Surveillance Technologies used in Intelligent Transportation Systems. Federal Highway Administration's (FHWA) Intelligent Transportation Systems Program Office, August 2007.

Miranda-Moreno, L.F., Chung, C., Amyot, D., Chapon, H. A System for Collecting and Mapping Traffic Congestion in a Network Using GPS Smartphones from Regular Drivers; Proceedings of the Transportation Research Board 94th Annual Meeting; Washington, DC, USA. 11–15 January 2015

Ortigosa, J., Menendez, M., and Tapia, H. Study on the number and location of measurement points for an mfd perimeter control scheme: a case study of zurich. EURO Journal on Transportation and Logistics, 3(3-4):245–266, 2014.

Papageorgiou, M., Diakaki, C., Dinopoulou, V., Kotsialos, A., and Wang, Y.. Review of Road Traffic Control Strategies. *Proceedings of the IEEE,* 91(12):2043-2067, 2003.

Robertson, D.I. and Bretherton, R.D.. Optimizing networks of traffic signals in real time-the SCOOT method. *IEEE Transactions on Vehicular Technology,* 40(1): 11-15, 1991.

Sekimoto,Y., Matsubayashi, Y., Yamada, H., Imai, R., Usui, T., and Kanasugi, H. 2012 Light weight lane positioning of vehicles using a smartphone GPS by monitoring the distance from the center line. In Proc. IEEE Conf. Intelligent Transportation Systems pp. 1561–1565

Simoni, M. D., Pel, A. J., Waraich, R. A., and Hoogendoorn, S. P. Marginal cost congestion pricing based on the network fundamental diagram. Transportation Research Part C: Emerging Technologies, 56:221–238, 2015.

Skog and P.Handel, “In-car positioning and navigation technologiesa survey,” IEEE Transactions on Intelligent Transportation Systems, vol. 10, no. 1, pp. 4–21, 2009.

Viktor. Knoop, L., De Bakker, P. F., Tiberius, C. C. J. M., and van Arem, B., “Lane determination with gps precise point positioning,”IEEE Transactions on Intelligent Transportation Systems , vol. PP, no. 99, pp.1–11, 2017

Warin, T., “Overcoming Barriers to ITS Implementation in the Asia Pacific Region,” presentation at 15th ITS World Congress, New York City, November 18, 2008.

Ybarra, S., Staley, S., “Sustainable Mobility in American Cities,” Reason Foundation, September 8, 2008, http://reason.org/news/show/sustainable-mobility-in-americ.

Yildirimoglu, M., Ramezani, M., and Geroliminis, N. Equilibrium analysis and route guidance in large-scale networks with mfd dynamics. Transportation Research Part C: Emerging Technologies, 59:404–420, 2015

Zheng, J., Liu, H. X.. Estimating traffic volumes for signalized intersections using connected vehicle data Transportation Research Part C 13 March 2017

ANNEX 1

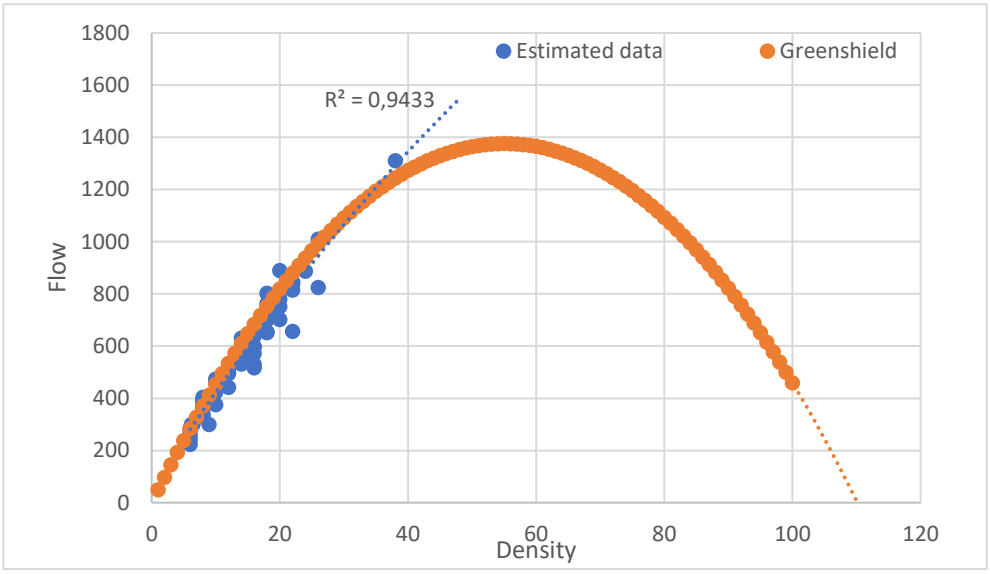

Fig. A.1. MFD Density- flow at 8-9 AM in Via Amendola southbound

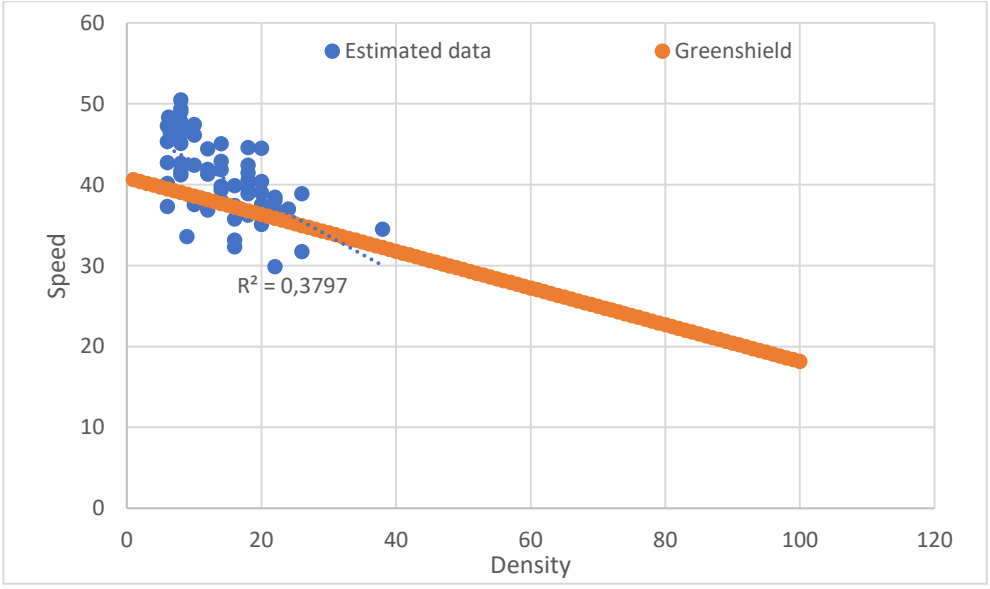

Fig. A.2. MFD Density- Speed at 8-9 AM in Via Amendola southbound

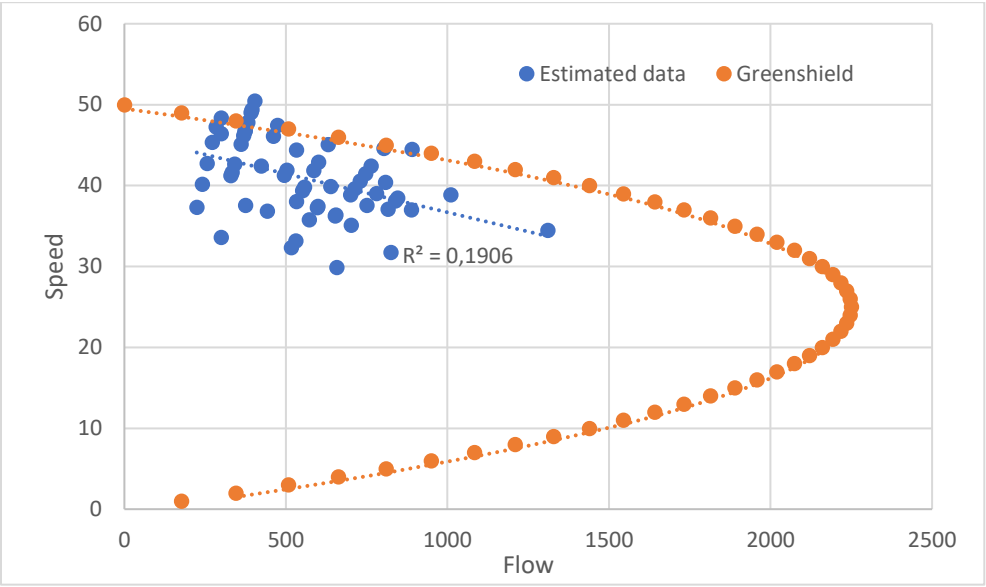

Fig. A.3. MFD Flow - Speed at 8-9 AM in Via Amendola southbound

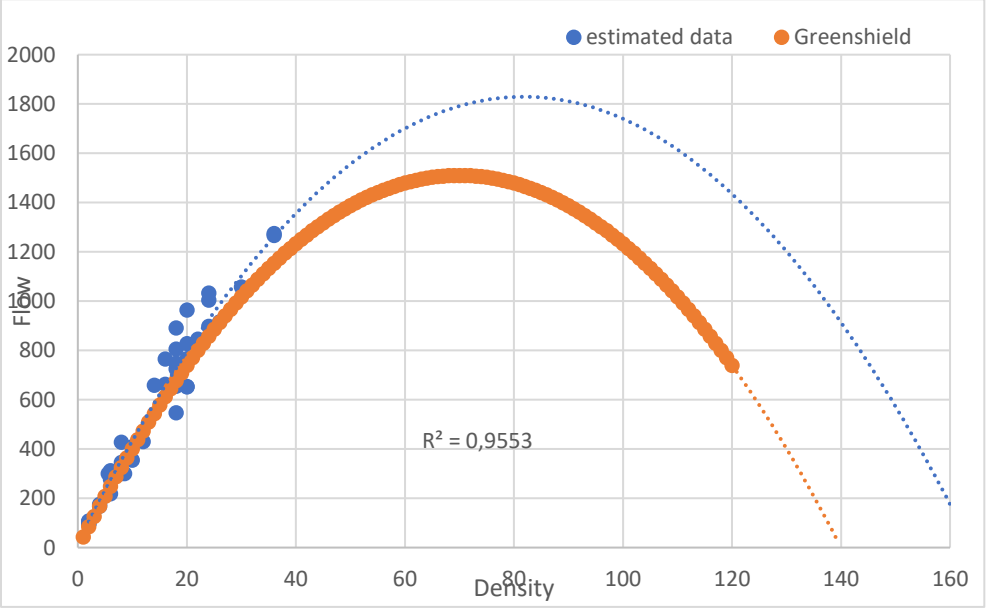

Fig. A.4. MFD Density- flow at 12 AM - 1 PM in Via Amendola northbound

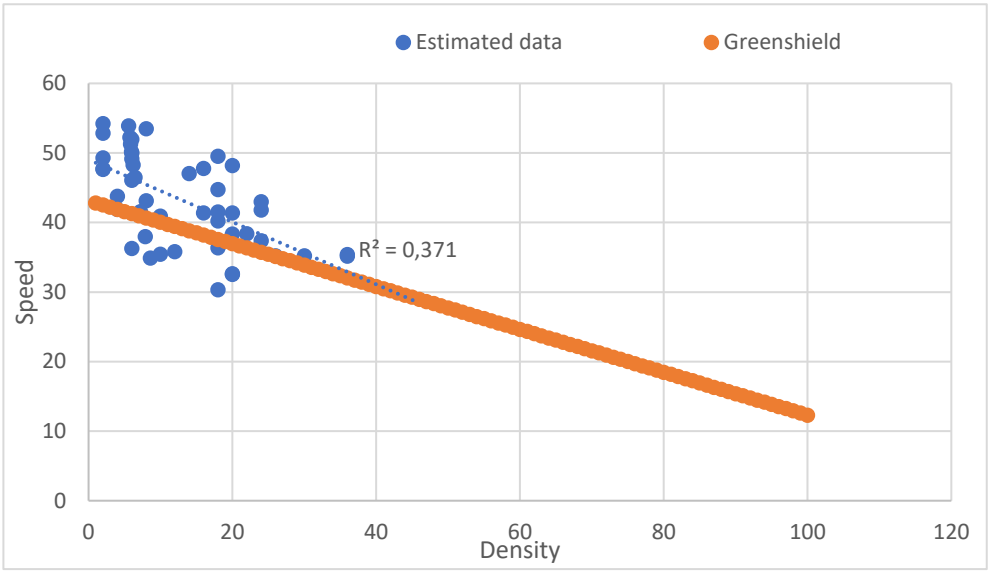

Fig. A.5. MFD Density- Speed at 12 AM - 1 PM in Via Amendola northbound

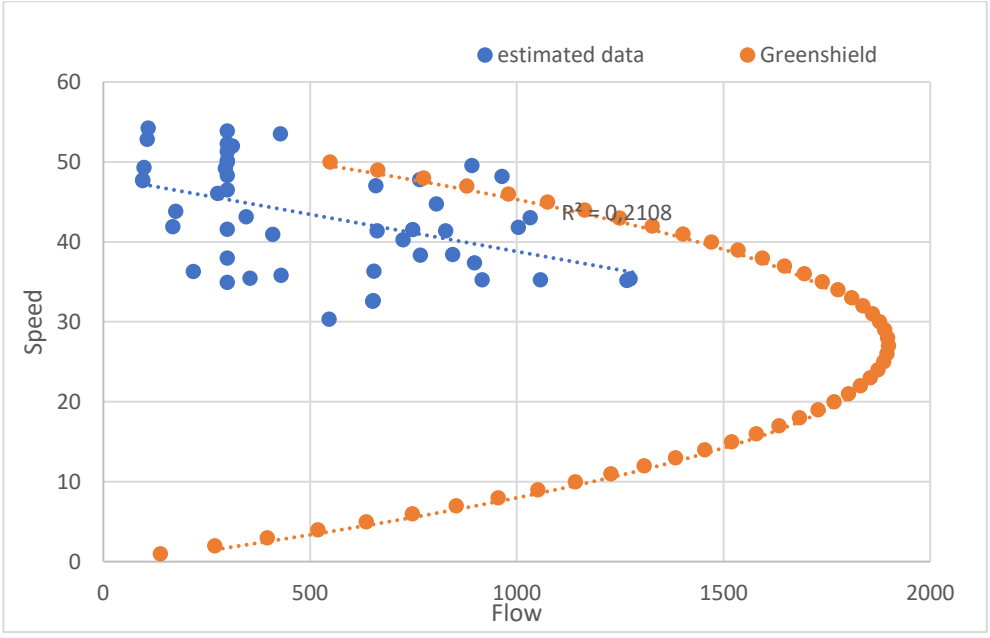

Fig. A.6. MFD Flow - Speed at 12 AM - 1 PM in Via Amendola northbound

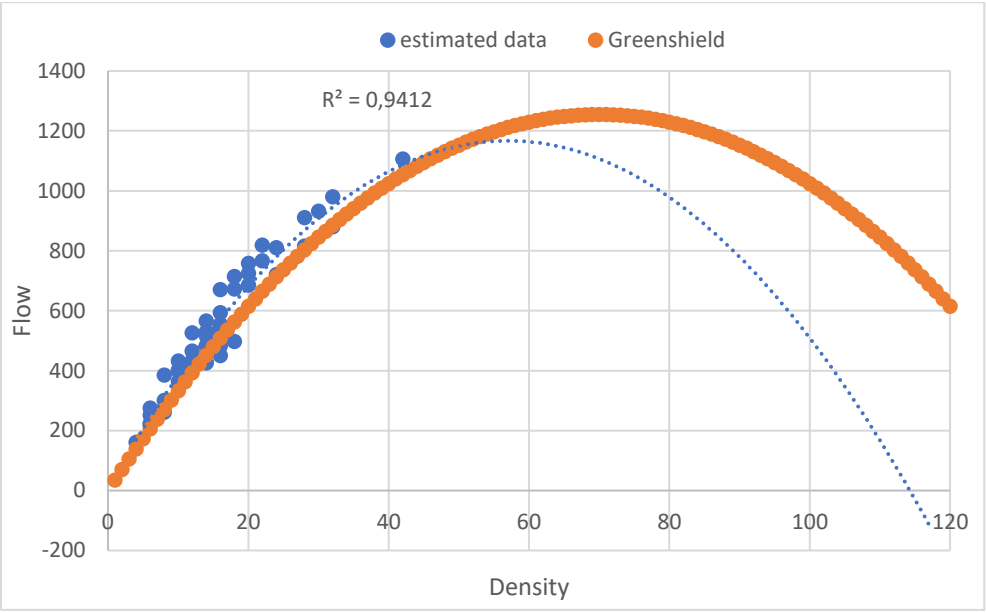

Fig. A.7. MFD Density- flow at 12 AM – 1 PM in Via Amendola southbound

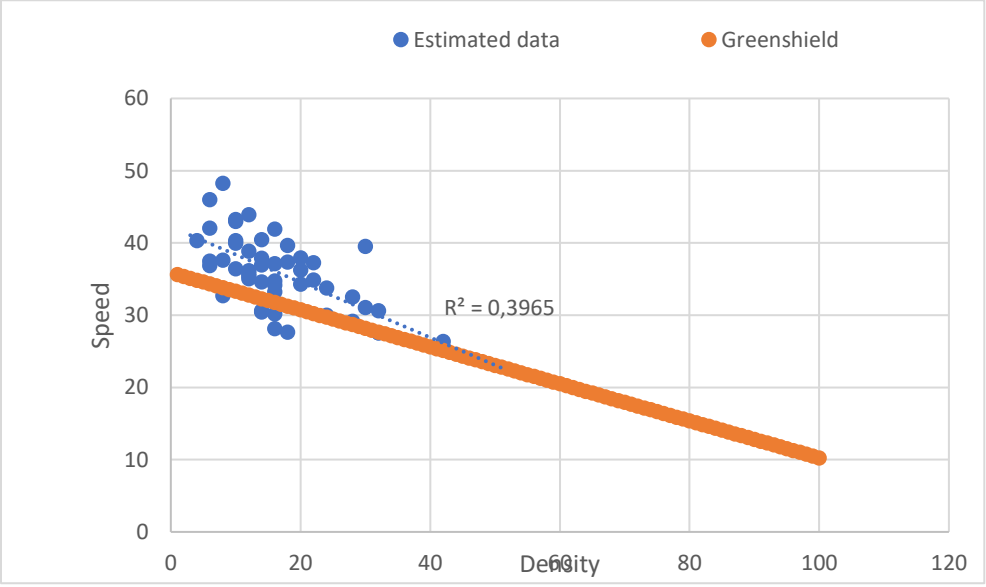

Fig. A.8. MFD Density- Speed at 12 AM – 1 PM in Via Amendola southbound

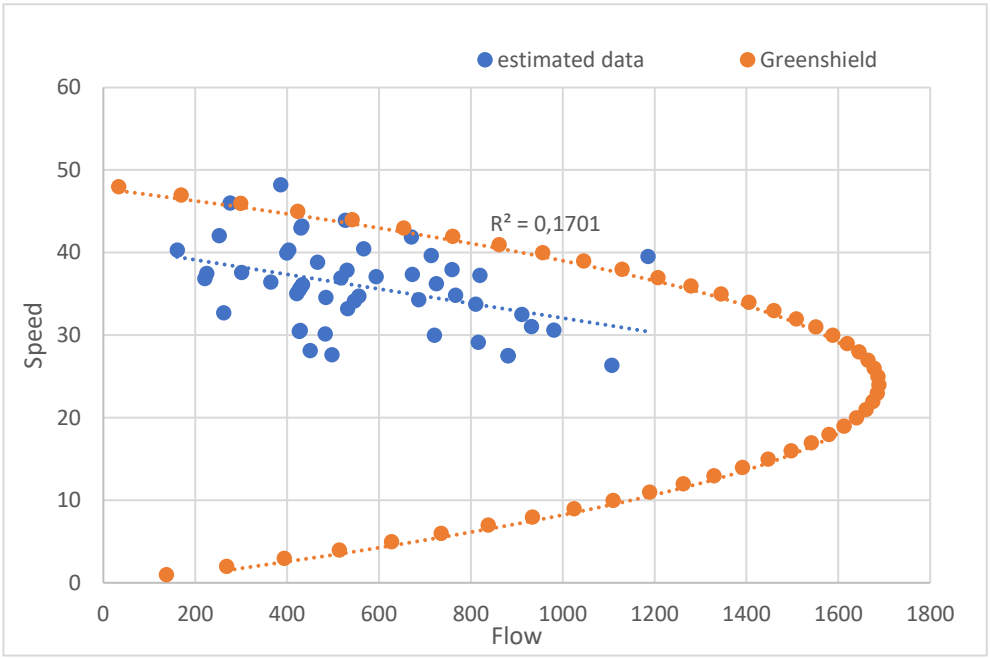

Fig. A.9. MFD Flow - Speed at 12 AM – 1 PM in Via Amendola southbound

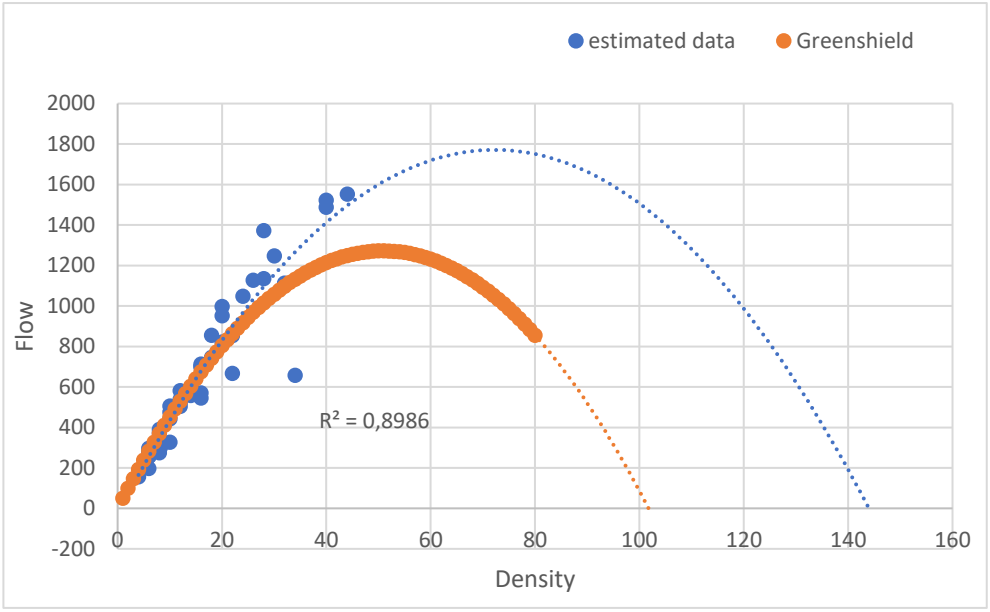

Fig. A.10. MFD Density- flow at 5 PM - 6 PM in Via Amendola northbound

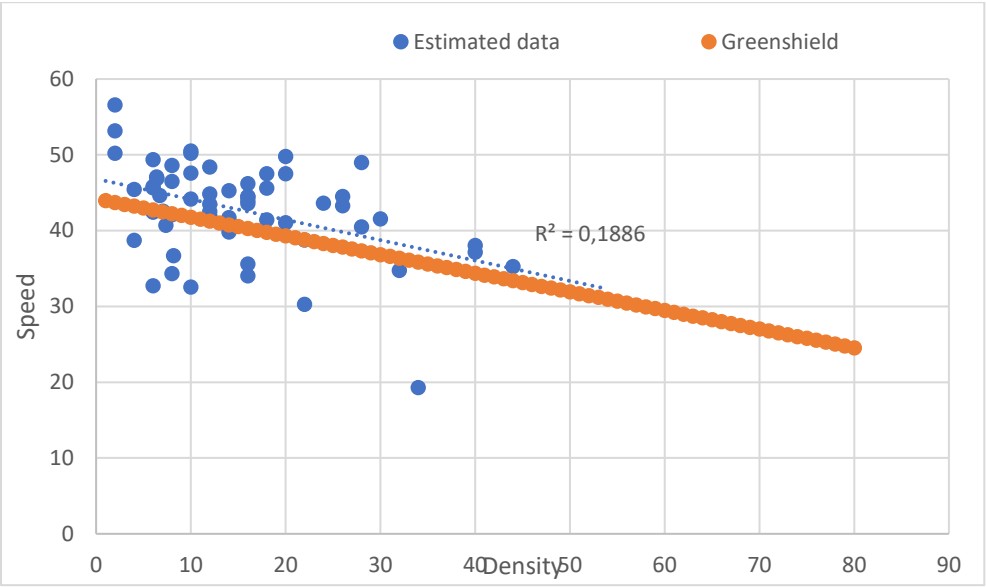

Fig. A.5. MFD Density- Speed at 5 PM – 6 PM in Via Amendola northbound

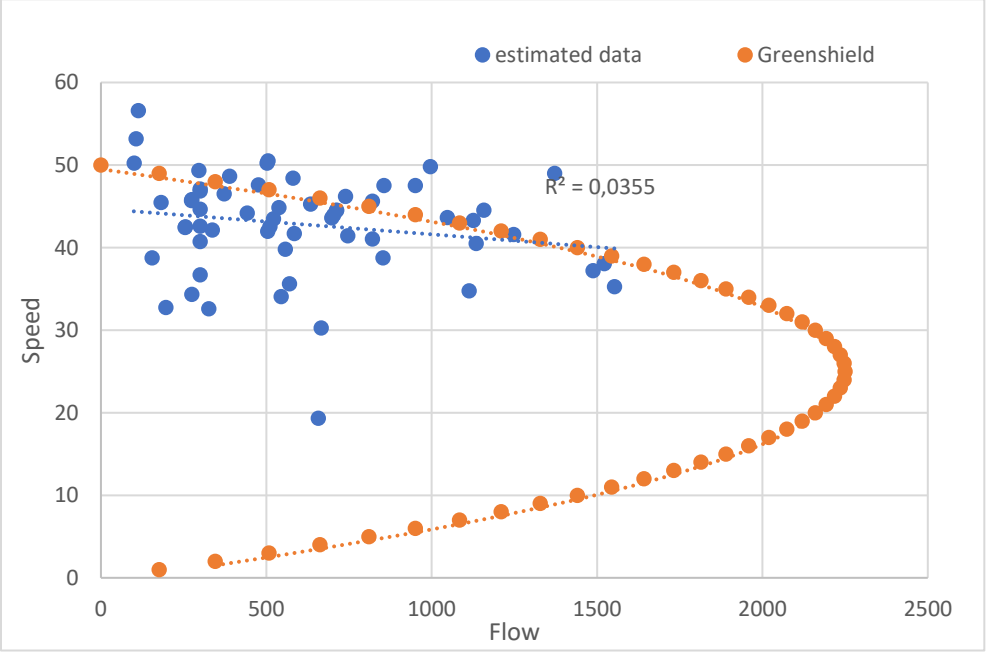

Fig. A.6. MFD Flow - Speed at 5 PM - 6 PM in Via Amendola northbound

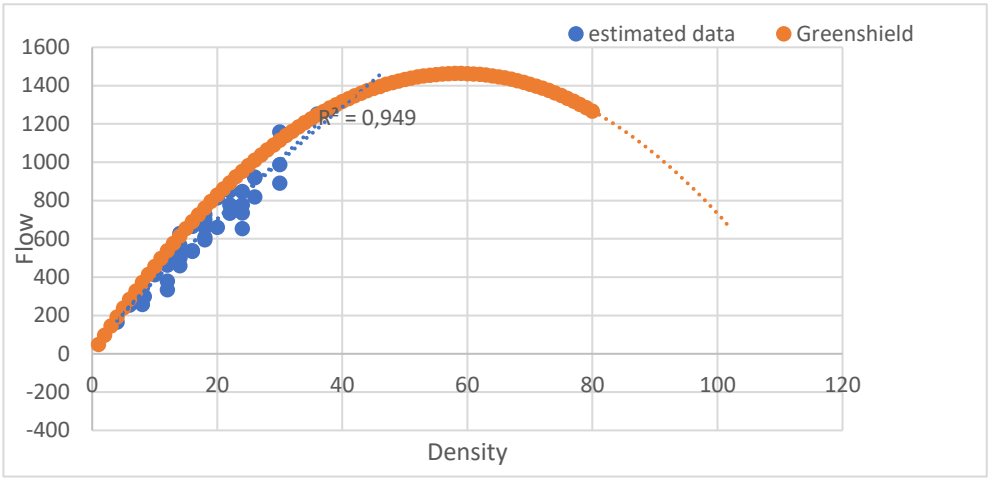

Fig. A.7. MFD Density- flow at 5 PM - 6 PM in Via Amendola southbound

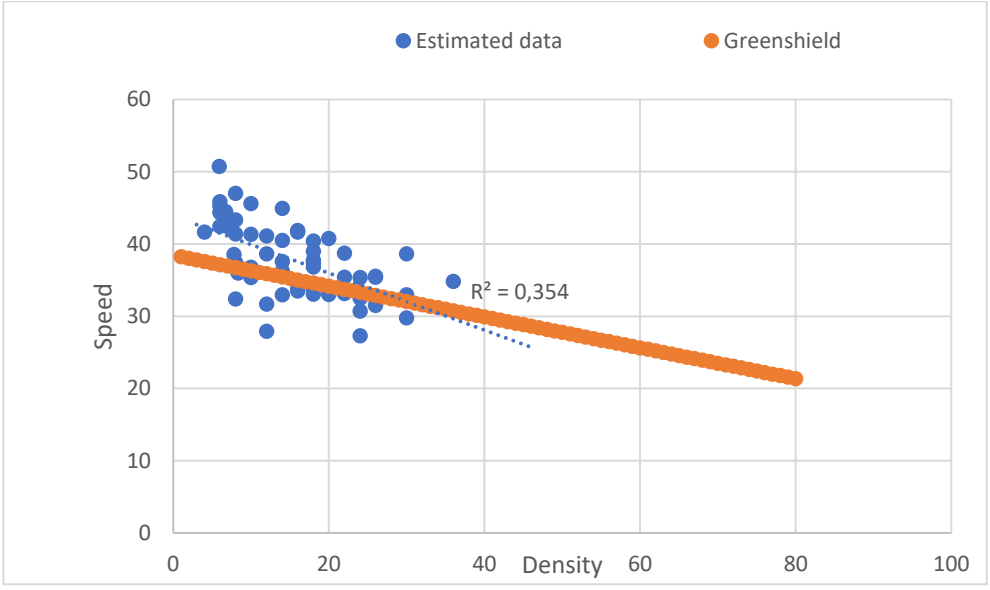

Fig. A.8. MFD Density- Speed at 5 PM - 6 PM in Via Amendola southbound

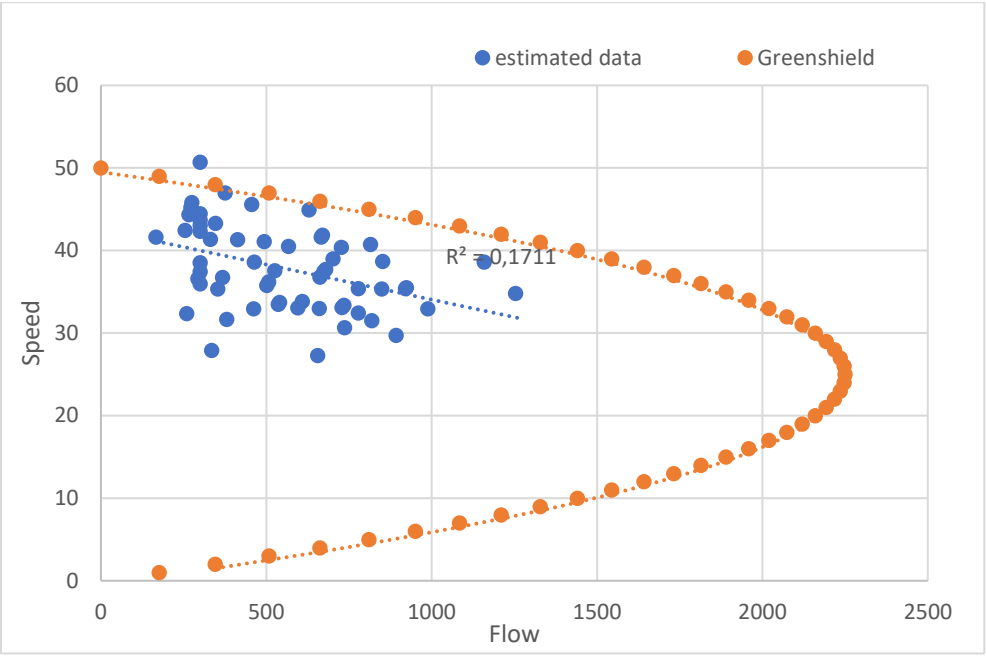

Fig. A.9. MFD Flow - Speed at 5 PM - 6 PM in Via Amendola southbound

ANNEX 2

Table A.1. O/D Matrix 2nd connected vehicle at 8-9

	1	2	3	4	5	6	7	8	9	10	11	12	13	14
1	0	0	0	0	0	0	672	0	0	0	0	0	0	0
2	0	0	58	173	0	0	346	0	0	0	0	0	0	0
3	0	0	0	0	0	0	26	0	0	62	0	0	0	0
4	0	0	0	0	0	0	0	0	0	0	0	0	0	0
5	0	0	0	0	0	0	0	0	0	238	0	0	0	0
6	0	0	0	0	0	0	35	0	0	318	0	0	0	0
7	0	0	0	0	0	0	0	0	0	0	0	0	0	0
8	0	0	0	0	0	0	0	0	0	0	0	0	0	587
9	0	0	0	0	0	0	0	0	0	162	0	0	0	379
10	0	0	0	0	0	0	0	0	0	0	0	0	0	0
11	0	0	0	270	0	0	0	0	0	0	0	0	0	0
12	0	0	30	200	0	0	0	0	0	0	0	0	0	0
13	0	0	0	0	0	0	0	0	0	0	0	0	0	333
14	0	0	0	0	0	0	0	0	0	0	0	0	0	0

Table A.2. O/D Matrix 3rd connected vehicle at 8-9

	1	2	3	4	5	6	7	8	9	10	11	12	13	14
1	0	0	0	0	0	0	423	0	0	0	0	0	0	0
2	0	0	63	188	0	0	376	0	0	0	0	0	0	0
3	0	0	0	0	0	0	28	0	0	65	0	0	0	0
4	0	0	0	0	0	0	0	0	0	0	0	0	0	0
5	0	0	0	0	0	0	0	0	0	238	0	0	0	0
6	0	0	0	0	0	0	35	0	0	318	0	0	0	0
7	0	0	0	0	0	0	0	0	0	0	0	0	0	0
8	0	0	0	0	0	0	0	0	0	0	0	0	0	554
9	0	0	0	0	0	0	0	0	0	153	0	0	0	356
10	0	0	0	0	0	0	0	0	0	0	0	0	0	0
11	0	0	0	270	0	0	0	0	0	0	0	0	0	0
12	0	0	30	200	0	0	0	0	0	0	0	0	0	0
13	0	0	0	0	0	0	0	0	0	0	0	0	0	333
14	0	0	0	0	0	0	0	0	0	0	0	0	0	0

Table A.3. O/D Matrix 4th connected vehicle at 8-9

	1	2	3	4	5	6	7	8	9	10	11	12	13	14
1	0	0	0	0	0	0	861	0	0	0	0	0	0	0
2	0	0	76	228	0	0	456	0	0	0	0	0	0	0
3	0	0	0	0	0	0	32	0	0	74	0	0	0	0
4	0	0	0	0	0	0	0	0	0	0	0	0	0	0
5	0	0	0	0	0	0	0	0	0	238	0	0	0	0
6	0	0	0	0	0	0	35	0	0	318	0	0	0	0
7	0	0	0	0	0	0	0	0	0	0	0	0	0	0
8	0	0	0	0	0	0	0	0	0	0	0	0	0	537
9	0	0	0	0	0	0	0	0	0	189	0	0	0	440
10	0	0	0	0	0	0	0	0	0	0	0	0	0	0
11	0	0	0	270	0	0	0	0	0	0	0	0	0	0
12	0	0	30	200	0	0	0	0	0	0	0	0	0	0
13	0	0	0	0	0	0	0	0	0	0	0	0	0	333
14	0	0	0	0	0	0	0	0	0	0	0	0	0	0

Table A.4. O/D Matrix 5th connected vehicle at 8-9

	1	2	3	4	5	6	7	8	9	10	11	12	13	14
1	0	0	0	0	0	0	820	0	0	0	0	0	0	0
2	0	0	68	203	0	0	407	0	0	0	0	0	0	0
3	0	0	0	0	0	0	29	0	0	69	0	0	0	0
4	0	0	0	0	0	0	0	0	0	0	0	0	0	0
5	0	0	0	0	0	0	0	0	0	238	0	0	0	0
6	0	0	0	0	0	0	35	0	0	318	0	0	0	0
7	0	0	0	0	0	0	0	0	0	0	0	0	0	0
8	0	0	0	0	0	0	0	0	0	0	0	0	0	562
9	0	0	0	0	0	0	0	0	0	187	0	0	0	435
10	0	0	0	0	0	0	0	0	0	0	0	0	0	0
11	0	0	0	270	0	0	0	0	0	0	0	0	0	0
12	0	0	30	200	0	0	0	0	0	0	0	0	0	0
13	0	0	0	0	0	0	0	0	0	0	0	0	0	333
14	0	0	0	0	0	0	0	0	0	0	0	0	0	0

O/D MATRIX 12-13

Table A.5. O/D Matrix 1st connected vehicle at 12-13

	1	2	3	4	5	6	7	8	9	10	11	12	13	14
1	0	0	0	0	0	0	378	0	0	0	0	0	0	0
2	0	0	70	211	0	0	422	0	0	0	0	0	0	0
3	0	0	0	0	0	0	28	0	0	65	0	0	0	0
4	0	0	0	0	0	0	0	0	0	0	0	0	0	0
5	0	0	0	0	0	0	0	0	0	238	0	0	0	0
6	0	0	0	0	0	0	35	0	0	318	0	0	0	0
7	0	0	0	0	0	0	0	0	0	0	0	0	0	0
8	0	0	0	0	0	0	0	0	0	0	0	0	0	516
9	0	0	0	0	0	0	0	0	0	177	0	0	0	414
10	0	0	0	0	0	0	0	0	0	0	0	0	0	0
11	0	0	0	270	0	0	0	0	0	0	0	0	0	0
12	0	0	23	200	0	0	0	0	0	0	0	0	0	0
13	0	0	0	0	0	0	0	0	0	0	0	0	0	333
14	0	0	0	0	0	0	0	0	0	0	0	0	0	0

Table A.6. O/D Matrix 2nd connected vehicle at 12-13

	1	2	3	4	5	6	7	8	9	10	11	12	13	14
1	0	0	0	0	0	0	448	0	0	0	0	0	0	0
2	0	0	63	188	0	0	375	0	0	0	0	0	0	0
3	0	0	0	0	0	0	35	0	0	82	0	0	0	0
4	0	0	0	0	0	0	0	0	0	0	0	0	0	0
5	0	0	0	0	0	0	0	0	0	238	0	0	0	0
6	0	0	0	0	0	0	35	0	0	318	0	0	0	0
7	0	0	0	0	0	0	0	0	0	0	0	0	0	0
8	0	0	0	0	0	0	0	0	0	0	0	0	0	522
9	0	0	0	0	0	0	0	0	0	172	0	0	0	401
10	0	0	0	0	0	0	0	0	0	0	0	0	0	0
11	0	0	0	270	0	0	0	0	0	0	0	0	0	0
12	0	0	55	200	0	0	0	0	0	0	0	0	0	0
13	0	0	0	0	0	0	0	0	0	0	0	0	0	333
14	0	0	0	0	0	0	0	0	0	0	0	0	0	0

Table A.7 O/D Matrix 3rd connected vehicle at 12-13

	1	2	3	4	5	6	7	8	9	10	11	12	13	14
1	0	0	0	0	0	0	535	0	0	0	0	0	0	0
2	0	0	66	197	0	0	395	0	0	0	0	0	0	0
3	0	0	0	0	0	0	27	0	0	62	0	0	0	0
4	0	0	0	0	0	0	0	0	0	0	0	0	0	0
5	0	0	0	0	0	0	0	0	0	238	0	0	0	0
6	0	0	0	0	0	0	35	0	0	318	0	0	0	0
7	0	0	0	0	0	0	0	0	0	0	0	0	0	0
8	0	0	0	0	0	0	0	0	0	0	0	0	0	612
9	0	0	0	0	0	0	0	0	0	158	0	0	0	368
10	0	0	0	0	0	0	0	0	0	0	0	0	0	0
11	0	0	0	270	0	0	0	0	0	0	0	0	0	0
12	0	0	23	200	0	0	0	0	0	0	0	0	0	0
13	0	0	0	0	0	0	0	0	0	0	0	0	0	333
14	0	0	0	0	0	0	0	0	0	0	0	0	0	0

Table A.8. O/D Matrix 4th connected vehicle at 12-13

	1	2	3	4	5	6	7	8	9	10	11	12	13	14
1	0	0	0	0	0	0	441	0	0	0	0	0	0	0
2	0	0	65	194	0	0	389	0	0	0	0	0	0	0
3	0	0	0	0	0	0	28	0	0	66	0	0	0	0
4	0	0	0	0	0	0	0	0	0	0	0	0	0	0
5	0	0	0	0	0	0	0	0	0	238	0	0	0	0
6	0	0	0	0	0	0	35	0	0	318	0	0	0	0
7	0	0	0	0	0	0	0	0	0	0	0	0	0	0
8	0	0	0	0	0	0	0	0	0	0	0	0	0	622
9	0	0	0	0	0	0	0	0	0	126	0	0	0	295
10	0	0	0	0	0	0	0	0	0	0	0	0	0	0
11	0	0	0	270	0	0	0	0	0	0	0	0	0	0
12	0	0	30	200	0	0	0	0	0	0	0	0	0	0
13	0	0	0	0	0	0	0	0	0	0	0	0	0	333
14	0	0	0	0	0	0	0	0	0	0	0	0	0	0

Table A.9. O/D Matrix 5th connected vehicle at 12-13

	1	2	3	4	5	6	7	8	9	10	11	12	13	14
1	0	0	0	0	0	0	460	0	0	0	0	0	0	0
2	0	0	61	182	0	0	364	0	0	0	0	0	0	0
3	0	0	0	0	0	0	27	0	0	63	0	0	0	0
4	0	0	0	0	0	0	0	0	0	0	0	0	0	0
5	0	0	0	0	0	0	0	0	0	238	0	0	0	0
6	0	0	0	0	0	0	35	0	0	318	0	0	0	0
7	0	0	0	0	0	0	0	0	0	0	0	0	0	0
8	0	0	0	0	0	0	0	0	0	0	0	0	0	640
9	0	0	0	0	0	0	0	0	0	140	0	0	0	326
10	0	0	0	0	0	0	0	0	0	0	0	0	0	0
11	0	0	0	270	0	0	0	0	0	0	0	0	0	0
12	0	0	30	200	0	0	0	0	0	0	0	0	0	0
13	0	0	0	0	0	0	0	0	0	0	0	0	0	333
14	0	0	0	0	0	0	0	0	0	0	0	0	0	0

O/D MATRIX 17-18

Table A.10. O/D Matrix 1st connected vehicle at 17-18

	1	2	3	4	5	6	7	8	9	10	11	12	13	14
1	0	0	0	0	0	0	196	0	0	0	0	0	0	0
2	0	0	26	77	0	0	179	0	0	0	0	0	0	0
3	0	0	0	0	0	0	17	0	0	39	0	0	0	0
4	0	0	0	0	0	0	0	0	0	0	0	0	0	0
5	0	0	0	0	0	0	0	0	0	238	0	0	0	0
6	0	0	0	0	0	0	35	0	0	318	0	0	0	0
7	0	0	0	0	0	0	0	0	0	0	0	0	0	0
8	0	0	0	0	0	0	0	0	0	0	0	0	0	655
9	0	0	0	0	0	0	0	0	0	162	0	0	0	377
10	0	0	0	0	0	0	0	0	0	0	0	0	0	0
11	0	0	0	270	0	0	0	0	0	0	0	0	0	0
12	0	0	30	200	0	0	0	0	0	0	0	0	0	0
13	0	0	0	0	0	0	0	0	0	0	0	0	0	333
14	0	0	0	0	0	0	0	0	0	0	0	0	0	0

Table A.11. O/D Matrix 2nd connected vehicle at 17-18

	1	2	3	4	5	6	7	8	9	10	11	12	13	14
1	0	0	0	0	0	0	275	0	0	0	0	0	0	0
2	0	0	27	82	0	0	192	0	0	0	0	0	0	0
3	0	0	0	0	0	0	17	0	0	40	0	0	0	0
4	0	0	0	0	0	0	0	0	0	0	0	0	0	0
5	0	0	0	0	0	0	0	0	0	238	0	0	0	0
6	0	0	0	0	0	0	35	0	0	318	0	0	0	0
7	0	0	0	0	0	0	0	0	0	0	0	0	0	0
8	0	0	0	0	0	0	0	0	0	0	0	0	0	778
9	0	0	0	0	0	0	0	0	0	150	0	0	0	351
10	0	0	0	0	0	0	0	0	0	0	0	0	0	0
11	0	0	0	270	0	0	0	0	0	0	0	0	0	0
12	0	0	30	200	0	0	0	0	0	0	0	0	0	0
13	0	0	0	0	0	0	0	0	0	0	0	0	0	333
14	0	0	0	0	0	0	0	0	0	0	0	0	0	0

Table A.12. O/D Matrix 3rd connected vehicle at 17-18

	1	2	3	4	5	6	7	8	9	10	11	12	13	14
1	0	0	0	0	0	0	504	0	0	0	0	0	0	0
2	0	0	70	211	0	0	492	0	0	0	0	0	0	0
3	0	0	0	0	0	0	30	0	0	70	0	0	0	0
4	0	0	0	0	0	0	0	0	0	0	0	0	0	0
5	0	0	0	0	0	0	0	0	0	238	0	0	0	0
6	0	0	0	0	0	0	35	0	0	318	0	0	0	0
7	0	0	0	0	0	0	0	0	0	0	0	0	0	0
8	0	0	0	0	0	0	0	0	0	0	0	0	0	595
9	0	0	0	0	0	0	0	0	0	158	0	0	0	368
10	0	0	0	0	0	0	0	0	0	0	0	0	0	0
11	0	0	0	270	0	0	0	0	0	0	0	0	0	0
12	0	0	30	200	0	0	0	0	0	0	0	0	0	0
13	0	0	0	0	0	0	0	0	0	0	0	0	0	333
14	0	0	0	0	0	0	0	0	0	0	0	0	0	0

Table A.13 O/D Matrix 4th connected vehicle at 17-18

	1	2	3	4	5	6	7	8	9	10	11	12	13	14
1	0	0	0	0	0	0	337	0	0	0	0	0	0	0
2	0	0	50	151	0	0	351	0	0	0	0	0	0	0
3	0	0	0	0	0	0	24	0	0	56	0	0	0	0
4	0	0	0	0	0	0	0	0	0	0	0	0	0	0
5	0	0	0	0	0	0	0	0	0	238	0	0	0	0
6	0	0	0	0	0	0	35	0	0	318	0	0	0	0
7	0	0	0	0	0	0	0	0	0	0	0	0	0	0
8	0	0	0	0	0	0	0	0	0	0	0	0	0	892
9	0	0	0	0	0	0	0	0	0	218	0	0	0	510
10	0	0	0	0	0	0	0	0	0	0	0	0	0	0
11	0	0	0	270	0	0	0	0	0	0	0	0	0	0
12	0	0	30	200	0	0	0	0	0	0	0	0	0	0
13	0	0	0	0	0	0	0	0	0	0	0	0	0	333
14	0	0	0	0	0	0	0	0	0	0	0	0	0	0

Table A.14. O/D Matrix 5th connected vehicle at 17-18

	1	2	3	4	5	6	7	8	9	10	11	12	13	14
1	0	0	0	0	0	0	96	0	0	0	0	0	0	0
2	0	0	30	90	0	0	210	0	0	0	0	0	0	0
3	0	0	0	0	0	0	18	0	0	42	0	0	0	0
4	0	0	0	0	0	0	0	0	0	0	0	0	0	0
5	0	0	0	0	0	0	0	0	0	238	0	0	0	0
6	0	0	0	0	0	0	35	0	0	318	0	0	0	0
7	0	0	0	0	0	0	0	0	0	0	0	0	0	0
8	0	0	0	0	0	0	0	0	0	0	0	0	0	300
9	0	0	0	0	0	0	0	0	0	90	0	0	0	210
10	0	0	0	0	0	0	0	0	0	0	0	0	0	0
11	0	0	0	270	0	0	0	0	0	0	0	0	0	0
12	0	0	30	200	0	0	0	0	0	0	0	0	0	0
13	0	0	0	0	0	0	0	0	0	0	0	0	0	333
14	0	0	0	0	0	0	0	0	0	0	0	0	0	0

ANNEX 3

Table A.1. Result 1st connected vehicle 12-13

Time Series	Current cycle length	New cycle length	improvement
Delay Time – Car [sec/km]	143.8	56.7	61%
Density – Car [veh/km]	8.8	5.7	36%
Mean Queue – Car [veh]	45.0	18.7	59%
Speed – Car [km/h]	26.6	33.6	21%
Stop Time – Car [sec/km]	119.7	43.4	64%
Total Number of Stops - Car	10074.7	7264.3	28%
Total Travel Time – Car [h]	84.2	54.4	35%
Travel Time – Car [sec/km]	209.8	122.8	41%

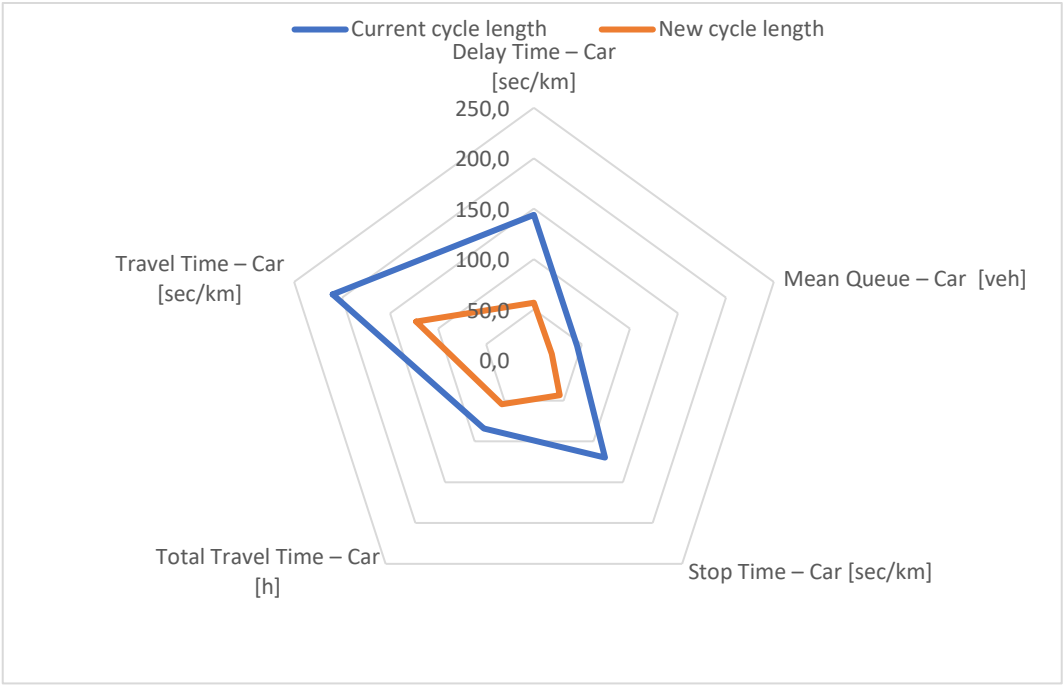

Fig. A.1. Improvement 1st connected vehicle 12-13

Table A.2. Result 2nd connected vehicle 12-13

Time Series	Current cycle length	New cycle length	improvement
Delay Time – Car [sec/km]	89.08	54.85	38%
Density – Car [veh/km]	6.63	5.48	17%
Mean Queue – Car [veh]	27.27	17.26	37%
Speed – Car [km/h]	30.16	34.04	11%
Stop Time – Car [sec/km]	72.48	41.21	43%
Total Number of Stops - Car	8044.57	7124.55	11%
Total Travel Time – Car [h]	63.99	52.94	17%
Travel Time – Car [sec/km]	155.22	120.95	22%

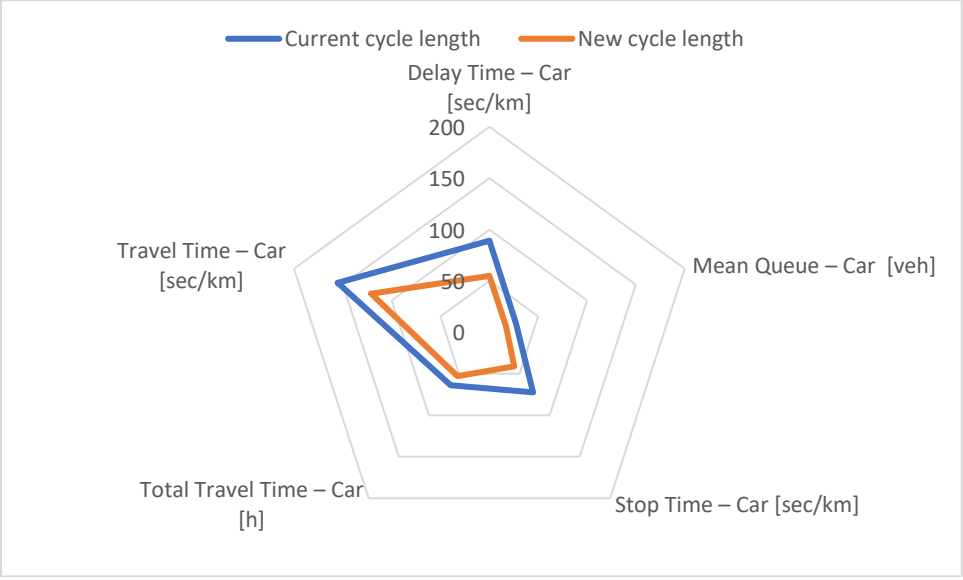

Fig. A.2. Improvement 2nd connected vehicle 12-13

Table A.3. Result 3rd connected vehicle 12-13

Time Series	Current cycle length	New cycle length	improvement
Delay Time – Car [sec/km]	105.6	55.09	48%
Density – Car [veh/km]	7.48	5.69	24%
Mean Queue – Car [veh]	33.15	18.42	44%
Speed – Car [km/h]	28.55	33.96	16%
Stop Time – Car [sec/km]	85.62	41.54	51%
Total Number of Stops - Car	9421.44	7289.11	23%
Total Travel Time – Car [h]	72.19	54.92	24%
Travel Time – Car [sec/km]	171.72	121.17	29%

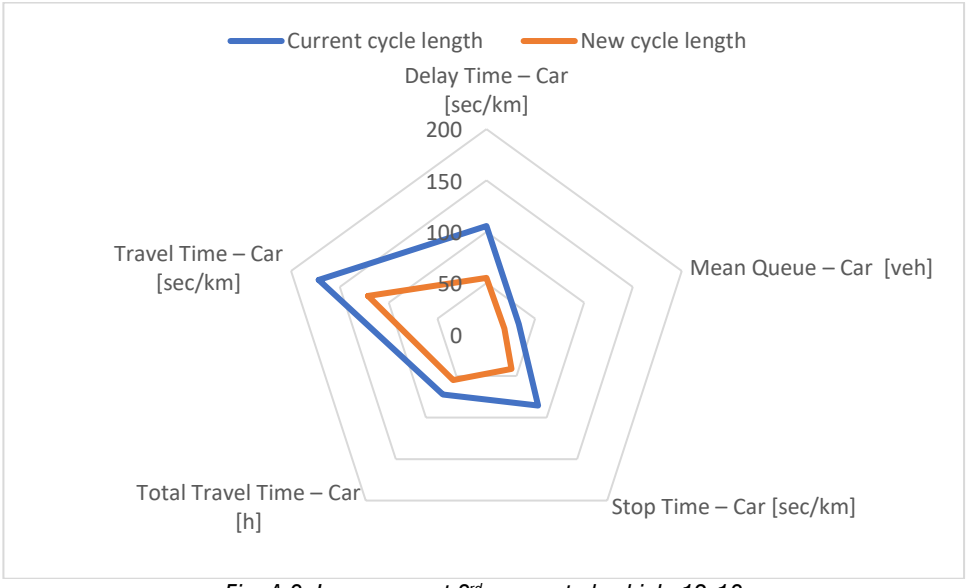

Fig. A.3. Improvement 3rd connected vehicle 12-13

Table A.4. Result 4th connected vehicle 12-13

Time Series	Current cycle length	New cycle length	improvement
Delay Time – Car [sec/km]	103.9	53.8	48%
Density – Car [veh/km]	7.0	5.5	22%
Mean Queue – Car [veh]	31.2	16.8	46%
Speed – Car [km/h]	29.6	34.5	17%
Stop Time – Car [sec/km]	85.8	40.6	53%
Total Number of Stops - Car	8398.1	7208.8	14%
Total Travel Time – Car [h]	67.4	52.8	22%
Travel Time – Car [sec/km]	170.0	119.9	29%

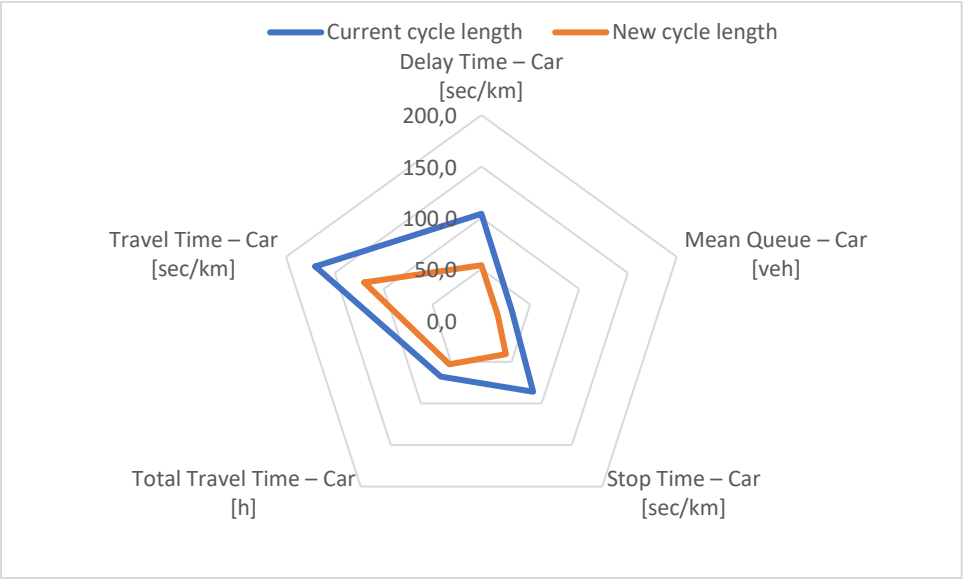

Fig. A.4. Improvement 4th connected vehicle 12-13

Table A.5. Result 5th connected vehicle 12-13

Time Series	Current cycle length	New cycle length	improvement
Delay Time – Car [sec/km]	84.0	53.4	36.4%
Density – Car [veh/km]	6.4	5.4	16.6%
Mean Queue – Car [veh]	25.8	16.8	34.8%
Speed – Car [km/h]	30.2	34.5	12.3%
Stop Time – Car [sec/km]	68.0	40.4	40.6%
Total Number of Stops - Car	7986.8	6971.8	12.7%
Total Travel Time – Car [h]	62.1	51.9	16.3%
Travel Time – Car [sec/km]	150.3	119.5	20.5%

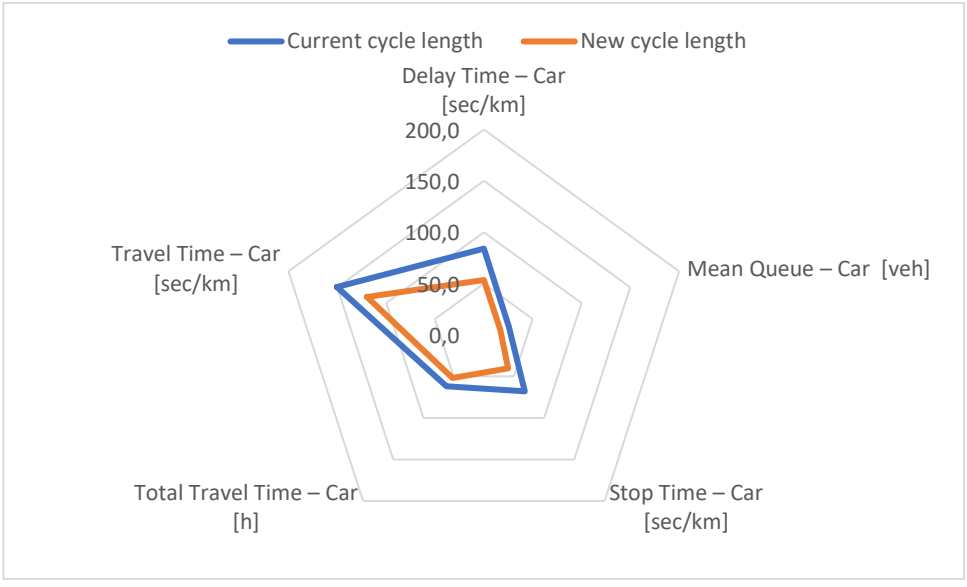

Fig. A.5. Improvement 5th connected vehicle 12-13

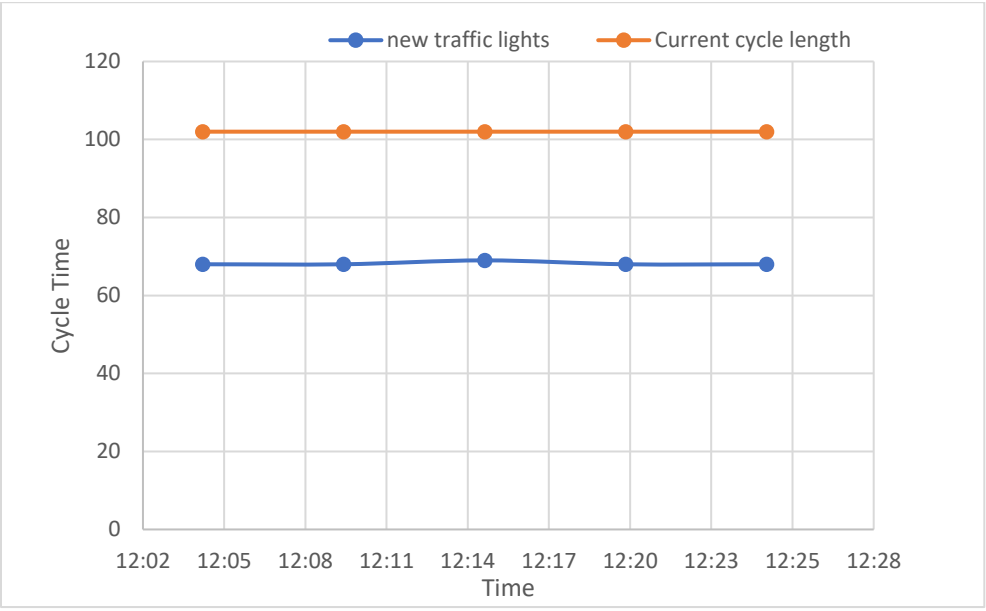

Fig. A.6. Cycle time

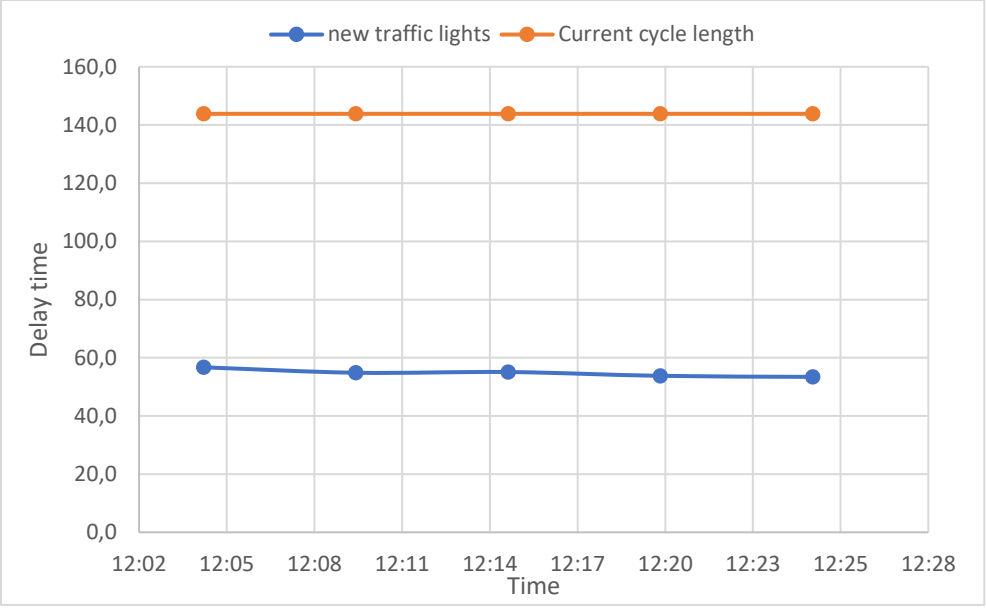

Fig. A.7. Delay time

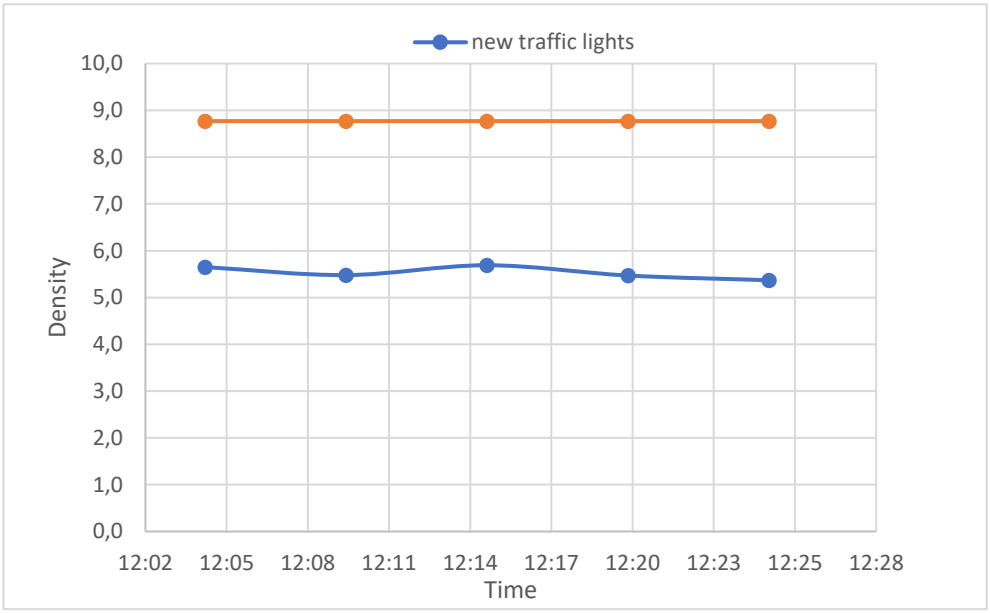

Fig. A.8. Density

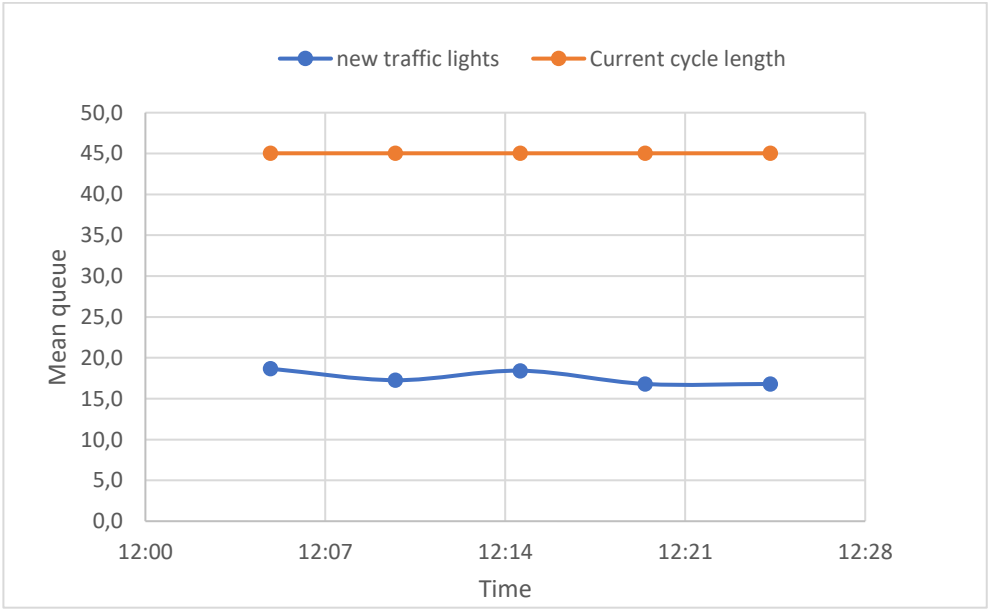

Fig. A.9. Mean queue

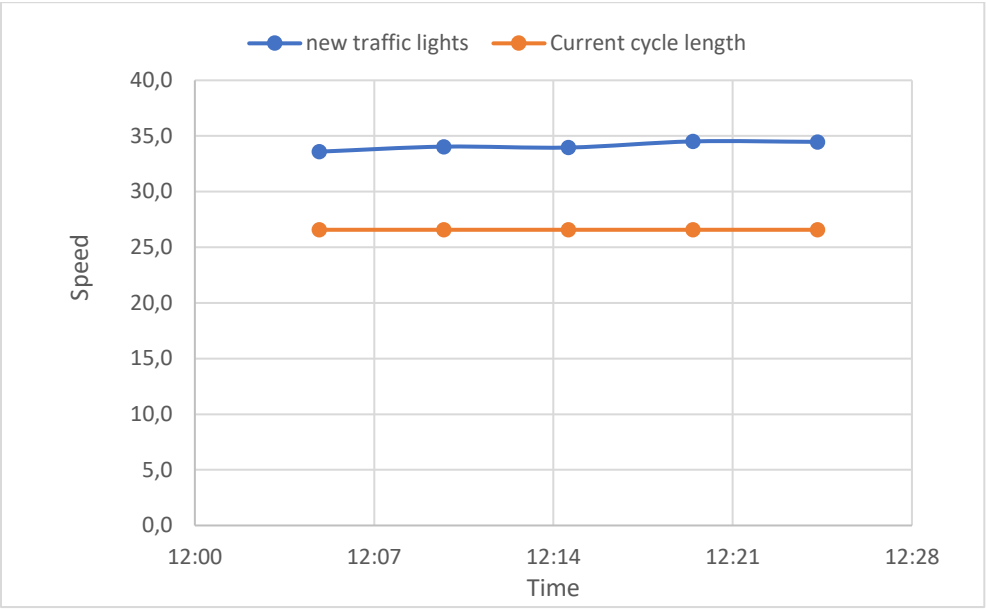

Fig. A.10. Speed

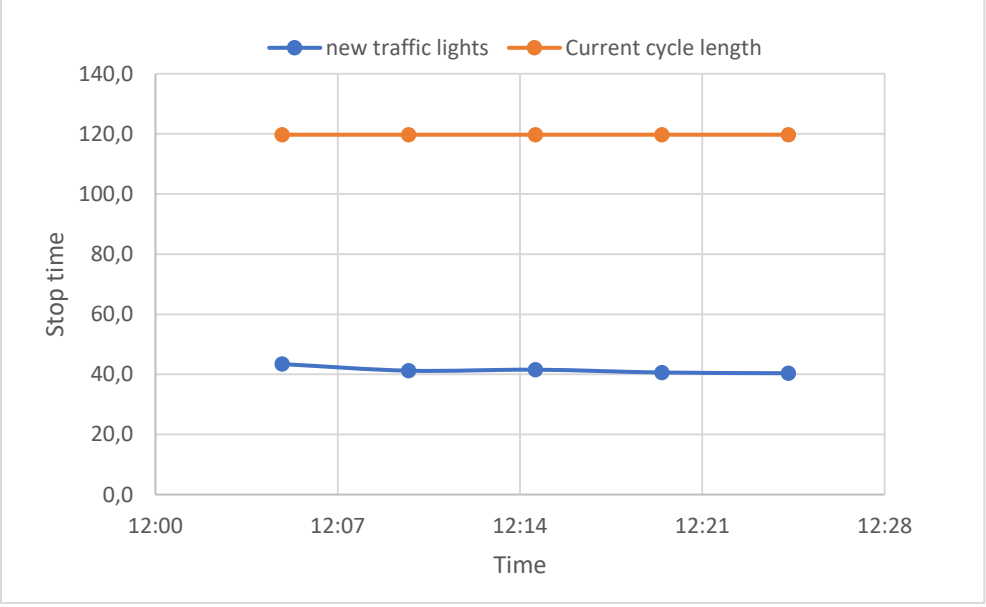

Fig. A.11. Stop time

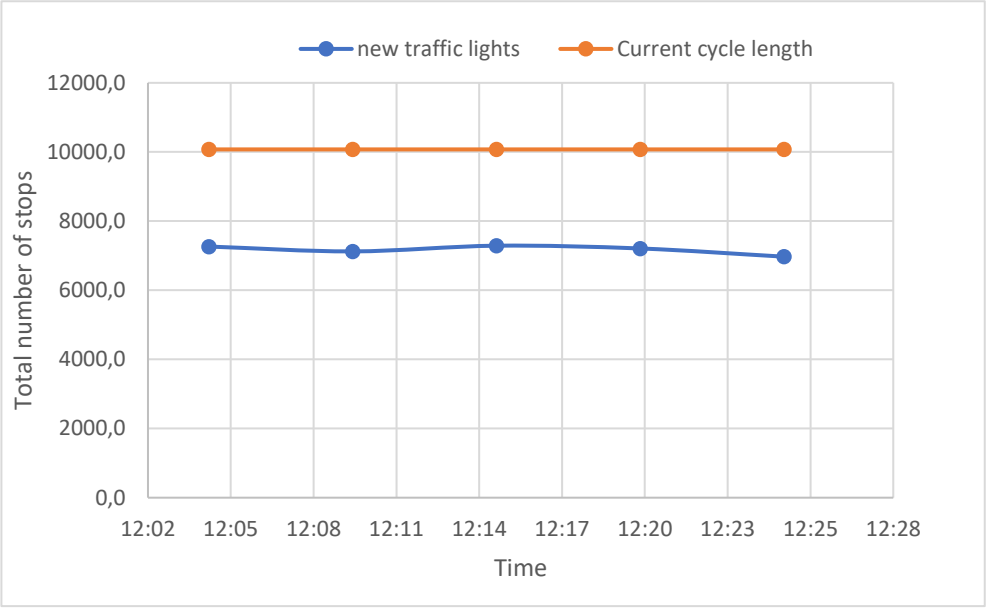

Fig. A.12. Total number of stops

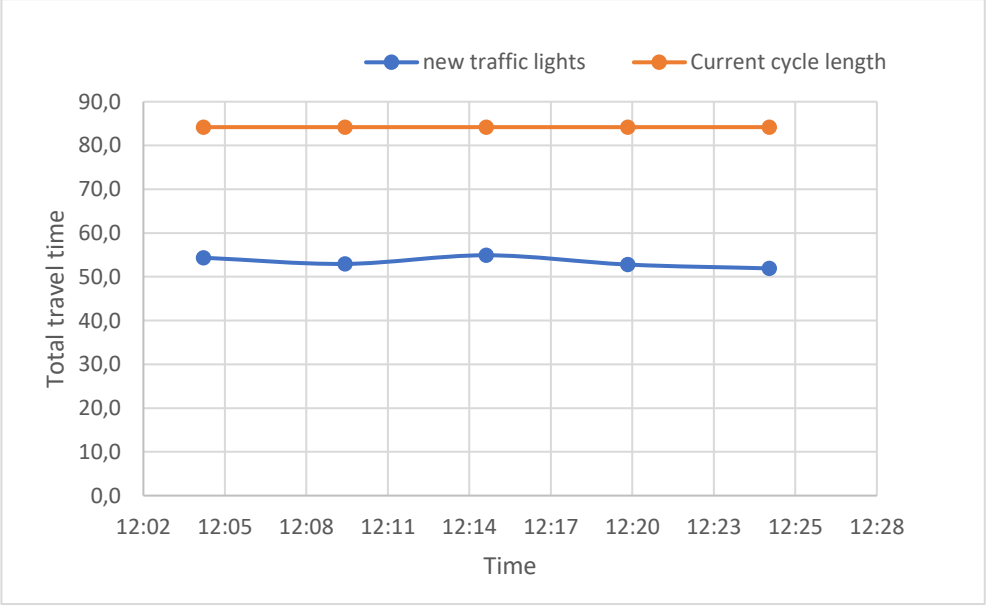

Fig. A.13. Total travel time

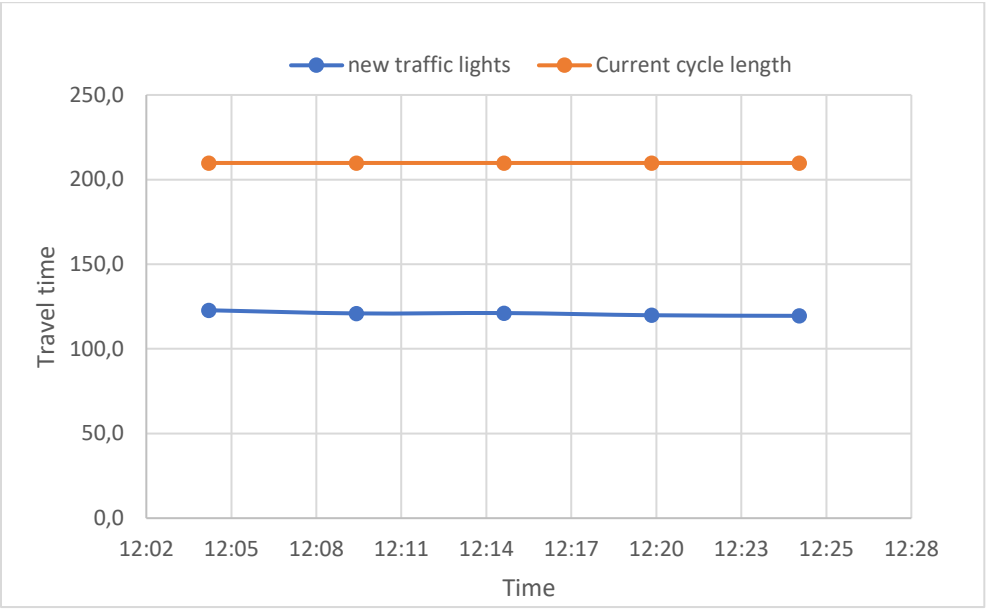

Fig. A.14 Travel time

Table A.6. Result 1st connected vehicle 17-18

Time Series	Current cycle length	New cycle length	improvement
Delay Time – Car [sec/km]	96.0	51.7	46%
Density – Car [veh/km]	6.0	4.7	22%
Mean Queue – Car [veh]	26.1	14.2	46%
Speed – Car [km/h]	31.0	35.3	12%
Stop Time – Car [sec/km]	80.7	39.7	51%
Total Number of Stops - Car	6440.8	5679.7	12%
Total Travel Time – Car [h]	57.9	45.0	22%
Travel Time – Car [sec/km]	162.2	117.8	27%

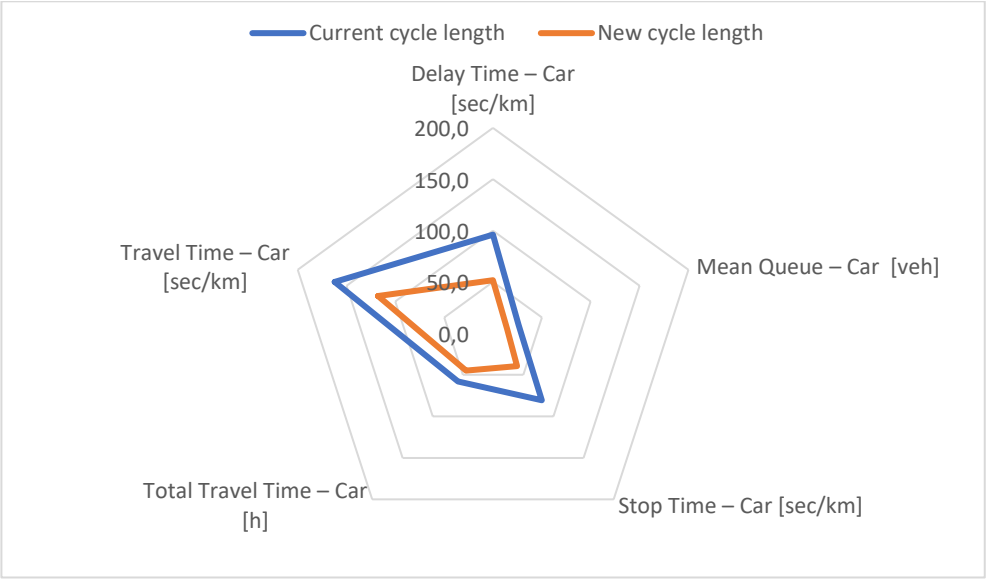

Fig. A.15. Improvement 1st connected vehicle 17-18

Table A.7. Result 2nd connected vehicle 17-18

Time Series	Current cycle length	New cycle length	improvement
Delay Time – Car [sec/km]	104.1	79.9	23%
Density – Car [veh/km]	6.2	5.9	5%
Mean Queue – Car [veh]	28.3	23.1	18%
Speed – Car [km/h]	30.7	31.6	3%
Stop Time – Car [sec/km]	88.3	64.1	27%
Total Number of Stops - Car	6405.9	5679.7	11%
Total Travel Time – Car [h]	59.4	56.3	5%
Travel Time – Car [sec/km]	170.2	146.0	14%

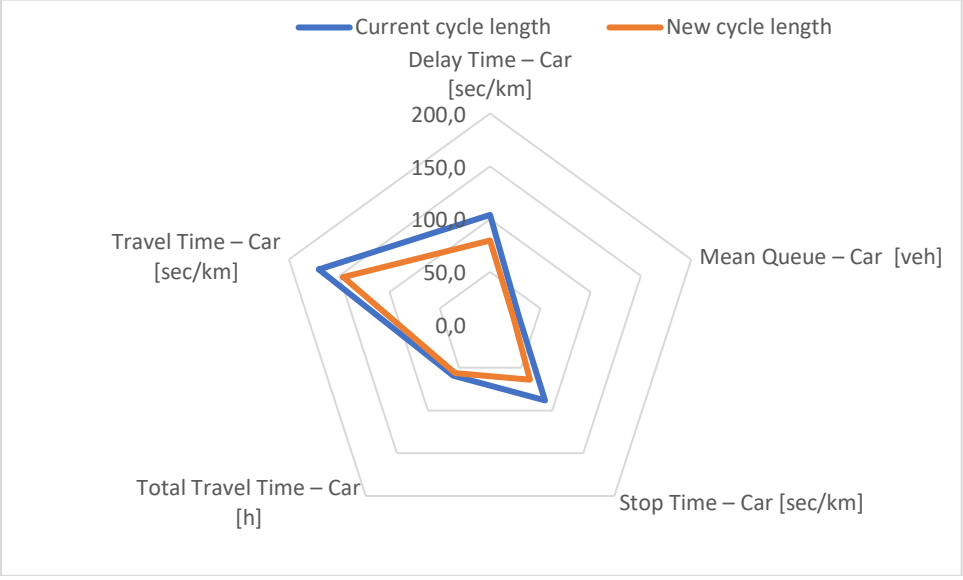

Fig. A.16. Improvement 2nd connected vehicle 17-18

Table A.8. Result 3rd connected vehicle 17-18

Time Series	Current cycle length	New cycle length	improvement
Delay Time – Car [sec/km]	120.3	60.4	50%
Density – Car [veh/km]	7.6	6.3	17%
Mean Queue – Car [veh]	35.5	21.7	39%
Speed – Car [km/h]	27.7	32.7	15%
Stop Time – Car [sec/km]	98.0	45.7	53%
Total Number of Stops - Car	10056.1	8387.7	17%
Total Travel Time – Car [h]	72.8	61.1	16%
Travel Time – Car [sec/km]	186.3	126.5	32%

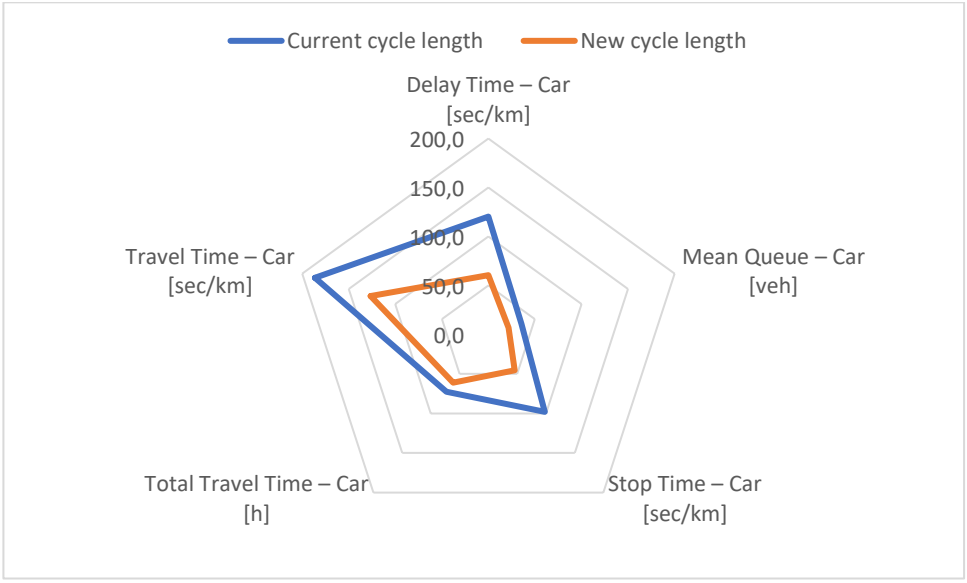

Fig. A.17. Improvement 3rd connected vehicle 17-18

Table A.9. Result 4th connected vehicle 17-18

Time Series	Current cycle length	New cycle length	improvement
Delay Time – Car [sec/km]	142.3	88.5	38%
Density – Car [veh/km]	8.5	7.3	14%
Mean Queue – Car [veh]	44.3	30.9	30%
Speed – Car [km/h]	27.2	29.6	8%
Stop Time – Car [sec/km]	120.8	70.2	42%
Total Number of Stops - Car	9185	8387.7	9%
Total Travel Time – Car [h]	81.5	70.3	14%
Travel Time – Car [sec/km]	208.4	154.6	26%

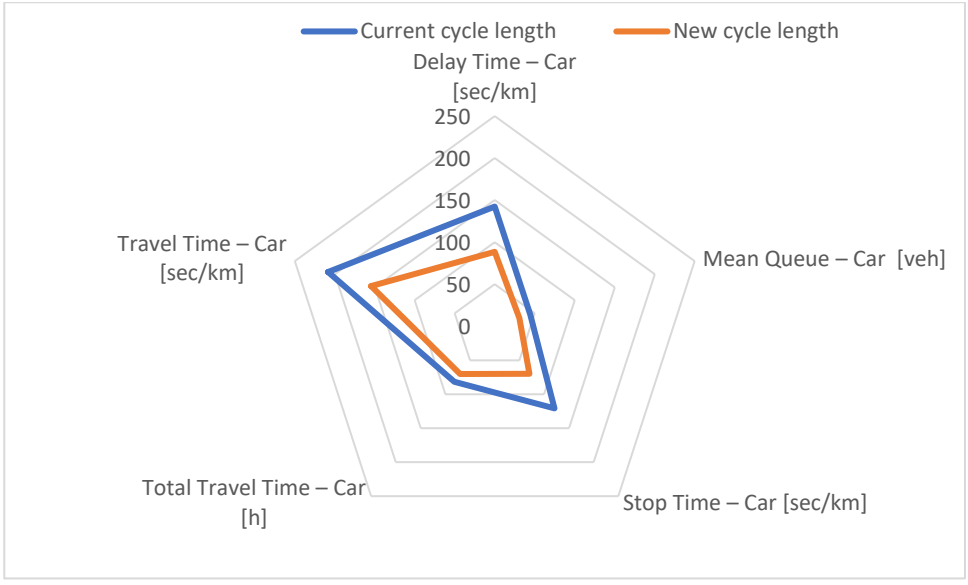

Fig. A.18. Improvement 4th connected vehicle 17-18

Table A.10. Result 5th connected vehicle 17-18

Time Series	Current cycle length	New cycle length	improvement
Delay Time – Car [sec/km]	47.2	39.8	16%
Density – Car [veh/km]	3.7	3.6	4%
Mean Queue – Car [veh]	11.2	9	19%
Speed – Car [km/h]	37.8	38.6	2%
Stop Time – Car [sec/km]	38.3	31.0	19%
Total Number of Stops - Car	3439.7	3175.4	8%
Total Travel Time – Car [h]	36	34.5	4%
Travel Time – Car [sec/km]	113.2	105.9	6%

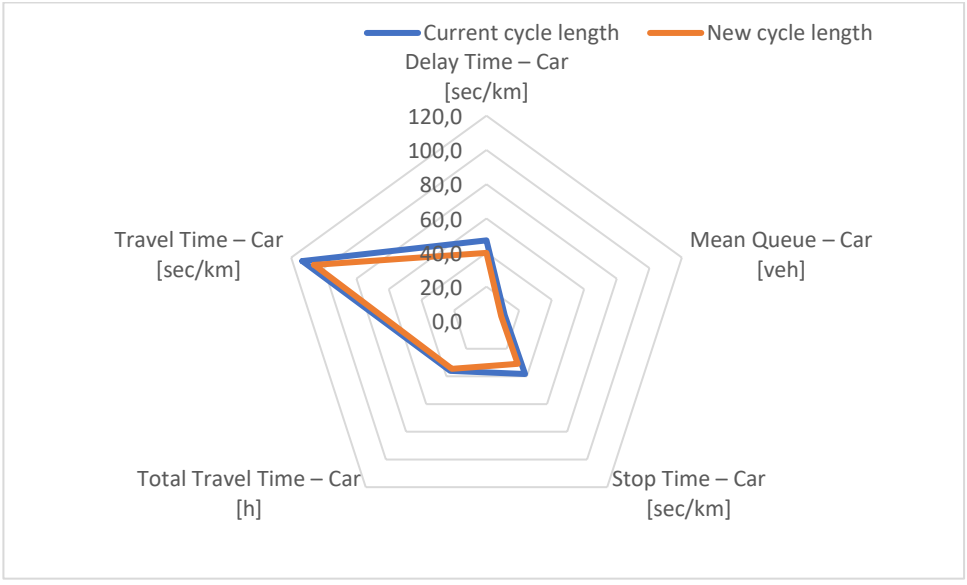

Fig. A.19. Improvement 5th connected vehicle 17-18

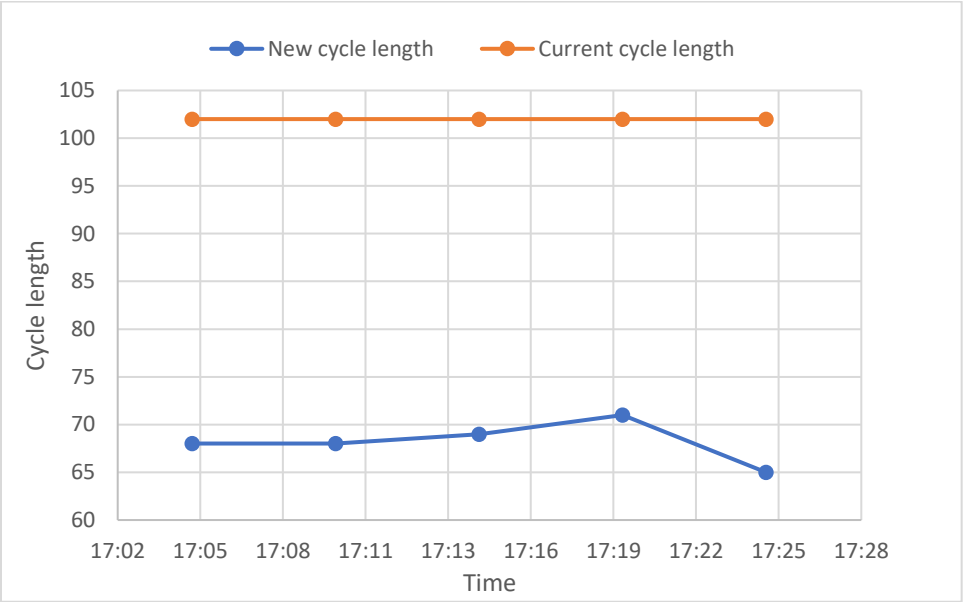

Fig. A.20. Cycle length time

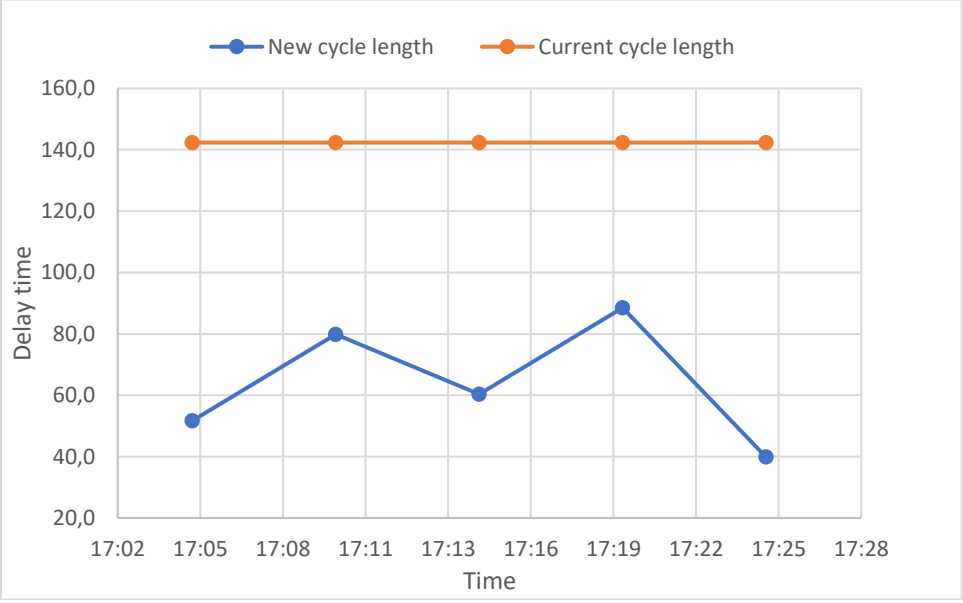

Fig. A.21. Delay time

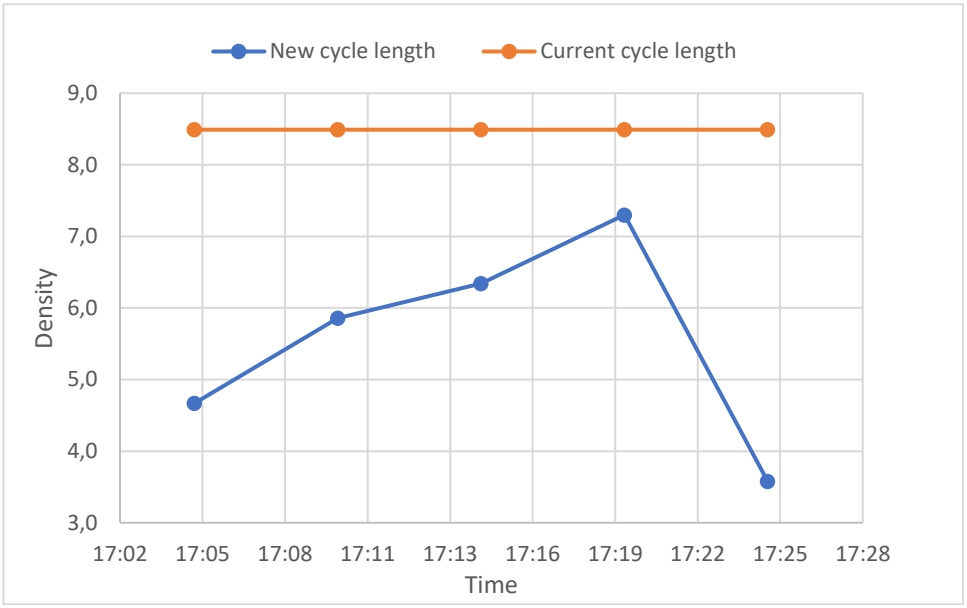

Fig. A.22. Density

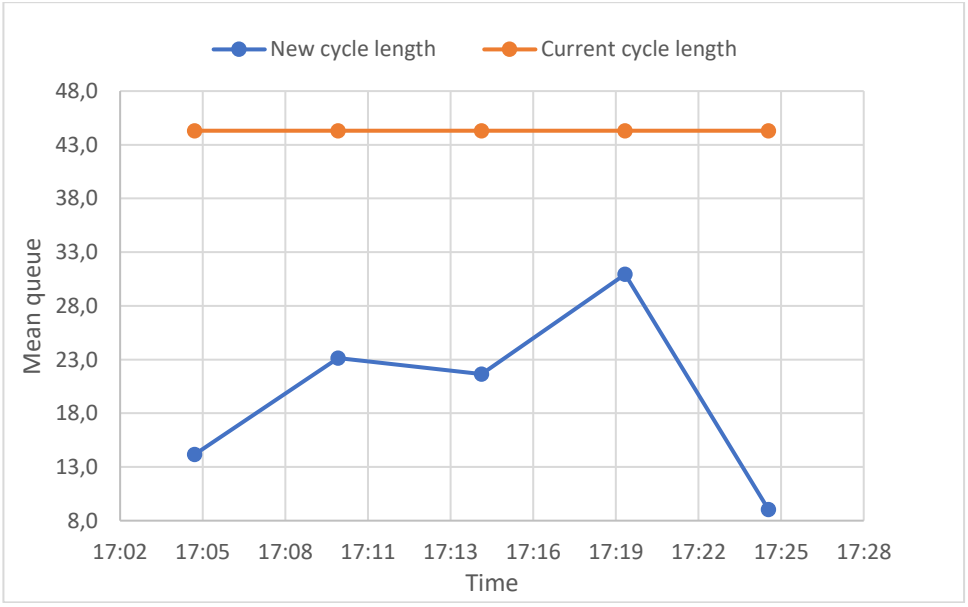

Fig. A.23. Mean queue

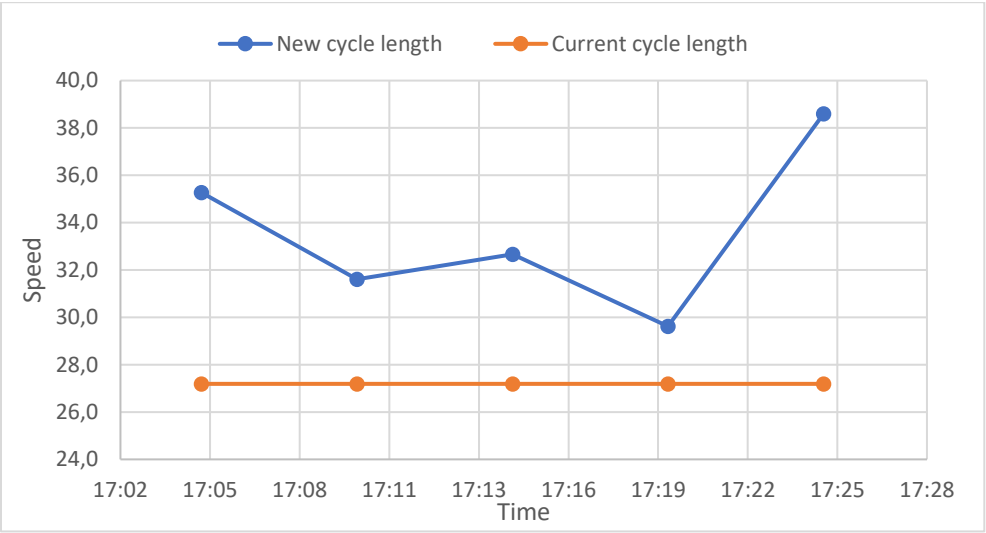

Fig. A.24. Speed

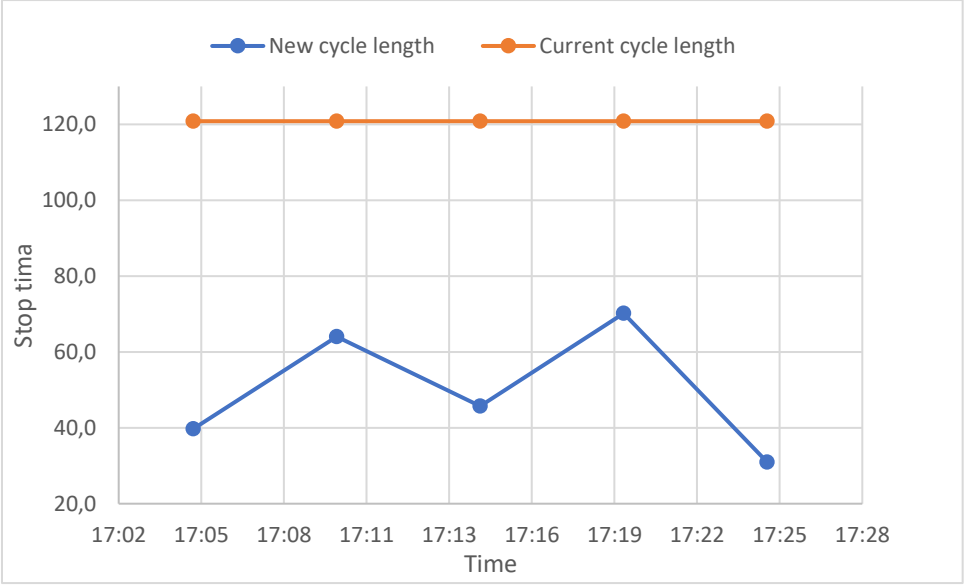

Fig. A.25. Stop time

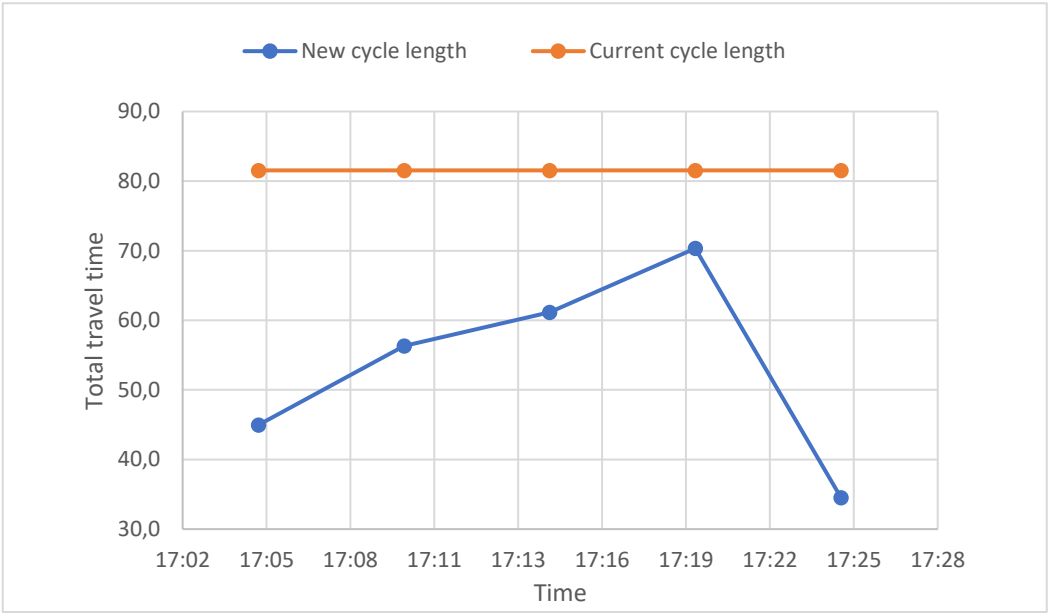

Fig. A.26. Total travel time

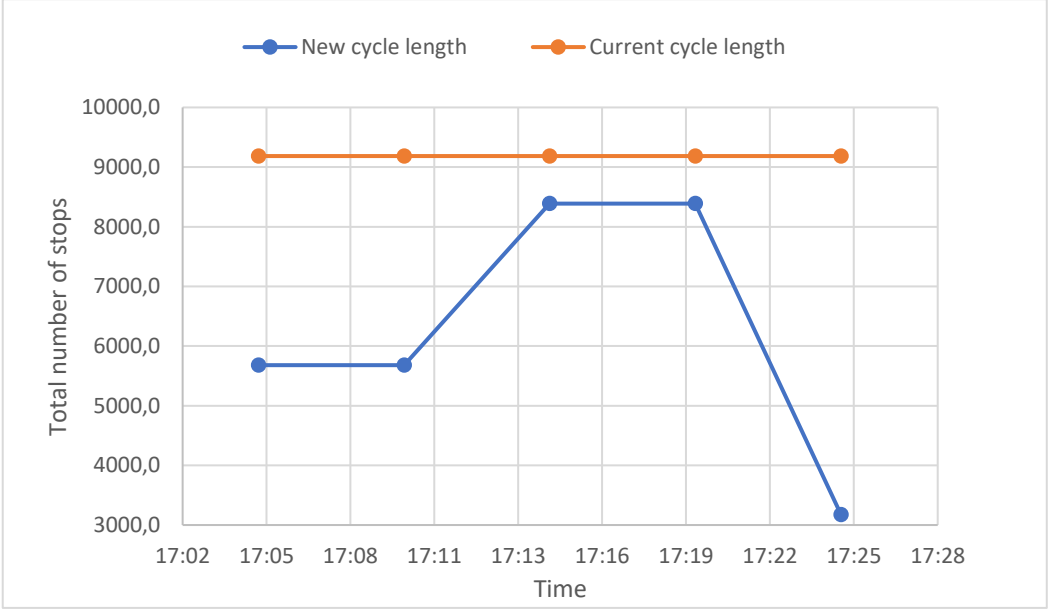

Fig. A.27. Total number of stops

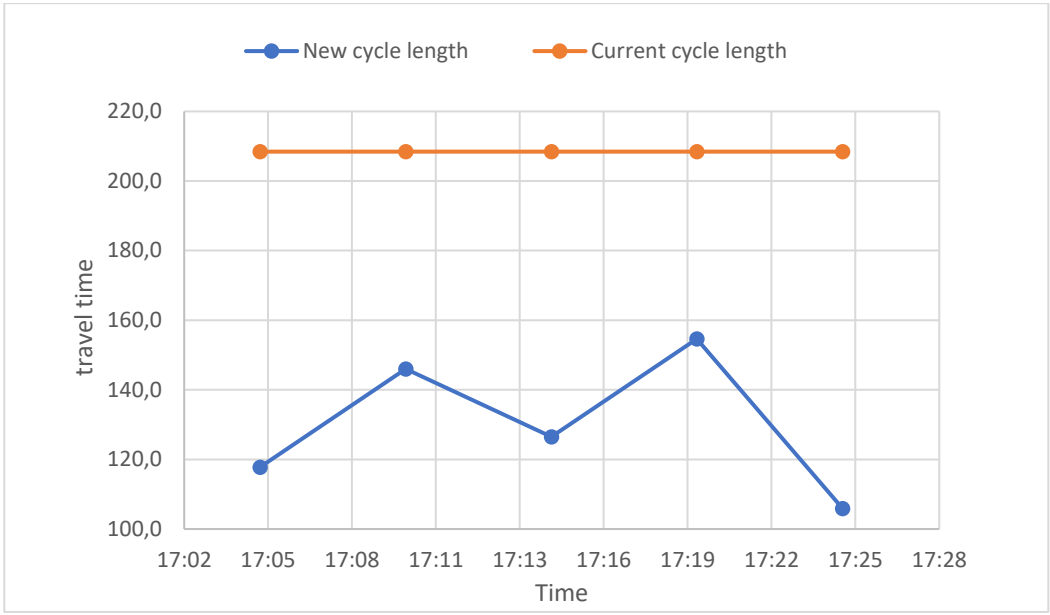

Fig. A.28. Travel time